

RECONSTRUÇÃO DE SOLUÇÕES NÃO-SUAVES DOS PROBLEMAS MAL POSTOS EM INVERSÃO GEOFÍSICA

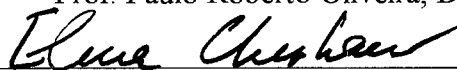
Hugo Richard Bertete Aguirre

TESE SUBMETIDA AO CORPO DOCENTE DA COORDENAÇÃO DOS PROGRAMAS DE PÓS-GRADUAÇÃO DE ENGENHARIA DA UNIVERSIDADE FEDERAL DO RIO DE JANEIRO COMO PARTE DOS REQUISITOS NECESSÁRIOS PARA A OBTENÇÃO DO GRAU DE DOUTOR EM CIÊNCIAS EM ENGENHARIA DE SISTEMAS E COMPUTAÇÃO.

Aprovada por:



Prof. Paulo Roberto Oliveira, Dr.Ing.



Prof. Elena Cherkaeva, Ph.D.



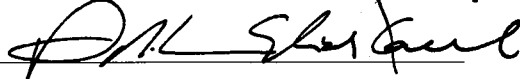
Prof. Michael Oristaglio, Ph.D.



Prof. Nelson Macular Filho, D.Sc.



Prof. Ammin Bassrrei, Ph.D.



Prof. Adilson Xavier, D.Sc.

AGUIRRE, HUGO RICHARD BERTETE

Reconstrução de Soluções Não-Suaves
dos Problemas Mal Postos em Inversão
Geofísica.

[Rio de Janeiro] 1997

VIII, 147p, 29,7 cm (COPPE/UFRJ, D.Sc., Engenharia de Sistemas e Computação, 1997)

Tese - Universidade Federal do Rio de Janeiro,
COPPE

1.Otimização

Problemas Inversos

I.COPPE/UFRJ II.Título(série)

Resumo da Tese apresentada à COPPE/UFRJ como parte dos requisitos necessários para a obtenção do grau de Doutor em Ciências(M.Sc.)

RECONSTRUÇÃO DE SOLUÇÕES NÃO-SUAVES
DOS PROBLEMAS MAL POSTOS EM INVERSÃO GEOFÍSICA.

Hugo Richard Bertete Aguirre

Agosto de 1997

Orientadores: Paulo Roberto Oliveira (Coppe-Sistemas, UFRJ)

Elena Cherkava (Mathematics Dept., University of Utah)

Programa: Engenharia de Sistemas e Computação

Estudamos neste trabalho a aplicação da teoria dos problemas inversos em geofísica. Analisamos analítica e numericamente um problema geofísico inverso. Desenvolvemos o operador do problema gravimétrico direto. Analisamos diferentes operadores de regularização e algoritmos para resolver problemas inversos. É proposta a minimização usando a norma "Total Variation, TV" para a reconstrução de estruturas em blocos em geofísica. Comparamos os resultados dos diferentes métodos numéricos para resolver o problema inverso em geofísica. Demonstramos que a abordagem através da norma de "Total Variation", permite a reconstrução das funções não-suaves da distribuição de densidade, e que não é possível a mesma, quando usados os métodos de regularização convencionais. Finalmente, um algoritmo "*regularized adaptive gradient minimization*" é apresentado para resolver o problema de TV.

Abstract of the Thesis presented to COPPE/UFRJ as a partial fulfillment of the requirements for the degree of Doctor of Science(D.Sc.)

RECONSTRUCTION OF NON-SMOOTH SOLUTIONS OF ILL-POSED GEOPHYSICAL INVERSE PROBLEMS

Hugo Richard Bertete Aguirre

August of 1997

Advisors: Paulo Roberto Oliveira (Coppe-Sistemas, UFRJ)

Elena Cherkaeva (Mathematics Dept., University of Utah)

Department: Computing Systems Engineering

This thesis analyzes analytically and numerically the geophysical inverse problem of gravimetry, which is the recovery of density variations in the earth from measurements of its gravity field on the surface or in boreholes. This inverse problem does not have a non-unique solution. Standard regularizing operators used for its solution and for the solution of other geophysical inverse problems tend to produce smooth models. I propose instead the use of the Total Variation norm (TV) for reconstruction of blocky structures in geophysics. Numerical simulations of the different regularization schemes suggest that an inversion based on the TV norm can effectively recover piecewise constant density functions which is usually not possible with conventional methods. An efficient algorithm minimizing the TV norm can be obtained by regularized adaptive gradient minimization of a discretized TV operator. Numerical results inverting 2D blocky structures using this algorithm allows to recover sharp density contrasts and edges present in the true model.

Agradecimentos

Gostaria de agradecer ao CNPq e a Schlumberger Doll Research , pelo auxílio financeiro.

Ao meus orientadores, Prof. Paulo Roberto Oliveira e Prof. Elena Cherkhaeva pela sua valiosa colaboração e preocupação pela qualidade do trabalho.

Aos Prof. Alan Tripp do Departamento de Geofísica da Universidade de Utah e Prof. Michael Ostraglio da Schlumberger Doll Research pelo seu importante apoio para o desenvolvimento desta pesquisa.

Ao professores da Universidade Federal do Rio de Janeiro, Prof. Nelson Maculan Filho, Prof. Luis Paulo Viera Braga e Prof. Adilson Xavier pelo seu invalorável incentivo e ajuda, ao longo do meu trabalho na Coppe-Sistemas.

Ao Prof. Amin Basrrei, da Universidade Federal da Bahia, pelas valiosas discussões sobre Regularização em Geofísica.

Ao Prof. Aaron Fogelson, do Departamento de Matemática da Universidade de Utah pelas importantes discussões durante esta pesquisa.

Ao Prof. Curtis Vogel, do Departamento de Matemática da Montana State University, pela agradável estadia naquela Universidade e as importantes referências do seu trabalho em métodos de "Total Variation".

Aos meus professores e colegas da Otimização da Coppe-Ufrj e da Matemática-UofU.

Índice

1	O problema	1
1.1	O problema gravimétrico inverso	2
1.2	O problema mal-posto	3
2	Soluções do problema de inversão gravimétrica	4
2.0.1	Regularização geral suave	4
2.1	Minimização regularizada não-linear	6
2.1.1	Método do "adaptive regularized gradient"	6
2.2	Problema discreto de inversão gravimétrica suave	8
3	Regularização alternativa não-suave	10
3.1	Definição da seminorma de Variação Total (TV)	10
3.1.1	TV para uma função contínua	10
3.1.2	TV para funções descontínuas	12
3.2	TV no problema gravimétrico inverso.	14
3.2.1	Equações de Euler-Lagrange para o problema $P_{TV}^\alpha(\rho, b)$	14
4	Discretização e Regularização	17
4.1	Discretização do operador do problema direto	17
4.2	Discretização semi-norma TV	21
4.2.1	Operador discreto das derivadas nas direções horizontal e vertical.	21
4.3	Calculo discreto da variação da semi-norma TV	22

4.4	Solução das equações de E-L usando o método de "Adaptive Gradient Minimization "	23
5	Resultados	26
6	Conclusões e Problemas em aberto	31
6.1	Conclusões	31
6.2	Problemas em aberto	32

Lista de Figuras

1.1	Esquema do problema de inversão gravimétrica	2
1.2	Instabilidade do operador gravimétrico inverso	3
2.1	Operador regularizado para o problema gravimétrico inverso	5
3.1	Exemplo função contínua 1D	11
3.2	Exemplo função descontínua 1D	13
4.1	Discretização usando blocos retangulares	18
4.2	Quantidades para o cálculo do efeito gravimétrico de um prisma	20
5.1	Distribuição de densidades do modelo verdadeiro	27
5.2	Solução sem regularização	28
5.3	Solução usando a primeira derivada em 2D como Funcional Estabilizante	29
5.4	Solução usando a Variação Total em 2D como Funcional Estabilizante	30

Capítulo 1

O problema

Neste trabalho estudamos o problema de reconstrução de funções não suaves a partir de dados gravimétricos na presença de ruído. As bases da teoria gravitacional foram estabelecidas pelo Marquês de Laplace em 1782, mostrando que o potencial Newtoniano fora de um corpo segue a equação,

$$\nabla^2\phi = 0$$

Não entanto, o problema direto que abordaremos neste trabalho, leva a uma equação mais geral que acima, válida também dentro de um corpo, e é chamada equação de Poisson.

$$\nabla^2\phi = -4\pi G\rho \tag{1.1}$$

onde, G é a Constante Gravitacional e $\rho(x)$ é a função densidade do meio.

A solução analítica da equação de Laplace é obtida usando o Teorema de Green, e para uma dada densidade $\rho(x)$ é,

$$\phi(y) = \int_{\Omega} \rho(x) G(y, x) dx \tag{1.2}$$

A equação 1.2 é um caso particular da Integral de Fredholm de primeira espécie e descreve a formulação para o problema gravimétrico.

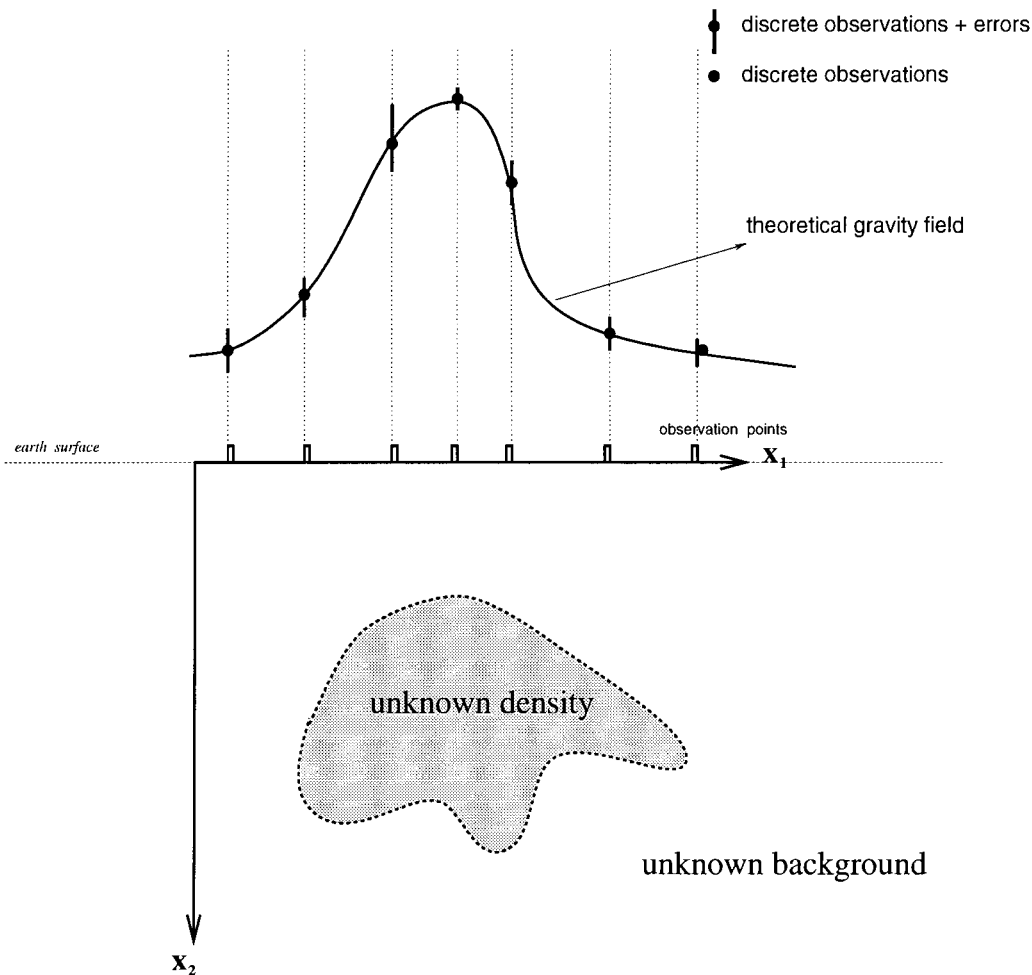


Figura 1.1: Esquema do problema de inversão gravimétrica

Em forma compacta pode ser escrita como

$$\phi = \bar{K}_{grav}(\rho) \quad (1.3)$$

onde o operador \bar{K} depende nos parâmetros do modelo do problema físico.

1.1 O problema gravimétrico inverso

O problema de inversão gravimétrica é, dadas algumas observações do potencial gravimétrico, queremos determinar a função densidade fonte.

$$K \rho = \phi$$

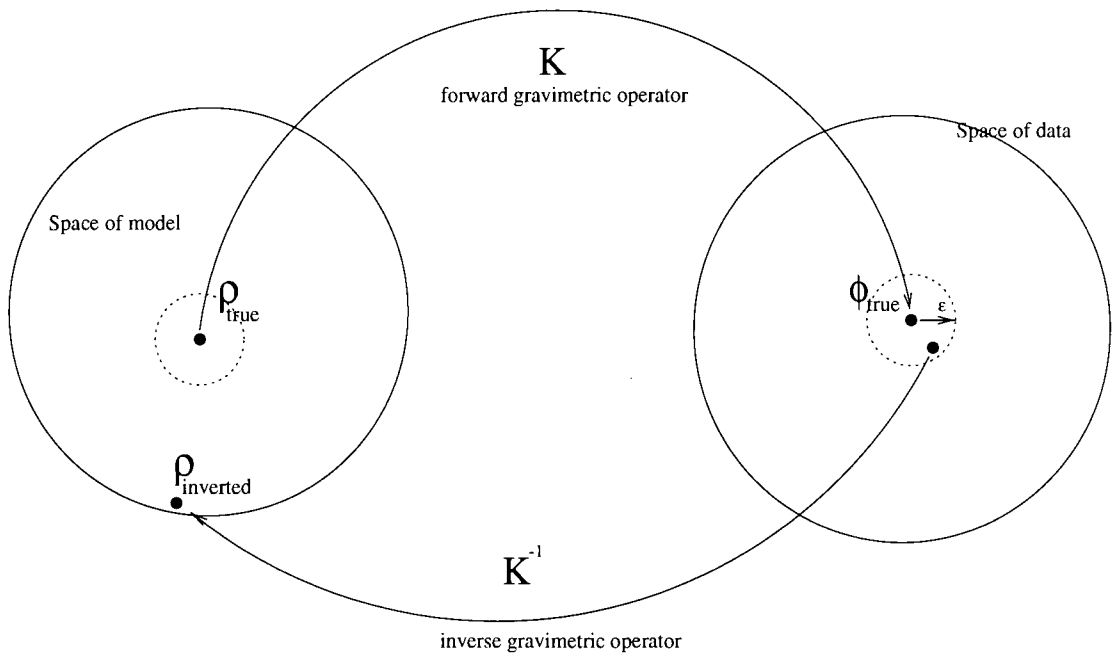


Figura 1.2: Instabilidade do operador gravimétrico inverso

1.2 O problema mal-posto

De acordo com (Hadamard, 1923) um modelo matemático de um problema físico e bem posto quando:

- 1) A solução do problema existe
- 2) Tem somente uma solução para o problema
- 3) A solução depende de forma contínua com os dados, (figura 1.2).

A solução da equação 1.3 não cumpre a terceira condição (estabilidade), nem a segunda (unicidade).

A equação 1.3 é mal posta. A unicidade da solução pode ser restringindo o espaço das soluções, mas devido a instabilidade do operador inverso \bar{K}^{-1} o problema requiere uma técnica especial para sua solução.

Capítulo 2

Soluções do problema de inversão gravimétrica

2.0.1 Regularização geral suave

A principal idéia da regularização é encontrar a solução do problema inverso, transformando um problema inverso mal-posto, dado pela equação

$$K(\rho) = b \tag{2.1}$$

numa seqüência de problemas inversos bem postos, dependendo num parâmetro (α), com a propriedade que quando ($\alpha \rightarrow 0$) a solução ($\rho^\alpha \rightarrow \rho$), ou em outras palavras, que pequenas variações nos dados representam pequenas variações na solução.

Regularização de Tikhonov

O problema de achar uma solução aproximada para o problema inverso mal posto 2.1 se reduz a construção do operador de regularização e a solução do problema para este operador [14].

O operador de regularização pode ser construído substituindo o problema mal-posto original em todo o espaço 2.1 por uma seqüência de equações bem condicionadas dentro de um conjunto *corrector*,

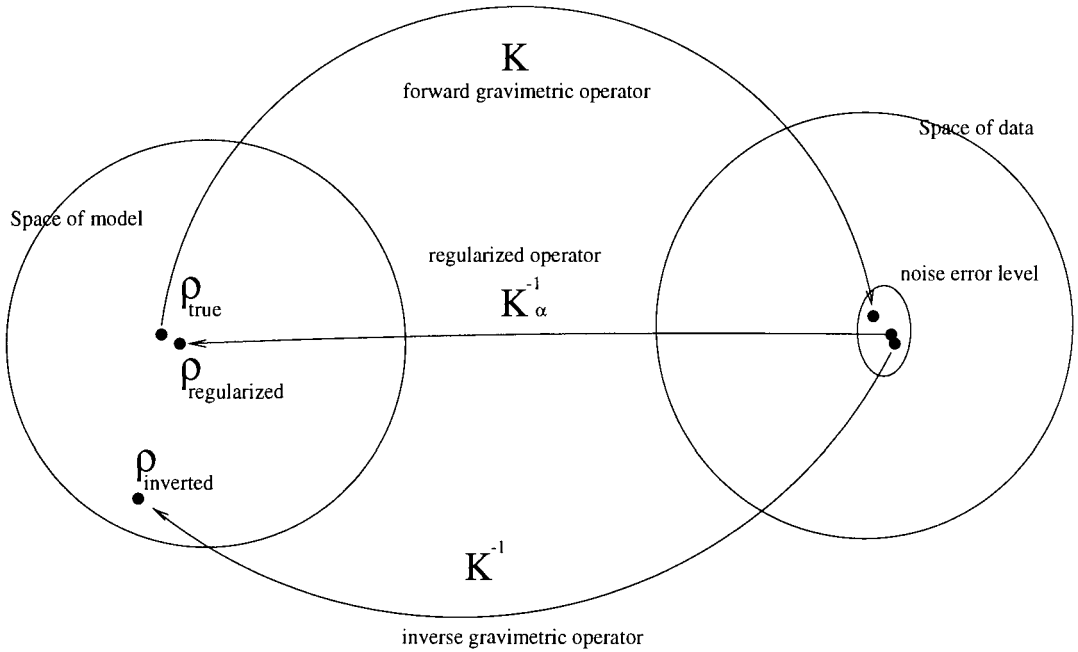


Figura 2.1: Operador regularizado para o problema gravimétrico inverso

$$\widetilde{K}_\alpha(\rho) = b$$

onde os operadores inversos $\widetilde{K}_\alpha^{-1}$ são contínuos (figura 2.1)

O parâmetro de regularização α , pode ser obtido a partir da amplitude do ruído nos dados. O conjunto *corrector* [14], selecionado a partir do espaço do modelo (X), é chamado *Estabilizador* ou *Funcional Estabilizante*.

Funcionais estabilizantes suaves

Baseados numa solução suave, as seguintes funcionais estabilizantes quadráticas são comumente utilizadas,

$$J_{mn}(\rho) = \int_{\Omega} [\rho(x)]^2 dx \quad (2.2)$$

ou

$$J_B(\rho) = \int_{\Omega} [\nabla \rho(x)]^2 dx \quad (2.3)$$

com $\nabla \rho(x) = \left(\frac{\partial}{\partial x}, \frac{\partial}{\partial y}, \frac{\partial}{\partial z} \right) \rho(x)$, ou

$$J_H(\rho) = \int_{\Omega} [\Delta \rho(x)]^2 dx \quad (2.4)$$

com $\Delta \rho(x) = \left(\frac{\partial^2}{\partial x^2}, \frac{\partial^2}{\partial y^2}, \frac{\partial^2}{\partial z^2} \right) \rho(x)$,

2.1 Minimização regularizada não-linear

Vários métodos podem ser desenvolvidos para a minimização da funcional de Tikhonov.

Apresentamos neste trabalho um método adaptativo baseado na direção de máxima descida.

2.1.1 Método do "adaptive regularized gradient"

O problema é minimizar o funcional de Tikhonov, usando como função estabilizante 2.2, a norma mínima da solução. Extensão para 2.3 e 2.4, é análoga.

$$\min_{\rho \in \mathbb{R}^n} P^\alpha(\rho) = \min \|F(\rho) - b\|_2^2 + \alpha \|\rho - \rho_0\|_2^2 \quad (2.5)$$

aonde F é operador não-linear do problema direto

ρ_0 é o modelo *a priori*

Escrevendo 2.5 em termos do produto interno, temos

$$\min \langle F(\rho) - b, F(\rho) - b \rangle + \langle \alpha \rho - \rho_0, \rho - \rho_0 \rangle$$

queremos $\delta_\rho P^\alpha(\rho) = 0$, (δ_ρ , é o operador variacional com respeito a ρ) e variando δ_ρ temos,

$$\delta_\rho P^\alpha(\rho) = \langle \delta_\rho F(\rho) - b, F(\rho) - b \rangle + \alpha \langle \delta_\rho \rho - \rho_0, \rho - \rho_0 \rangle$$

ou

$$= 2 \langle \delta_\rho (F(\rho) - b), F(\rho) - b \rangle + 2\alpha \langle \delta_\rho (\rho - \rho_0), \rho - \rho_0 \rangle$$

e finalmente,

$$= 2 \langle \delta_\rho F(\rho), F(\rho) - b \rangle + 2\alpha \langle \delta_\rho, \rho - \rho_0 \rangle$$

agora, lembrando que se K é diferenciável podemos escreve-lo em termos da derivada de Frechet F'_ρ então,

$$\delta_x F(x) \cong F(x + \delta_x) - F(x) = F'_\rho \delta_\rho$$

então

$$\delta_\rho P^\alpha(\rho) = 2 \langle F'_\rho \delta_\rho, F(\rho) - b \rangle + 2\alpha \langle \delta_\rho, \rho - \rho_0 \rangle$$

usando a definição de operador adjunto em [14] temos,

$$= 2 \langle \delta_\rho, (F'_\rho)^* (F(\rho) - b) \rangle + 2\alpha \langle \delta_\rho, \rho - \rho_0 \rangle$$

então

$$= 2 \langle \delta_\rho, (F'_\rho)^* (F(\rho) - b) + \alpha (\rho - \rho_0) \rangle$$

mas, queremos $\delta_\rho P^\alpha(\rho) = 0$ para qualquer δ_ρ , então é necessário que

$$(F'_\rho)^* (F(\rho) - b) + \alpha (\rho - \rho_0) = 0$$

que são as equações de Euler-Lagrange. Para construir um processo iterativo para achar a solução, consideremos ρ_{k+1} como,

$$\rho_{k+1} \leq \rho_k + \delta\rho$$

usando a parte linear de $\delta_\rho P^\alpha(\rho)$,

$$\delta\rho = -\theta^\alpha \left[\left(F'_\rho \right)^* (F(\rho) - b) + \alpha(\rho - \rho_0) \right]_\alpha = -\theta^\alpha g^\alpha(\rho)$$

onde θ^α é o tamanho do passo

$$g^\alpha(\rho) = \left[\left(F'_\rho \right)^* (F(\rho) - b) + \alpha(\rho - \rho_0) \right]_\alpha$$

e $g^\alpha(\rho)$ é a direção de máxima descida da funcional $P^\alpha(\rho)$.

Para verificar que $g^\alpha(\rho)$ é uma direção de descida da funcional $P^\alpha(\rho)$, calculemos $\delta_\rho P^\alpha(\rho)$;

$$\delta_\rho P^\alpha(\rho) = 2 \langle -\theta^\alpha g^\alpha(\rho), g^\alpha(\rho) \rangle < 0$$

devido a que $\langle g^\alpha(\rho), g^\alpha(\rho) \rangle \geq 0$.

Então, temos,

$$\rho_{k+1} \leq \rho_k - \theta_k^\alpha g_k^\alpha(\rho_k)$$

o tamanho do passo pode ser determinado utilizando uma minimização unidirecional da funcional de Tikhonov.

$$\min_{\theta_n \in \mathbb{R}^n} \Theta(\theta_n) = P^\alpha(\rho_{k+1}) = P^\alpha(\rho_k - \theta_k^\alpha g_k^\alpha(\rho_k))$$

O parâmetro de regularização α é uma seqüência de números reais $(\alpha_0 \dots \alpha_n)$, com $\alpha_0 > N$, e $\alpha_n < M$, aonde N e M são usualmente um valor grande e pequeno, respectivamente e depende da natureza do problema.

2.2 Problema discreto de inversão gravimétrica suave

O problema discreto pode ser obtido a partir da redução do problema a dimensão finita.

Representaremos como K , a matriz obtida do operador linear \bar{K} .

teremos então, quando a função estabilizante é a norma mínima da solução,

$$\min_{\rho} P^{\alpha}(\rho) = \min \|K\rho - b\|_2^2 + \alpha \|I(\rho)\|_2^2$$

e no caso da função estabilizante é o operador 2D ∇ ,

$$\min \|K\rho - b\|_2^2 + \alpha \left(\left\| \frac{\partial(\rho)}{\partial x_1} \right\|_2^2 + \left\| \frac{\partial(\rho)}{\partial x_2} \right\|_2^2 \right)$$

Capítulo 3

Regularização alternativa não-suave

3.1 Definição da seminorma de Variação Total (TV)

A definição de seminorma de Variação Total (TV) é, como em [3],

$$J_{tv} =^{def} \sup_{v \in \nu} \int_{\Omega} (-u \operatorname{div} v) \, dx \quad (3.1)$$

aonde v são funções teste que,

$$\nu = \left\{ v \in C_0^1(\Omega, \mathbb{R}^d) \mid |v(x)| \leq 1 \text{ para todo } x \in \Omega \right\}$$

Analizemos a seminorma TV. Por simplicidade consideremos o caso de uma função contínua 1D (fig. 3.1).

3.1.1 TV para uma função continua

Da definição 3.1 podemos escrever.

Caso: 1D, e $u \in C^1(\Omega_{0,1})$

$$J_{tv} = \sup_{v \in \nu} \int_{\Omega} -u \, v_x \, dx =$$

integrando por parte temos,

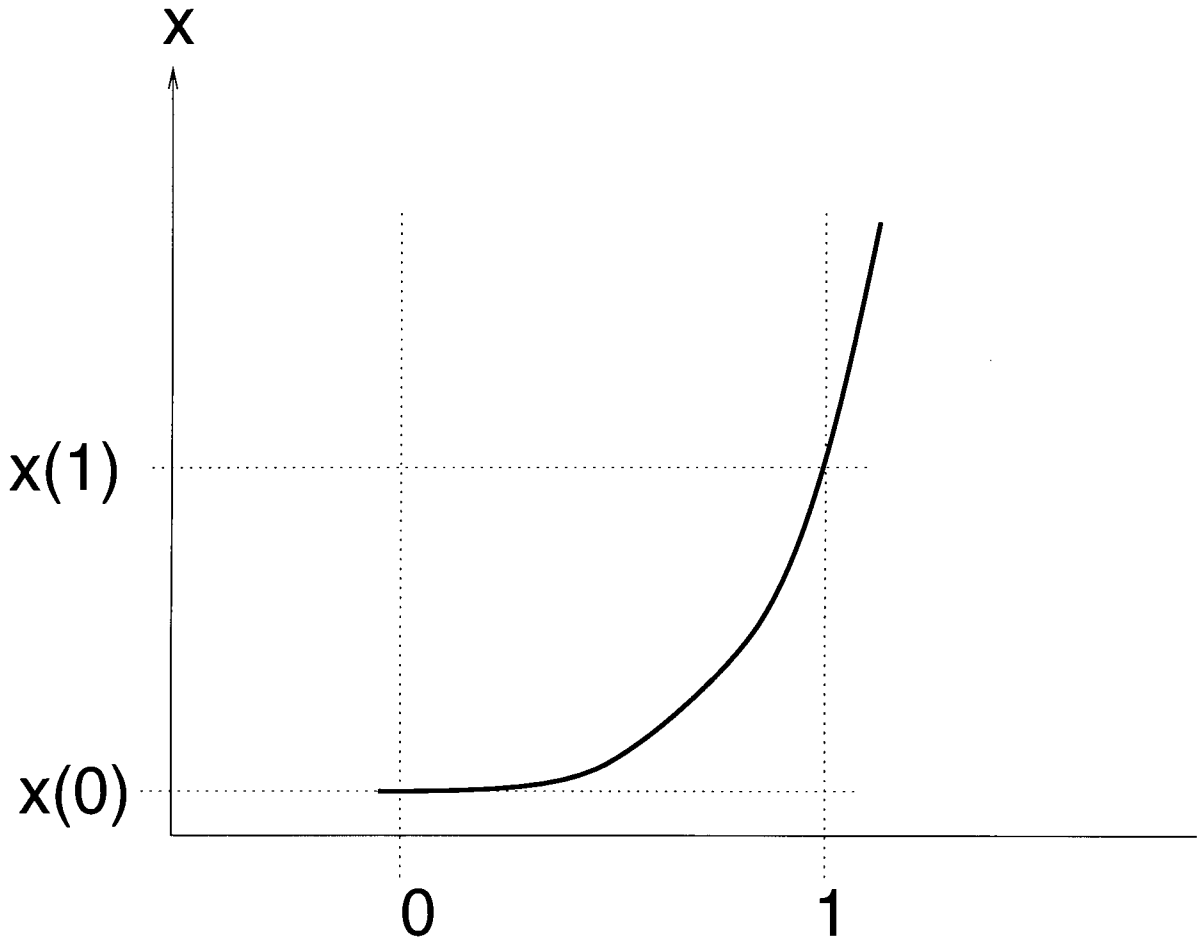


Figura 3.1: Exemplo função contínua 1D

$$\sup_{v \in \nu} - \int_{\Omega} (-u_x \ v) \, dx + uv|_0^1 =$$

mas como, $v \in C_0^1(\Omega, R^d)$, então

$$J_{tv} = \sup_{v \in \nu} \int_{\Omega} v \, u_x \, dx$$

e se ter

$$v \equiv \begin{cases} +1, & u_x > 0 \\ -1, & u_x < 0 \end{cases}$$

então obtemos

$$J_{tv} = \int_{\Omega} |u_x| \, dx \quad (3.2)$$

De 3.2 podemos ver que a definição 3.1 nos da a variação da função no domínio Ω

Consideremos agora para o caso descontínuo (fig. 3.2).

3.1.2 TV para funções descontínuas

Da definição 3.1 podemos escrever para uma função descontínua (fig. 3.2,

Caso: 1D, e $u \in C^0(\Omega_{0,1})$

$$J_{tv} = \sup_{v \in \nu} \int_{\Omega} -u \, v_x \, dx =$$

dividindo a integral a cada lado da descontinuidade teremos,

$$J_{tv} = \sup_{v \in \nu} \left\{ \lim_{\dot{a} \rightarrow a^-} - \int_0^{\dot{a}} -u \, v_x \, dx + \right. \\ \left. \lim_{\dot{a} \rightarrow a^+} \int_{\ddot{a}}^1 -u \, v_x \, dx \right\}$$

e integrando por partes em ambos termos, obtemos

$$J_{tv} = \sup_{v \in \nu} \left\{ \lim_{\dot{a} \rightarrow a^-} \int_0^{\dot{a}} u \, v_x \, dx - u(\dot{a})v(\dot{a}) + \right.$$

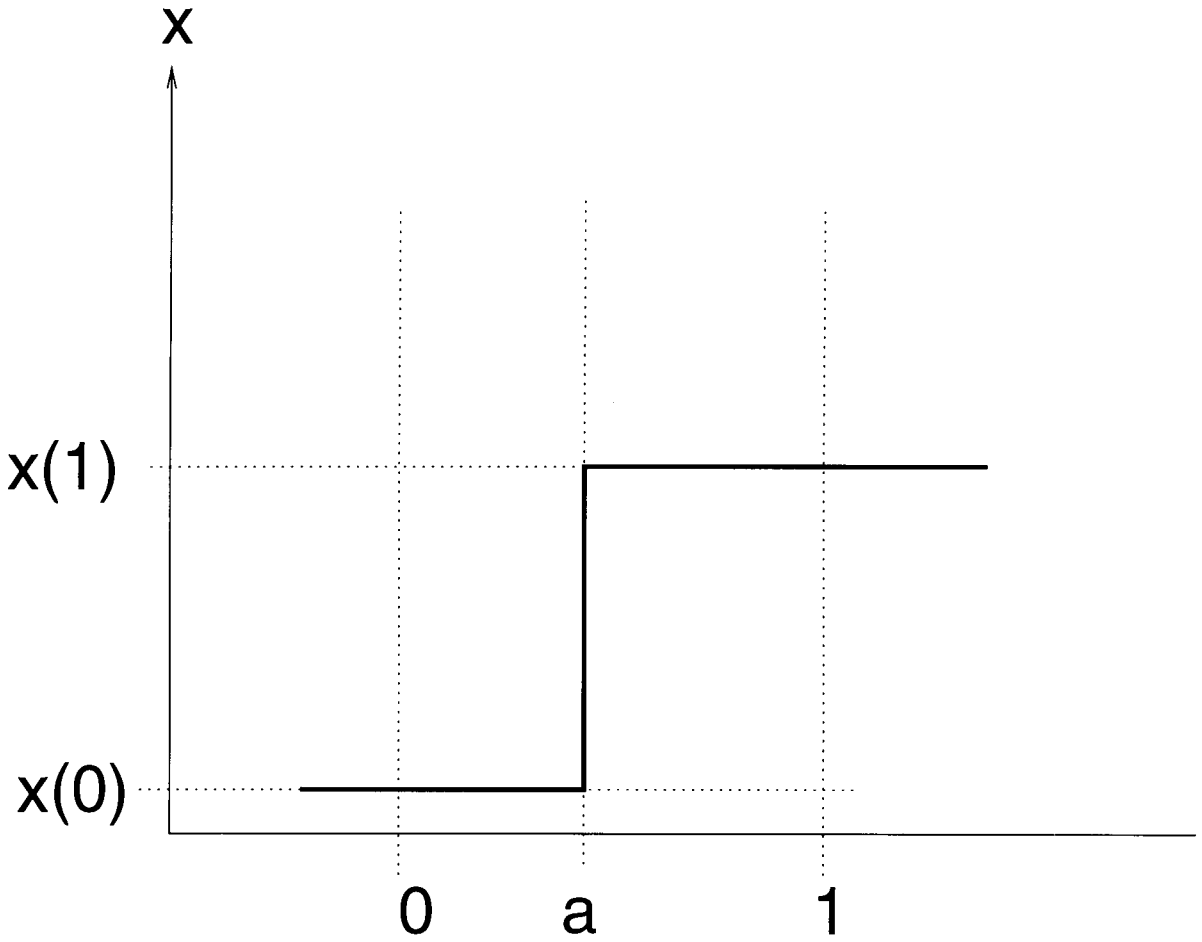


Figura 3.2: Exemplo função descontínua 1D

$$\lim_{\ddot{a} \rightarrow a^+} \int_{\ddot{a}}^1 u \ v_x dx + u(\ddot{a})v(\ddot{a}) \}$$

e como $v \in C_0^1(\Omega, \mathbb{R}^d)$, então

$$J_{tv} = \sup_{v \in \mathcal{V}} [-v(a)u(a^-) + v(a)u(a^+)]$$

ou

$$J_{tv} = \sup_{v \in \mathcal{V}} [v(a) (u(a^+) - u(a^-))]$$

e para

$$v(a) \equiv \begin{cases} +1, & (u(a^+) - u(a^-)) > 0 \\ -1, & (u(a^+) - u(a^-)) < 0 \end{cases}$$

então obteremos,

$$J_{tv} = |u(a^+) - u(a^-)|$$

e também neste caso, pode ser visto que é obtida a variação da função no domínio Ω .

Apresentaremos agora, o problema de inversão gravimétrica usando a TV como *estabilizador*.

3.2 TV no problema gravimétrico inverso.

Usando a definição 3.1 podemos escrever para o problema gravimétrico em 2D,

$$\min P_{TV}^\alpha(\rho, b) = \min \|K\rho - b\|_2^2 + \alpha \int_{\Omega} \sqrt{\left(\frac{\partial(\rho)}{\partial x_1}\right)^2 + \left(\frac{\partial(\rho)}{\partial x_2}\right)^2} dx \quad (3.3)$$

3.2.1 Equações de Euler-Lagrange para o problema $P_{TV}^\alpha(\rho, b)$

As equações de Euler-Lagrange para o primeiro termo de 3.3 podem ser deduzidas a partir do apresentado no Capítulo 2. Para o segundo termo de 3.3 teremos,

$$\delta_\rho TV(\rho) = \delta_\rho \int_\Omega \sqrt{\left(\frac{\partial \rho}{\partial x_1}\right)^2 + \left(\frac{\partial \rho}{\partial x_2}\right)^2} dx_1 dx_2 =$$

e colocando o operador δ_ρ dentro da integral

$$\int_\Omega \delta_\rho \sqrt{\left(\frac{\partial \rho}{\partial x_1}\right)^2 + \left(\frac{\partial \rho}{\partial x_2}\right)^2} dx_1 dx_2 =$$

variando δ_ρ , obtemos

$$\frac{1}{2} \int_\Omega \frac{1}{\sqrt{\left(\frac{\partial \rho}{\partial x_1}\right)^2 + \left(\frac{\partial \rho}{\partial x_2}\right)^2}} \left(2 \frac{\partial \rho}{\partial x_1} \delta_\rho \frac{\partial \rho}{\partial x_1} + 2 \frac{\partial \rho}{\partial x_2} \delta_\rho \frac{\partial \rho}{\partial x_2} \right) dx_1 dx_2 =$$

e reagrupando,

$$\int_\Omega \frac{\frac{\partial \rho}{\partial x_1} \delta_\rho \frac{\partial \rho}{\partial x_1}}{\sqrt{\left(\frac{\partial \rho}{\partial x_1}\right)^2 + \left(\frac{\partial \rho}{\partial x_2}\right)^2}} + \frac{\frac{\partial \rho}{\partial x_2} \delta_\rho \frac{\partial \rho}{\partial x_2}}{\sqrt{\left(\frac{\partial \rho}{\partial x_1}\right)^2 + \left(\frac{\partial \rho}{\partial x_2}\right)^2}} dx_1 dx_2 =$$

ou

$$\int_\Omega \frac{\nabla \rho}{\sqrt{\left(\frac{\partial \rho}{\partial x_1}\right)^2 + \left(\frac{\partial \rho}{\partial x_2}\right)^2}} + \delta_\rho \left(\frac{\partial \rho}{\partial x_1}, \frac{\partial \rho}{\partial x_2} \right) dx_1 dx_2 =$$

e usando o Teorema de Green podemos escrever,

$$\int_{\partial \Omega} \delta_\rho \left(\frac{\frac{\partial \rho}{\partial x_1}}{\sqrt{\left(\frac{\partial \rho}{\partial x_1}\right)^2 + \left(\frac{\partial \rho}{\partial x_2}\right)^2}}, \frac{\frac{\partial \rho}{\partial x_2}}{\sqrt{\left(\frac{\partial \rho}{\partial x_1}\right)^2 + \left(\frac{\partial \rho}{\partial x_2}\right)^2}} \right) \cdot \vec{n} \, ds \quad (3.4)$$

então 3.4 sera satisfeita quando,

$$\begin{cases} \frac{\partial \rho}{\partial n} = 0 & \text{on } \partial \Omega \\ \nabla \cdot \left(\frac{\nabla \rho}{|\nabla \rho|} \right) = 0 & \text{in } \Omega \end{cases}$$

finalmente as equações de Euler-Lagrange 3.3 podem ser escritas como,

$$\frac{\partial \rho}{\partial n} = 0 \quad (3.5)$$

e

$$(K^*K\rho - K^*\rho) + \alpha\nabla \cdot \left(\frac{\nabla\rho}{|\nabla\rho|} \right) = 0 \quad (3.6)$$

Capítulo 4

Discretização e Regularização

O problema de minimização para o problema de inversão gravimétrica é,

$$\min \|K\rho - b\|_2^2 + \alpha \int_{\Omega} \sqrt{\left(\frac{\partial(\rho)}{\partial x_1}\right)^2 + \left(\frac{\partial(\rho)}{\partial x_2}\right)^2} dx \quad (4.1)$$

4.1 Discretização do operador do problema direto

Na Figa. 4.1, apresentamos o esquema de um modelo discreto usado em diferentes aplicações geofísicas, aonde $\Omega = \{\Omega_{ij}, i = 1 \dots n, j = 1 \dots m\}$.

A função $\rho(x)$ é "piece-wise constant" e é dada. A mesma pode ser escrita como,

$$\rho(x) = \sum_{i=1}^{i=nx_1} \sum_{j=1}^{j=nx_2} \rho_{ij} \chi_{ij}(x), \quad x \in \Omega$$

onde $\chi_{i,j}(x) = \begin{cases} 1, & x \in \Omega_{i,j} \\ 0 & \text{nos outros casos} \end{cases}$

e $b(y)_j$ são os dados discretos obtidos em alguma parte do domínio $\partial\Omega$.

Da solução da equação de Poisson temos,

$$\phi(y) = \gamma \int_{\Omega} \rho(x) \frac{1}{r} d\Omega = K(\rho)$$

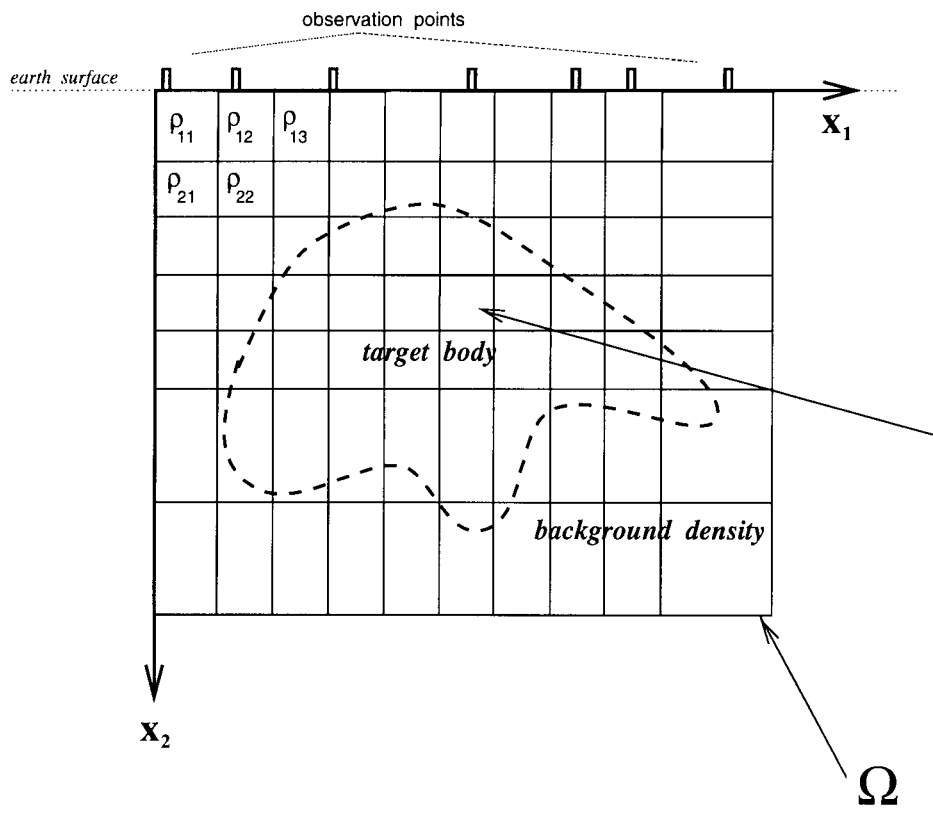


Figura 4.1: Discretização usando blocos rectangulares

e

$$\mathbf{g}(y) = \nabla\phi = \gamma \int_{\Omega} \rho(x) \nabla \frac{1}{r} d\Omega$$

mas, os gravímetros medem somente a componente vertical do vetor da gravidade, então teremos,

$$b = \gamma \int_{\Omega} \frac{\partial}{\partial x_2} \frac{1}{r} \rho(x) d\Omega \quad (4.2)$$

A avaliação desta integral para diferentes geometrias é bem conhecida, alguns exemplos são [18], [29]. Uma abordagem comum é integrar 4.2 ao longo do eixo (x_3) que tem densidade constante obtendo uma integral da forma,

$$b = \gamma \int_S \frac{\partial}{\partial x_2} \log \frac{1}{r} \rho(x) dS = \gamma \int_S f(x_1, x_2) dS$$

Usando a observação que esta superfície de integração é equivalente a integração em dos passos ao longo do contorno da superfície (F_x), teremos

$$b = \int_S f(x_1, x_2) dS = \oint_{\partial S} F_x(x_1, x_2) dx_2 \quad (4.3)$$

a solução numérica de 4.3 para um prisma rectangular pode ser encontrada em [18], [29], etc. e pode ser escrita,

$$b = 2\gamma \left[D\theta_2 - d\theta - x \log \left(\frac{r_1 r_4}{r_2 r_3} \right) + b \log \left(\frac{r_4}{r_3} \right) \right] \rho \quad (4.4)$$

A figura 4.2 mostra as quantidades envolvidas em 4.4.

Seja $b_j =$ dado discretos observados no ponto $j, \{j = 1, \dots, m\}$ e $\rho(x)_i =$ densidade constante no bloco i , então usando a notação matricial podemos escrever

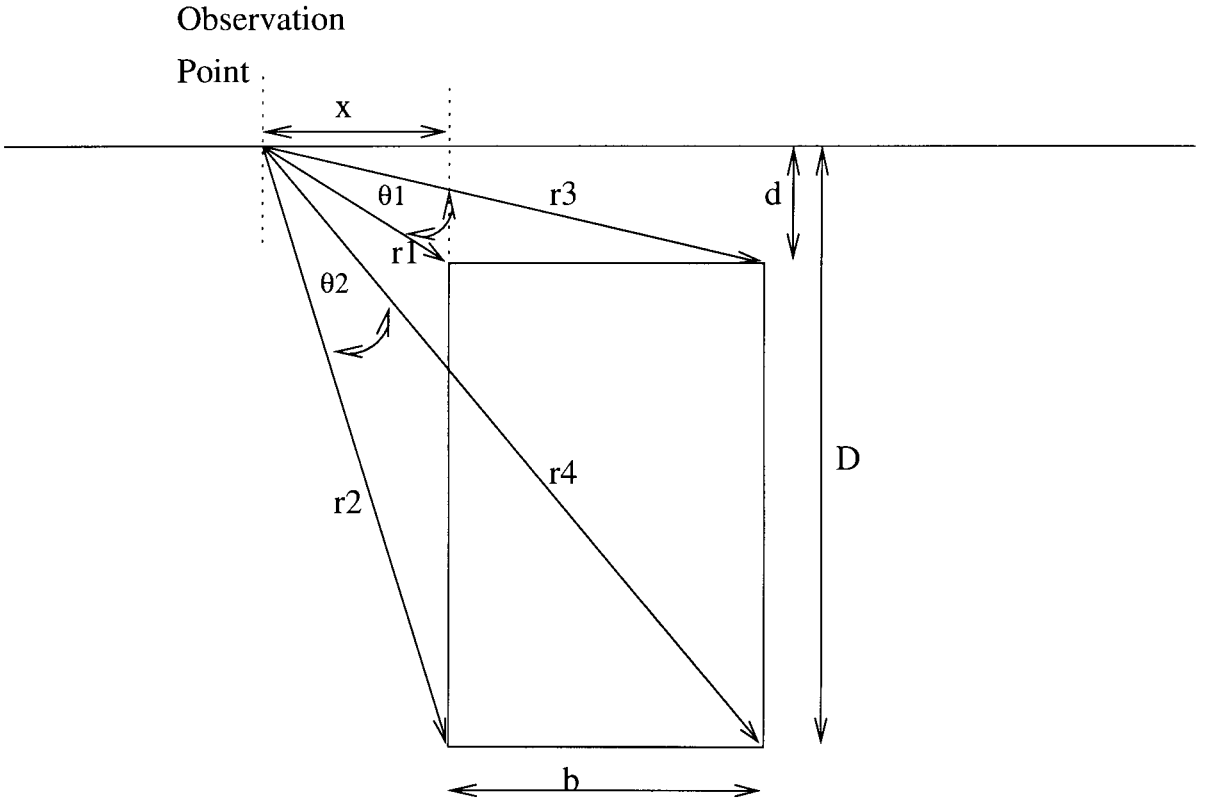


Figura 4.2: Quantidades para o cálculo do efeito gravimétrico de um prisma

$$K(\rho) = \begin{pmatrix} k_{11} & \cdot & \cdot & k_{1n} \\ \cdot & \cdot & \cdot & \cdot \\ \cdot & \cdot & \cdot & \cdot \\ \cdot & \cdot & \cdot & \cdot \\ k_{m1} & \cdot & \cdot & k_{mn} \end{pmatrix} \begin{pmatrix} \rho^1 \\ \cdot \\ \cdot \\ \rho^n \end{pmatrix} = \begin{pmatrix} b^1 \\ \cdot \\ \cdot \\ \cdot \\ b^m \end{pmatrix} \quad (4.5)$$

aonde

$$k_{ij}(x, y) = 2\gamma \left[D\theta_2 - d\theta - x \log \left(\frac{r_1 r_4}{r_2 r_3} \right) + b \log \left(\frac{r_4}{r_3} \right) \right]$$

e K é o operador gravimétrico direto.

4.2 Discretização semi-norma TV

Na figure 4.1 a densidade a ser calculada $\rho(x)$ está representada num espaço em 2D , com $x = (x_1, x_2)$ e $\rho(x) = \rho(x_1, x_2)$. Para o cálculo dos operadores da derivadas discretas na expressão da semi-norma TV 4.1, converteremos $\rho(x_1, x_2)$ em um vetor em 1D vetor, usando uma ordenação linha a linha.

4.2.1 Operador discreto das derivadas nas direções horizontal e vertical.

Para a direções horizontal (x_1) e vertical (x_2), as derivadas discretas da função de distribuição de densidade no ponto i, j podem ser escritas como,

$$\left(\frac{\partial(\rho)}{\partial x_1}\right)_{i,j} \cong \frac{\rho_{i,j} - \rho_{i+1,j}}{\Delta x_1}$$

e

$$\left(\frac{\partial(\rho)}{\partial x_2}\right)_{i,j} \cong \frac{\rho_{i,j} - \rho_{i,j+1}}{\Delta x_2}$$

aonde Δx_1 e Δx_2 são o comprimento do bloco.

Ou então podemos escrever,

$$\left(\frac{\partial(\rho)}{\partial x_1}\right) \cong DX_1 \begin{pmatrix} \rho_{11} \\ \cdot \\ \cdot \\ \rho_{ij} \\ \cdot \\ \cdot \\ \rho_{ZX} \end{pmatrix} \quad (4.6)$$

e

$$\left(\frac{\partial(\rho)}{\partial x_2} \right) \cong DX_2 \begin{pmatrix} \rho_{11} \\ \cdot \\ \cdot \\ \rho_{ij} \\ \cdot \\ \cdot \\ \cdot \\ \rho_{ZX} \end{pmatrix} \quad (4.7)$$

Usando os operadores acima nas (eqs. 4.6 e 4.7) podemos escrever o operador discreto da variação total da densidade como,

$$TV(\rho) \cong \sum_{ij} \sqrt{[DX_1(\rho)]_{ij}^2 + [DX_2(\rho)]_{ij}^2} \Delta x_1 \Delta x_2 \quad (4.8)$$

então o funcional discreto de Tikhonov pode ser escrita como,

$$P_{dT}^\alpha = \|K\rho - b\|_2^2 + \alpha \sum_{ij} \sqrt{[DX_1(\rho)]_{ij}^2 + [DX_2(\rho)]_{ij}^2} \Delta x_1 \Delta x_2 \quad (4.9)$$

e nosso objetivo é $P_{dT}^\alpha \rightarrow \min$.

4.3 Cálculo discreto da variação da semi-norma TV

A variação da semi-norma TV usando uma "forward approximation" da primeira derivada de 4.8 pode ser avaliada como,

$$\frac{\partial TV(\rho)}{\partial \rho_{kl}} \cong \frac{1}{\delta_\rho} TV(\rho + \eta^{kl} \delta_\rho) - TV(\rho) \quad (4.10)$$

onde, $\eta_{ij}^{kl} = \begin{cases} 1 & \text{se } i = k, j = l \\ 0 & \text{nos outros casos} \end{cases}$.

Substituindo 4.8 em 4.10 obtemos,

$$\frac{\partial TV(\rho)}{\partial \rho_{kl}} \cong$$

$$\frac{1}{\delta_\rho} \left[\left\{ \sum_{ij} [DX_1(\rho + \eta^{kl}\delta_\rho)]_{ij} + [DX_2(\rho + \eta^{kl}\delta_\rho)]_{ij} \right\}^{\frac{1}{2}} \Delta x_1 \Delta x_2 - \sum_{ij} \{ [DX_1(\rho)]_{ij} + [DX_2(\rho)]_{ij} \}^{\frac{1}{2}} \Delta x_1 \Delta x_2 \right]$$

então as equações discretas de E-L são,

$$0 = \frac{\partial \rho}{\partial n} \quad \text{on } \partial\Omega$$

$$0 = l^\alpha(\rho) = (\widetilde{K}^* \widetilde{K} \rho - \widetilde{K}^* \hat{b}) +$$

$$\alpha \frac{1}{\delta_\rho} \left[\left\{ \sum_{ij} [DX_1(\rho + \eta^{kl}\delta_\rho)]_{ij} + [DX_2(\rho + \eta^{kl}\delta_\rho)]_{ij} \right\}^{\frac{1}{2}} \Delta x_1 \Delta x_2 - \sum_{ij} \{ [DX_1(\rho)]_{ij} + [DX_2(\rho)]_{ij} \}^{\frac{1}{2}} \Delta x_1 \Delta x_2 \right] \quad \text{in } \Omega$$

$$\left[\left\{ \sum_{ij} [DX_1(\rho + \eta^{kl}\delta_\rho)]_{ij} + [DX_2(\rho + \eta^{kl}\delta_\rho)]_{ij} \right\}^{\frac{1}{2}} \Delta x_1 \Delta x_2 - \sum_{ij} \{ [DX_1(\rho)]_{ij} + [DX_2(\rho)]_{ij} \}^{\frac{1}{2}} \Delta x_1 \Delta x_2 \right] \quad \text{in } \Omega$$

aonde,

$$\eta_{ij}^{kl} = \begin{cases} 1 & \text{se } i = k, \quad j = l \\ 0 & \text{nos outros casos} \end{cases}$$

4.4 Solução das equações de E-L usando o método de "Adaptive Gradient Minimization"

O algoritmo pode ser descrito sumariamente como,

$$\text{set } \alpha = \alpha_L, \quad \rho = \rho_0$$

do until stopping criteria for $[\alpha]$

do until stopping criteria for $[\rho_{k+1}]$

set, $(\rho_{k+1}) = \rho_k - \xi_k^\alpha g^\alpha(\rho_k)$;

using $P^\alpha(\rho_{k+1}) = P^\alpha(\rho_k - \xi_k^\alpha g^\alpha(\rho_k)) = \min$

end do $[\rho_{k+1}]$

choose new α by decreasing criteria

end do $[\alpha]$

aonde α_L parâmetro de regularização, tomado para o problema sendo resolvido. Uma escolha muito grande do α_L fará o processo de minimização lento e uma escolha muito pequena de α_L fará o processo de minimização instável.

ρ_0 é o modelo *a priori*. Este é um ponto crítico do algoritmo. Usualmente esta informação é providenciada por levantamentos geológicos ou geofísicos prévios. Neste trabalho o objetivo são estruturas geológicas não-suaves.

A importância do modelo *a priori* (ρ_0), pode ser entendida se olharmos para o processo de regularização, como uma forma inteligente de introduzir informação para resolver o problema inverso mal-posto. Outra importante informação, pode ser introduzida através da escolha apropriada da função estabilizante, que melhor reflitam as propriedades da solução esperada.

O algoritmo de "adaptive gradient minimization" avalia a solução sempre em menos de um par de minutos no pior caso, usando uma estação de trabalho "DEC3100".

O código do programa foi escrito em Matlab altamente vetorizado. Uma interface amigável está em desenvolvimento.

Capítulo 5

Resultados

A figura 5.2 uma tentativa de recuperar a função densidade quando não é usada nenhuma regularização e o domínio da função é dividido em 240 blocos, tornando o problema altamente mal condicionado.

O resultado é esperado e mostrado na figura 5.2 , aonde a amplitude da função solução é correta, mas sem nenhum significado físico (geológico).

O resultado usando o operador da primeira derivada em 2D como apresentado no cap '3, é mostrado na figura 5.3 . Este resultado é um avanço importante na correta solução física do problema, quando comparado como 5.2 , mas falha em recuperar as características da função distribuição de densidade verdadeira.

Um novo avanço na recuperação das características quando a função da distribuição de densidade é não suave, é apresentada na figura 5.4, aonde foi utilizada a minimização da Variação Total da densidade na solução do problema inverso.

Uma imagem mais próxima da função não-suave original, foi possível ser recuperada, devido ao fato que a funcional de TV não penaliza as discontinuidades ou variações rápidas na solução.

A regularização convencional é fundamental para a obtenção de uma solução física viável. A regularização usando a norma de TV permite também a possibilidade

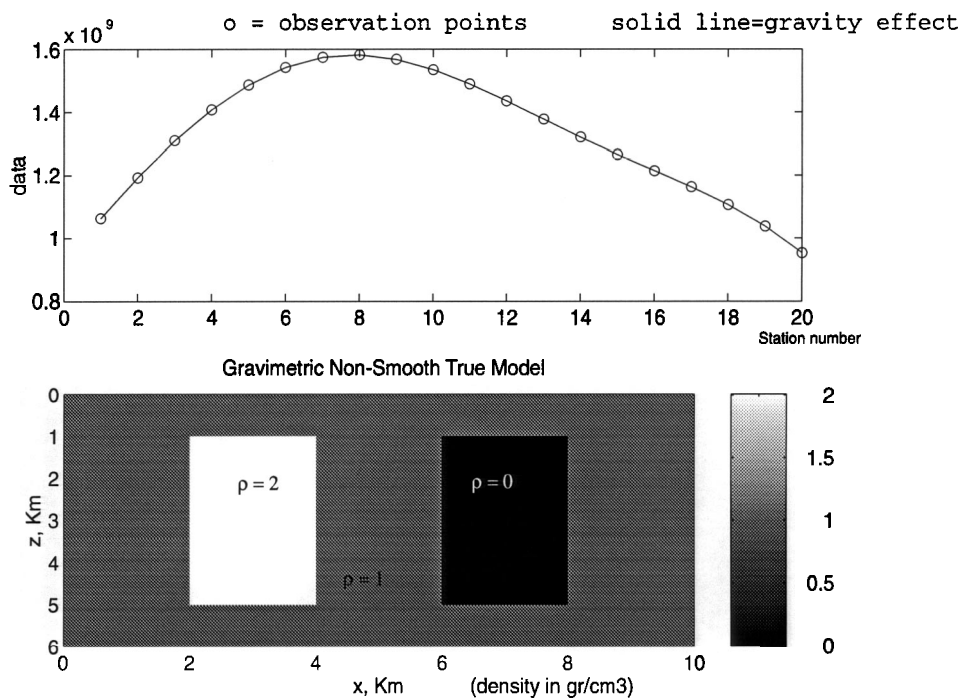


Figura 5.1: Distribuição de densidades do modelo verdadeiro

de reconstruir funções de densidade não suave, o que não era possível dentro das aplicações geofísicas até o presente.

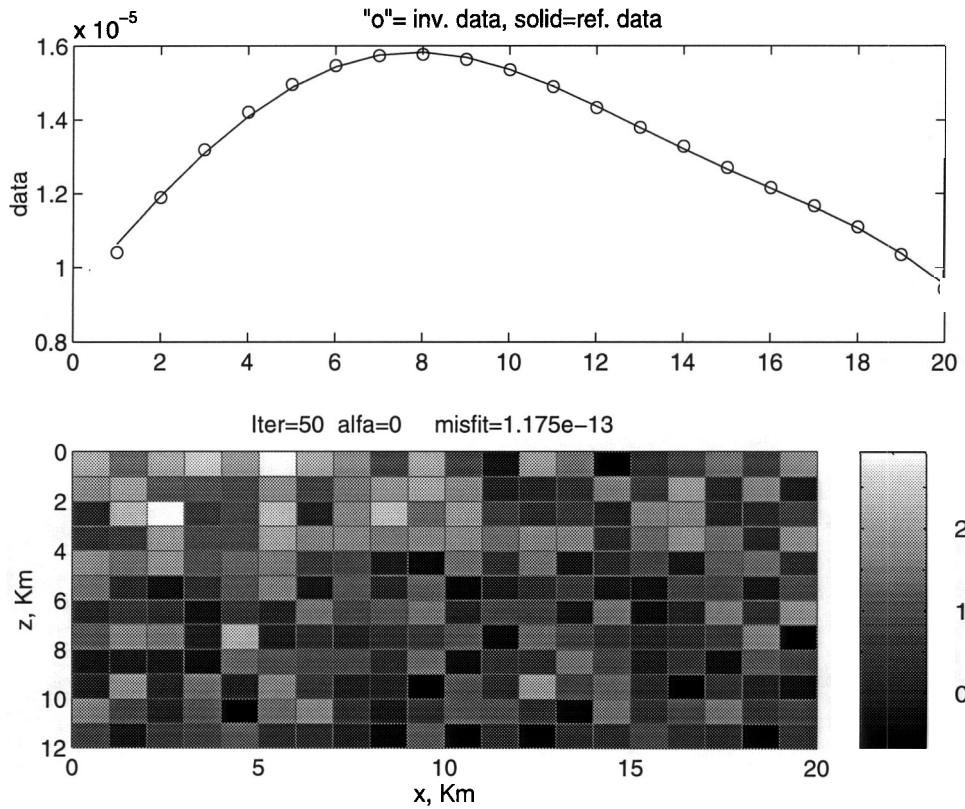


Figura 5.2: Solução sem regularização

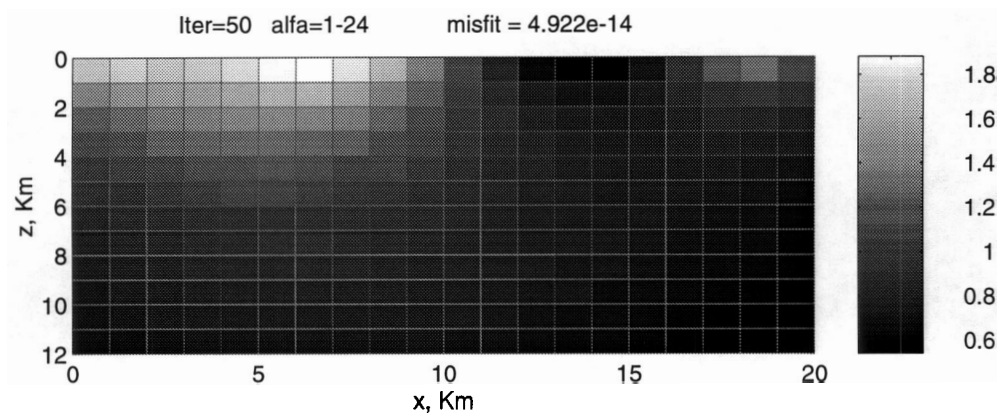
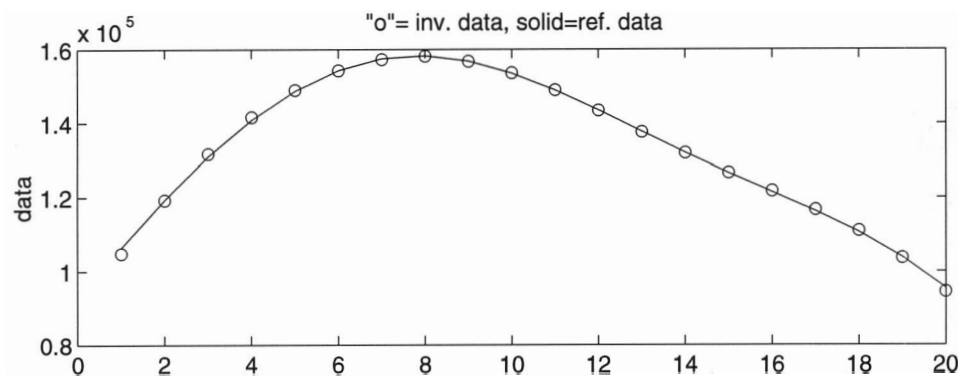


Figura 5.3: Solução usando a primeira derivada em 2D como Funcional Estabilizante

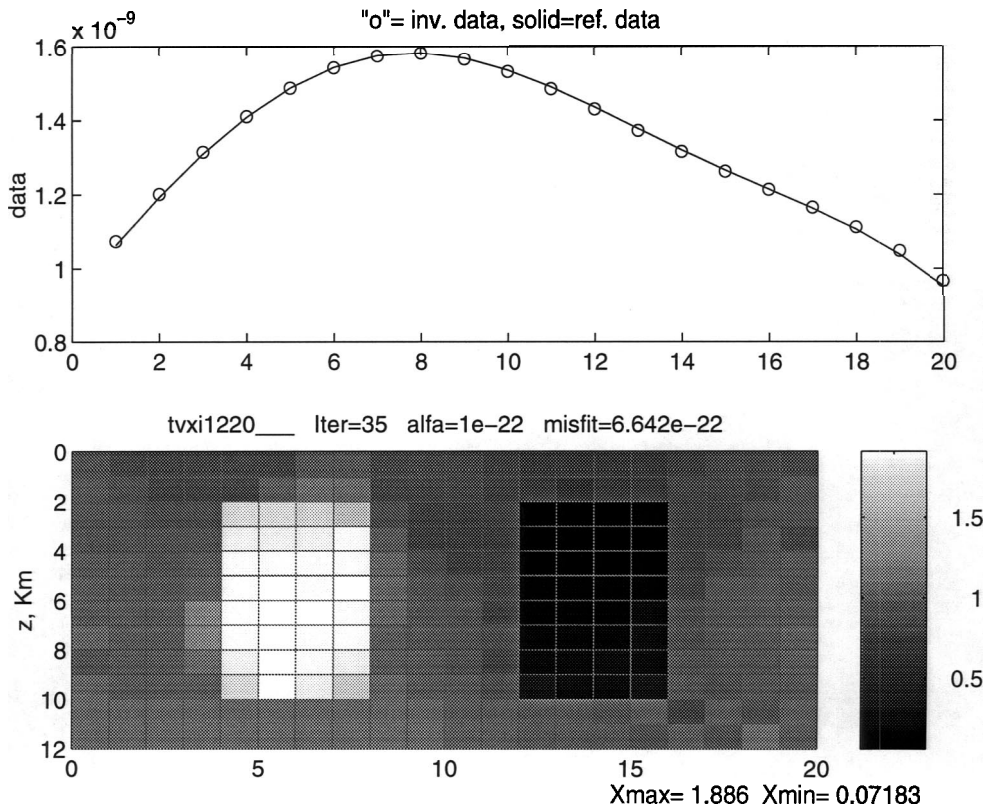


Figura 5.4: Solução usando a Variação Total em 2D como Funcional Estabilizante

Capítulo 6

Conclusões e Problemas em aberto

6.1 Conclusões

Uma forma de "definir" regularização, é *como uma forma inteligente de introduzir informação a priori no processo de inversão do problema físico mal posto*. O método de regularização proposto baseado na funcional de TV é uma ferramenta mais apropriada que os métodos convencionais quando o objetivo é recuperar soluções não-suaves.

Para o problema de inversão do potencial gravitacional, distribuições não suaves e com formas não-suaves, são melhor reconstruídas quando usada a norma de Variação Total da solução como funcional estabilizante, ao invés dos operadores de regularização standard.

Um algoritmo computacionalmente efetivo foi desenvolvido, usando uma aproximação discreta das equações de Euler-Lagrange do problema de inversão gravimétrica, evitando a solução de uma equação de derivadas parciais em cada iteração.

O algoritmo de "adaptive gradient minimization" foi implementado para resolver o problema numericamente, e mostrou ser eficiente para este tipo de problemas.

E mostrado que os resultados obtidos neste trabalho para o problema de inversão gravimétrica podem ser estendidos para outras aplicações geofísicas.

6.2 Problemas em aberto

a) Discretização e regularização ou regularização e discretização como estratégia de solução.

b) Um melhor entendimento dos efeitos da norma TV, além dos analisados neste trabalho.

c) Extensão para outras aplicações geofísicas.

d) Definição da norma de Variação Total Variação vetorial em problemas geofísicos não-lineares e anisotrópicos.

e) Algoritmos eficientes para problemas de grande porte.

Referências Bibliográficas

- [1] A. BASSREI, *Regularization and Inversion of 2-D Gravity Data*, Expanded Abstracts of 63th. Annual Meeting, S.E.G., Washington, D.C., September 26-30, 1993
- [2] A. ACAR AND C. VOGEL, *Analysis of bounded Variation penalty methods for ill-posed problems*, Inverse Problems 10, (1994), 1217-1229.
- [3] E. GIUSTI, *Minimal Surfaces and Function of Bounded Variation*, Birkhäuser, (1984).
- [4] D. R. ADAMS, *Function spaces and potential theory*, Springer-Verlag Berlin Heidelberg New York, (1991).
- [5] L. RUDIN, *Nonlinear Total Variation Based Algorithms*, Physica D, 60 (1992), pp. 259–268.
- [6] L. ALVAREZ, P. LIONS AND J. MOREL, *Image selective smoothing and edge detection by nonlinear diffusion*, SIAM J. Numer. Anal. Vol. 29- 3, (1992), pp. 845-866.
- [7] D. DOBSON AND F. SANTOSA, *Recovery of blocky images from noisy and blurred data*, Tech. Report No. 94-7, Center for the Mathematics of Waves, University of Delaware (1994).

- [8] T. F. CHAN, H. M. ZHOU, AND R. H. CHAN, *Continuation method for total variation denoising problems*, Advanced Signal Processing Algorithms, Vol. 2563, (1995).
- [9] C. R. VOGEL AND M. E. OMAN, *Fast Numerical methods for total variation minimization in image reconstruction*, Advanced Signal Processing Algorithms, Vol. 2563, (1995).
- [10] H. BERTETE-AGUIRRE, E. CHERKAEVA, AND A. FOGELSON, *Comparison between total variation regularization operators and standard regularization operators for gravimetric inverse problems*, Fourth SIAM Conference on Mathematical and Computational Issues in Geosciences, June 16-19, Albuquerque, New Mexico, (1997)
- [11] H. BERTETE-AGUIRRE, E. CHERKAEVA, AND A. FOGELSON, *Total variation methods for finding non-smooth solutions to the inverse gravimetric problem*, II PanAmerican Workshop in Applied and Computational Mathematics, Gramado, Brazil, September 8-12 (1997).
- [12] H. BERTETE-AGUIRRE AND A. XAVIER, *Mínimos cuadrados aplicados à inversão geofísica*, Coppe-Sistemas report, UFRJ, (1994).
- [13] A. N. TIKHONOV, *On the stability of inverse problems*, Soviet. Math. Dokl., 39 (1943), pp. 1035–1038.
- [14] A. N. TIKHONOV AND V. Y. ARSENIN, *Solutions of ill-posed problems*, Willey, N.Y., 1977.
- [15] M. M. LAVRENTIEV, V. G. ROMANOV AND S. P. SHISHASKY, *Ill-posed problems in mathematical physics and analyses*, Nauka, Moscow, 1980.
- [16] N. J. FISHER, AND L. E. HOWARD, *Gravity interpretation with the aid of quadratic programming*, Geophysics, 45 (1980), pp. 403–419.

- [17] C. SAFON, G. VASSEUR, AND M. CUER, *Some applications of linear programming to the inverse gravity problem*, Geophysics, 42 (1977), pp. 1215–1229.
- [18] W. M. TELFORD, L. P. GELDART AND, R. E. SHERIFF, *Applied geophysics*, 2nd ed., Cambridge University Press, Cambridge (1990)
- [19] G. H. GOLUB AND C. F. VAN LOAN, *Matrix computations*, 2nd ed., The Johns Hopkins University Press, Baltimore (1989)
- [20] J. WERMER, *Potential theory*, Lecture Notes in Mathematics 408, (1974).
- [21] H. AIKAWA AND M. ESSEN, *Potential theory - Selected Topics*, Lecture Notes in Mathematics 1633, (1996).
- [22] O. P. GUPTA, *A least-squares approach to depth determination from gravity data*, Geophysics, 48, (1983), pp. 357-360.
- [23] E. M. ABDELRAHMAN, A. I. BAYYOUMI AND H. M. EL-ARABY, *A least-squares minimization approach to invert gravity data* , Geophysics, 56, (1991), pp. 115-118.
- [24] M. AL-CHALABI, *Some studies relating to nonuniqueness in gravity and magnetic inverse problems* , Geophysics, 36, (1971), pp. 835-855.
- [25] F. GUSPI, *Noniterative nonlinear gravity inversion*, Geophysics, 58, (1993), pp. 935-940.
- [26] C. T. BARNET, *Theoretical modeling of the magnetic and gravitational fields of an arbitrarily shaped Three-Dimensional Body* , Geophysics, 41, (1976), pp. 1353-1364.
- [27] R. E. CHAVEZ AND G. D. GARLAND, *On the application of the inverse theory to gravity interpretation* , Geophysics, 31, (1983), pp. 119-130.

- [28] D. W. OLDENBURG, *The inversion and interpretation of gravity anomalies*, Geophysics, 39, (1974), pp. 526-536.
- [29] G. D. GARLAND, *The earth's shape and gravity*, Pergamon Press, London 1965
- [30] A. BJÖRCK, *Numerical methods for least squares problems*, SIAM, Philadelphia, (1996).
- [31] C. L. LAWSON AND R. J. HANSON, *Solving least squares problems*, Prentice Hall, Englewood Cliff, NJ, (1995).
- [32] C. L. LAWSON AND R. J. HANSON, *Solving least squares problems*, Classics in Applied Mathematics, SIAM, Philadelphia, (1995).

**RECONSTRUCTION OF NON-SMOOTH
SOLUTIONS OF ILL-POSED GEOPHYSICAL
INVERSE PROBLEMS**

by

Hugo Bertete Aguirre

A dissertation submitted to the faculty of
The Federal University of Rio de Janeiro
in partial fulfillment of the requirements for the degree of

Doctor of Science

Department of Computing System Engineering

The Federal University of Rio de Janeiro

August 1997

Copyright © Hugo Bertete Aguirre 1997

All Rights Reserved

THE DEPARTMENT OF COMPUTING SYSTEM ENGINEERING

SUPERVISORY COMMITTEE APPROVAL

of a dissertation submitted by

Hugo Bertete Aguirre

This dissertation has been read by each member of the following supervisory committee and by majority vote has been found to be satisfactory.

Chair: Prof. Paulo Roberto Oliveira, Ph.D.

Prof. Elena Cherkaeva, Ph.D.

Prof. Michael Oristaglio, Ph.D.

Prof. Nelson Maculan Filho, Ph.D.

Prof. Amin Bassrei, Ph. D.

Prof. Adilson Xavier, Ph. D.

ABSTRACT

This thesis analyzes analytically and numerically the geophysical inverse problem of gravimetry, which is the recovery of density variations in the earth from measurements of its gravity field on the surface or in boreholes. This inverse problem does not have a non-unique solution. Standard regularizing operators used for its solution and for the solution of other geophysical inverse problems tend to produce smooth models. I propose instead the use of the Total Variation norm (TV) for reconstruction of blocky structures in geophysics. Numerical simulations of the different regularization schemes suggest that an inversion based on the TV norm can effectively recover piecewise constant density functions which is usually not possible with conventional methods. An efficient algorithm minimizing the TV norm can be obtained by regularized adaptive gradient minimization of a discretized TV operator. Numerical results inverting 2D blocky structures using this algorithm allows to recover sharp density contrasts and edges present in the true model.

To the memory of my grandfather

CONTENTS

ABSTRACT	iv
LIST OF FIGURES	viii
LIST OF TABLES	x
ACKNOWLEDGEMENTS	xi
CHAPTERS	
1. EXTENDED ABSTRACT OF THE WORK	1
1.1 Structure of the thesis	2
1.2 Introduction	4
1.3 Gravimetric Forward Models	6
1.4 The inverse gravimetric problem	9
1.5 Ill-Posed Problem	11
1.5.1 Noisy data	11
2. SOLUTIONS FOR THE INVERSE GRAVITY PROBLEM	14
2.1 No Regularization	14
2.2 General Smooth Regularization	14
2.2.1 Tikhonov Regularization	15
2.2.1.0.1 Regularized Minimization Problem, Tikhonov Ap- proach	16
2.2.2 Smoothing Stabilization Functional	17
2.3 Regularized non-linear gradient minimization	18
2.3.1 Euler Lagrange Equations	18
2.3.2 Gradient technique	19
2.3.2.1 Euler Lagrange Equations for gravitational problem	20
2.4 Choosing the regularization parameter	21
2.5 Discrete inverse gravimetric problem	21
2.5.1 Regularized Gravimetric Minimization Problems	22
2.5.2 Regularized Direct solution	22
2.5.3 Analysis of the discrete Tikhonov solution	23
2.5.4 Derivation of GSVD of Tikhonov solution	25
3. NON-SMOOTH ALTERNATIVE REGULARIZATION	35
3.1 Previous Reference Work	35
3.1.1 Inverse Gravitational Problem for a non-smooth density function	38
3.2 Definition of Bounded Variation seminorm or Total Variation (TV) .	38

3.2.1	TV for continuous functions	39
3.2.2	TV for discontinuous functions	39
3.3	TV minimization for the inverse gravity problem	42
3.3.1	Regularization and Discretization	43
3.3.2	Euler-Lagrange Equations for the $P_{TV}^\alpha(\rho, b)$ problem	43
4.	DISCRETIZATION AND REGULARIZATION	46
4.1	Discretization of the forward operator	46
4.2	Discretization of the TV semi-norm	49
4.2.1	Discrete horizontal and vertical derivative operators	52
4.3	Discrete calculation of variation of the TV semi-norm	54
4.4	Solving the Euler-Lagrange equations	55
5.	ANALYSIS OF THE NUMERICAL RESULTS	60
5.1	Model considerations	60
5.2	General Inversion results for large discretizations	60
5.2.1	Comparison of the inversion schemes	66
5.2.2	Smooth regularization results	66
5.2.3	Non-smooth regularization results	74
5.2.4	Large Discretization	74
5.2.5	Reduced discretization	74
5.3	Application of TV method to noisy data	81
6.	CONCLUSIONS AND FURTHER WORK	86
6.1	Extension to other geophysical problems.	86
6.2	Conclusions	88
6.3	Further Work	89
	REFERENCES	90

LIST OF FIGURES

1.1 Gravimetric Model Scheme	7
1.2 Gravitational attraction due to a density distribution ρ	7
1.3 Inverse Gravimetric Scheme	10
1.4 Instability of the inverse gravimetric operator	12
2.1 Regularized operator for the gravimetric problem	29
2.2 regularization parameter choice	30
2.3 Exponential decay of singular values of K (60×20)	31
2.4 Singular values and first left and right singular vectors of the discretized operator K (8×20)	32
2.5 Singular values and first left and right singular vectors of the discretized operator K (8×20) corresponding to the second singular value	33
2.6 Singular values and first left and right singular vectors of the discretized operator K (8×20) corresponding to the last singular value	34
3.1 Denoising problem, example 1	36
3.2 Denoising problem, example 2	37
3.3 1D continuous example	40
3.4 1D discontinuous example	41
4.1 Discretization using rectangular blocks	47
4.2 Quantities for calculation of a prism gravity effect	50
4.3 Row and Column order in the 2D discretization	51
4.4 Convergence results	59
5.1 Non-Smooth density model	62
5.2 Solution for a Non-Regularized scheme	63
5.3 Solution for a 2D First Derivative scheme	64
5.4 Solution for a 2D Total Variation Scheme	65
5.5 True initial density function	68
5.6 Minimum Norm Stabilizer, second iteration	69
5.7 2D First Derivative operator, third iteration	70

5.8 Intermediate smooth iteration (2D grad. stabilizer)	71
5.9 Minimum Norm Stabilizer, final iteration	72
5.10 2D First Derivative operator, final iteration	73
5.11 TV semi-norm Stabilizer, starting model (240 cells)	75
5.12 TV semi-norm stabilizer, intermediate iteration (240 cells)	76
5.13 TV semi-norm stabilizer, final solution (240 cells)	77
5.14 TV semi-norm Stabilizer, starting model (60 cells)	78
5.15 TV semi-norm stabilizer, intermediate iteration (60 cells)	79
5.16 TV semi-norm stabilizer, final solution (60 cells)	80
5.17 Fault model with noisy gravity data	82
5.18 Inversion result, fault model with noisy data	83
5.19 Oil reservoir model with noisy gravity data	84
5.20 Inversion result, oil reservoir model with noisy data	85

LIST OF TABLES

ACKNOWLEDGEMENTS

I wish to acknowledge and thank my advisors, Professor Paulo Roberto Oliveira from the Computing and System Sciences at the Federal University of Rio de Janeiro and Professor Elena Cherkaeva, from the Department of Mathematics at the University of Utah for their support and valuable help to complete my academic and thesis work.

I would like to thank Professor Aaron Fogelson from the Mathematics Department at the University of Utah, who provided me with fruitful discussions during the development of the numerical scheme presented in chapter 3.

I also want to express my deep appreciation for the help received from Professor Alan Tripp from the Department of Geology and Geophysics at the University of Utah and Professor Michael Oristaglio from Schlumberger Doll Research, for their encouragement and support of this research.

I would also like to express my gratitude to Professor Nelson Maculan Filho, Professor Luis Paulo Viera Braga and Professor Adilson Xavier, for their encouragement and help during my academic time at the Computing and System Sciences Department at the Federal University of Rio de Janeiro.

Professor Amin Bassrei from the Geophysics Department of Bahia Federal University and Professor Curtis Vogel from the Mathematics Department of State Montana University provided me with much information and helpful discussions during the development of this work, I wish to thank them.

Thanks also are due to my professors and colleagues from the Optimization group at the Federal University of Rio de Janeiro, Department of Geology and Geophysics and Department of Mathematics at the University of Utah.

The research in this thesis was supported in part by the CNPq and Schlumberger Doll Research.

CHAPTER 1

EXTENDED ABSTRACT OF THE WORK

Inverse problem of gravimetry is to determine the density distribution in the earth from measurements on its Gravity field (or its derivatives) on the surface or in boreholes. It is well known to be non-unique in its general form. Discrete numerical formulations which can be unique are often ill-posed - a small variation in data can cause very large variation in the solution.

Since, data can only be obtained at a discrete number of points and are contaminated with noise, the inverse problem needs regularization.

Different regularization techniques commonly used for solution of this inverse problem, and others inverse problems give reasonable solutions; however, they fail to recover non-smooth density functions.

I propose to use the Total Variation norm (TV) as a stabilization functional in a Tikhonov regularization scheme for reconstruction of blocky geophysical structures (i.e. piecewise constant density models).

We show for a number of models in geophysics that the minimization of Total Variation norm permits reconstruction of sharp density contrast, which is not possible with conventional regularization methods. This new approach is a promising research area since recover of non-smooth solutions to geophysical inverse problems has economically important application in exploration for ore bodies, detection of faults, mapping the shape of oil reservoirs, and in geotechnical surveying.

We developed an alternative scheme to solve the Tikhonov parametrical functional with a TV stabilizer for the inverse gravitational problem, having the advantage to avoid to solving a partial differential equation on each iteration, as did the

procedures that have been used before in image denoising. The algorithm is based on discretizing the original problem first and then regularizing.

A regularized adaptive gradient minimization algorithm is presented to solve the Tikhonov parametrical functional with a TV stabilizer.

Finally an extension to other geophysical problems is shown, presenting the basic background involved in the construction of the forward operator for the other two main areas in geophysics, electromagnetic and seismic. It can be seen that electromagnetic and seismic problems can be reduced to an analogous operator equation as for the inverse gravimetric problem studied in this thesis. Hence we expect that the results of the research are applicable in these situations as well.

1.1 Structure of the thesis

In chapter one we introduce the problem. We present the concepts for the evaluation of the forward operator for the gravitational potential problem. We discuss the inverse gravimetric problem and the special features of the inverse operator. It is shown that the problem has non-unique solution and that the solution does not depend continuously on the data. Therefore it is ill-posed in the Hadamard sense. In the situation when the available data are discrete and contaminated with noise, its solution requires application of regularized technique.

In chapter two, we analyze analytically and numerically the inverse problem of gravitational potential. We introduce the Tikhonov regularization operator and the common stabilization functionals in use in geophysics to solve the inverse problem, which are quite efficient for reconstruction of smooth solutions, however they fail to recover non-smooth functions.

We introduce the adaptive minimization basis for the minimization algorithm for the Tikhonov parametrical functional and show how the regularization parameter can be chosen.

In chapter three, we present an alternative regularization. For non-smooth functions we introduce the Total Variation semi-norm and describe previous works in image processing. We illustrate the TV semi-norm for a 1D continuous and discontinuous functions.

We present the 3D inverse gravity problem (where the function density is constant in one direction) when use the TV stabilization functional.

We discuss a technique used in all denoising problems which ends up with a partial differential equation.

In chapter four, we present an alternative solution scheme for the solution of the inverse gravity problem with a TV stabilizer, discretizing the parametrical functional and then regularizing the obtained finite dimensional operator. We present the discretization of the forward operator, the discrete derivative operators in both (x_1, x_2) directions, build the discrete Total Variation operator and the discrete first variation of the discrete TV operator.

We present an adaptive gradient minimization technique to solve the discrete Euler-Lagrange equations, avoiding solution of a PDE in each step of iteration as in the previous approaches.

In chapter five we analyze the numerical results. We use a simulated example of density distribution (Bassrei, 1993 [1]) with sharp edges and sharp contrast, which make this function ideal to evaluate results from the different inversion schemes.

We show an unphysical result, when no regularization is applied. We show the improvement obtained in the results, when used a smoothing criteria, like the 2D first derivative stabilization functional. For large discretization the solution is stable and is more close to the true function, however fails to reconstruct the sharp features of the original density distribution function.

We show the result obtained when the minimization of the total variation of the density function is performed, bringing the non-smooth features that were not able to be recovered with the standard regularization techniques. This result represents an important advance in the geophysical inversion schemes, since many practically important density distributions are non-smooth functions.

To better illustrate and compare the numerical results obtained in the different inversion schemes, we present the results of a sequence of iterations obtained during the inversion process for different inversion algorithms for the same problem, using the true model as a starting point. These numerical results obtained in the different

inversion schemes, show how the initial solution is destroyed when smoothness is imposed by stabilizing operators. On the other hand, results show how TV stabilizer preserves the initial information during the inversion process, denoises it and fits the observed data.

We analyze the monitoring result of the implemented adaptive gradient minimization in several situations, showing the algorithm performance in terms of the number of iterations.

In chapter six we present the conclusions of this thesis and the further research to be done in the direction of this work, which represents the first step in the recovering non-smooth density functions for the inverse problem of gravitational potential.

Finally, we discuss the extension of this work for other fields in geophysics.

1.2 Introduction

In this work we study the inverse gravimetric problem. Geological structures such as a mineral deposit, an oil reservoir, a fault, a geotechnical structure, etc., having different density than the background earth, generate a gravitational field which changes slightly the gravitational field of the earth. This difference in gravitational field is noticeable on the surface of the earth and can be measured. It is called gravitational anomaly due to the underground body.

The forward gravimetric problem is to calculate the gravity anomaly generated by the underground body when the location of the body and its density contrast are known. The solution of this problem helps to build more accurately instruments that fit the necessary requirements and can be used in comparing anomalies caused by different gravimetric bodies. The opposite problem which is known as the inverse problem in geophysics is to recover the location of the body and its density distribution from measured gravitational anomaly due to this underground body.

More generally, the forward problem in geophysical research consists in the study of the response of a media with certain physical properties to different kinds of natural or artificial excitations. The most important geophysical fields are gravitational, magnetic, electromagnetic and seismic. These fields depend primary

on the physical properties of the media (for example, properties of the rocks in an underground study). The inverse problem is to determine the physical properties of the medium from measurements of its response to different natural or artificial excitations.

Different geophysical methods are available today for solution of the forward and inverse problems, which are one of the main interest in the geophysics research.

In this work we study the inverse gravimetric problem and, especially, reconstruction of non-smooth functions from the data in the presence of noise. The basis of the theory of gravity fields was established in 1782 when Marquis de Laplace showed that the Newtonian potential (ϕ) outside a body obeys a differential equation which is called now Laplace equation,

$$\nabla^2 \phi = 0$$

Inside of the body the potential (ϕ) satisfies the Poisson equation.

$$\nabla^2 \phi = -4\pi\gamma\rho \tag{1.1}$$

where γ is the Gravitational Constant and $\rho(x)$ is the density function of the medium. When the function $\rho(x)$ is known this equation describes the forward problem for gravitational potential.

The analytical solution for the Poisson equation (1.1) is given by the Green's Theorem. For a given density $\rho(x)$ the potential (ϕ) at point y is,

$$\phi(y) = \int_{\Omega} \rho(x) G(y, x) dx \tag{1.2}$$

where $G(y, x)$ is the solution for a point mass and Ω is the domain of integration corresponding to the underground domain.

The equation (1.2) is a particular case of a Fredholm integral of the first kind and describes the forward formulation for the gravimetry problem, or operator equation of the first kind ([4]),

$$\phi = K (\rho) \quad (1.3)$$

where the operator K is defined by equation (1.2). A more detailed derivation for the gravimetric problem will be approached in the next sections.

1.3 Gravimetric Forward Models

In this work we want to determine the location and shape of a blocky structure in the subsurface. The previous works dealing with gravimetric inverse problem developed effective and stable algorithms of solution of problem when the density function is smooth, for example [1].

In the contrast, we are not interested in structures that present smooth changes in densities or bodies without sharp shapes in the structure.

Blocky structure is an often encountered object among geological and geotechnical structures, examples are faults, mineral deposits, dikes, etc..

The methods developed previously for solutions of inverse problems give good results when recovering geological models where can be imposed smoothness of the solution, however, they fail to recover non-smooth density function distributions.

Our model is schematically represented in fig. 1.1.

The forward problem is to calculate the gravitational potential generated on the surface by the underground distribution of mass. The corresponding operator is (1.3).

We can consider a continuous distribution of mass as a collection of individual infinitesimal masses. The gravitational potential of a collection of masses is the sum of the gravitational attraction of the individual masses (superposition principle). The attraction of two particles is stated by Newton law, so we can write the potential of a body (figure 1.2) with density function ρ in the domain Ω , as

$$\phi(x', y', z') = \gamma \int_{\Omega} \frac{1}{r} dm = \gamma \int_{\Omega} \frac{\rho(x, y, z)}{r} dv \quad (1.4)$$

where dm is the mass of an element of the volume dv , $dv = dx dy dz$.

The gravitational field is the gradient of the potential,

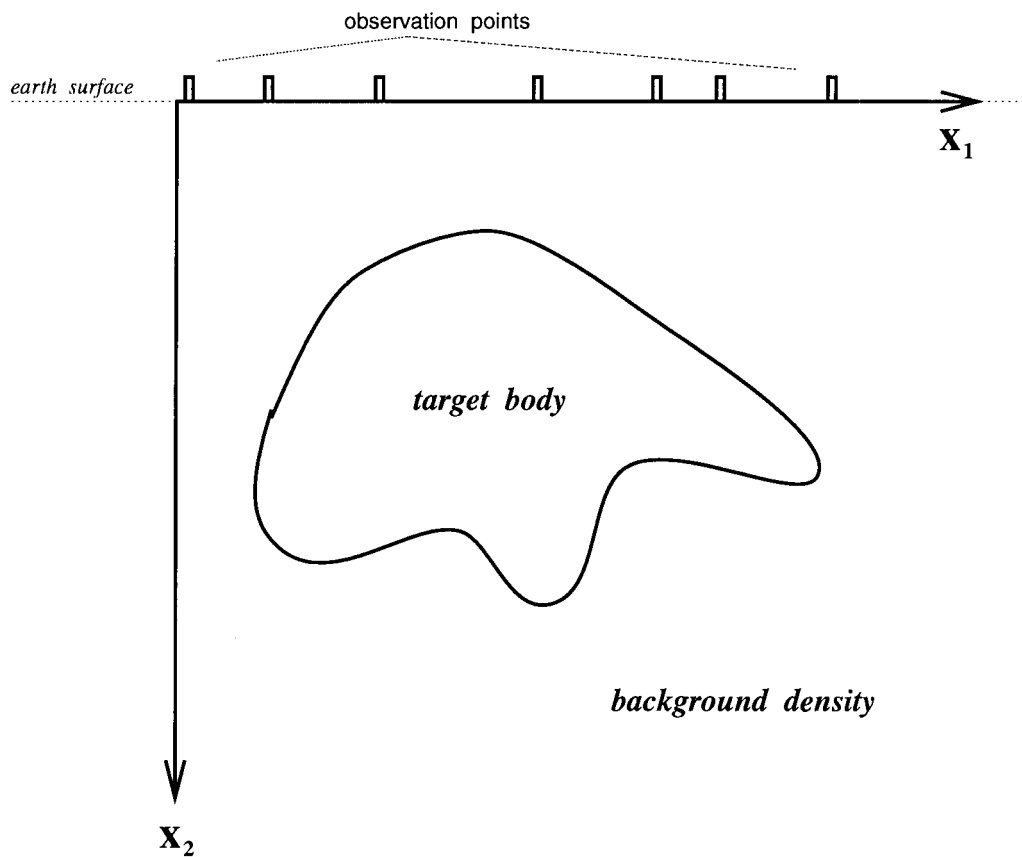


Figure 1.1. Gravimetric Model Scheme

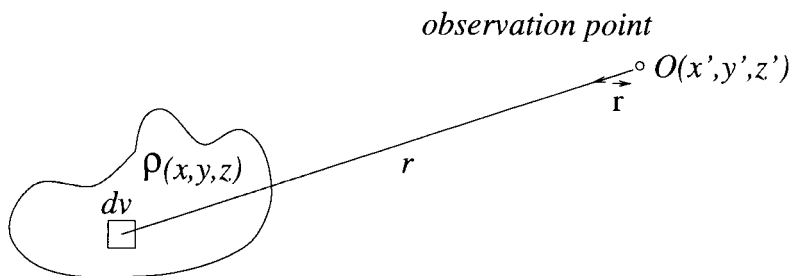


Figure 1.2. Gravitational attraction due to a density distribution ρ .

$$F = \nabla\phi$$

The component F_i of the vector field F in any direction \vec{i} is equal to the derivative of the potential ϕ (work) in that direction, then in a Cartesian coordinate system the field in the x direction is

$$F_x = \frac{\partial\phi}{\partial x} = -\gamma \int_{\Omega} \rho(x, y, z) \frac{\partial}{\partial x} \frac{1}{r} dv$$

analogously, we can obtain the component in the y direction,

$$F_y = \frac{\partial\phi}{\partial y} = -\gamma \int_{\Omega} \rho(x, y, z) \frac{\partial}{\partial y} \frac{1}{r} dv$$

and in the z direction

$$F_z = \frac{\partial\phi}{\partial z} = -\gamma \int_{\Omega} \rho(x, y, z) \frac{\partial}{\partial z} \frac{1}{r} dv$$

The function r is the distance from the observation point (x', y', z') to the point (x, y, z) inside the body,

$$r = \sqrt{(x' - x)^2 + (y' - y)^2 + (z' - z)^2}$$

Taking derivative of the function r we obtain

$$-\frac{\partial}{\partial x} \frac{1}{r} = \frac{(x' - x)}{r^3},$$

$$-\frac{\partial}{\partial y} \frac{1}{r} = \frac{(y' - y)}{r^3},$$

$$-\frac{\partial}{\partial z} \frac{1}{r} = \frac{(z' - z)}{r^3}$$

Adding the three components of the field we obtain

$$F(x', y', z') = \nabla\phi = F_x \vec{i}_x + F_y \vec{i}_y + F_z \vec{i}_z$$

or

$$F = -\gamma \int_{\Omega} \frac{1}{r^3} \left[(x - x') \vec{i}_x + (y - y') \vec{i}_y + (z - z') \vec{i}_z \right] \rho(x, y, z) dv \quad (1.5)$$

This is the total gravity field at the point (x', y', z') for a given mass distribution.

Let \vec{r}' be the unit vector

$$\vec{r}' = \frac{\left[(x - x') \vec{i}_x + (y - y') \vec{i}_y + (z - z') \vec{i}_z \right]}{r}$$

Substituting this expression in (1.5) we obtain the final expression for the total gravity vector for a given anomalous mass.

$$F = \gamma \int_{\Omega} \frac{1}{r^2} \rho(x, y, z) \vec{r}' dv \quad (1.6)$$

Calculation of F for a given density function ρ is called the gravitational forward problem.

1.4 The inverse gravimetric problem

The inverse gravimetric problem is the following: given some observations of the gravity field, we want to determine the density function generating this gravitational field. Most gravimeters used in geophysical exploration do not measure the vector field F , they measure instead the variation in the vertical component of the total field (1.6). Hence the observed field gravity data are measurements of z -component of the gravitational field.

Then the inverse gravimetric problem is to determine the unknown density function from measured vertical derivative of the potential:

$$\text{observed_field_data}(z') = -\gamma \int_{\Omega} \frac{1}{r^3} (z - z') \rho(x, y, z) dv \quad (1.7)$$

The inverse gravimetric problem is illustrated in Figure 1.3. In operator form:

$$b = K_{grav} \rho \quad (1.8)$$

where b is measured vertical component of the field and K_{grav} is an integral operator (1.7). Hence the inverse problem for the gravitational potential can be

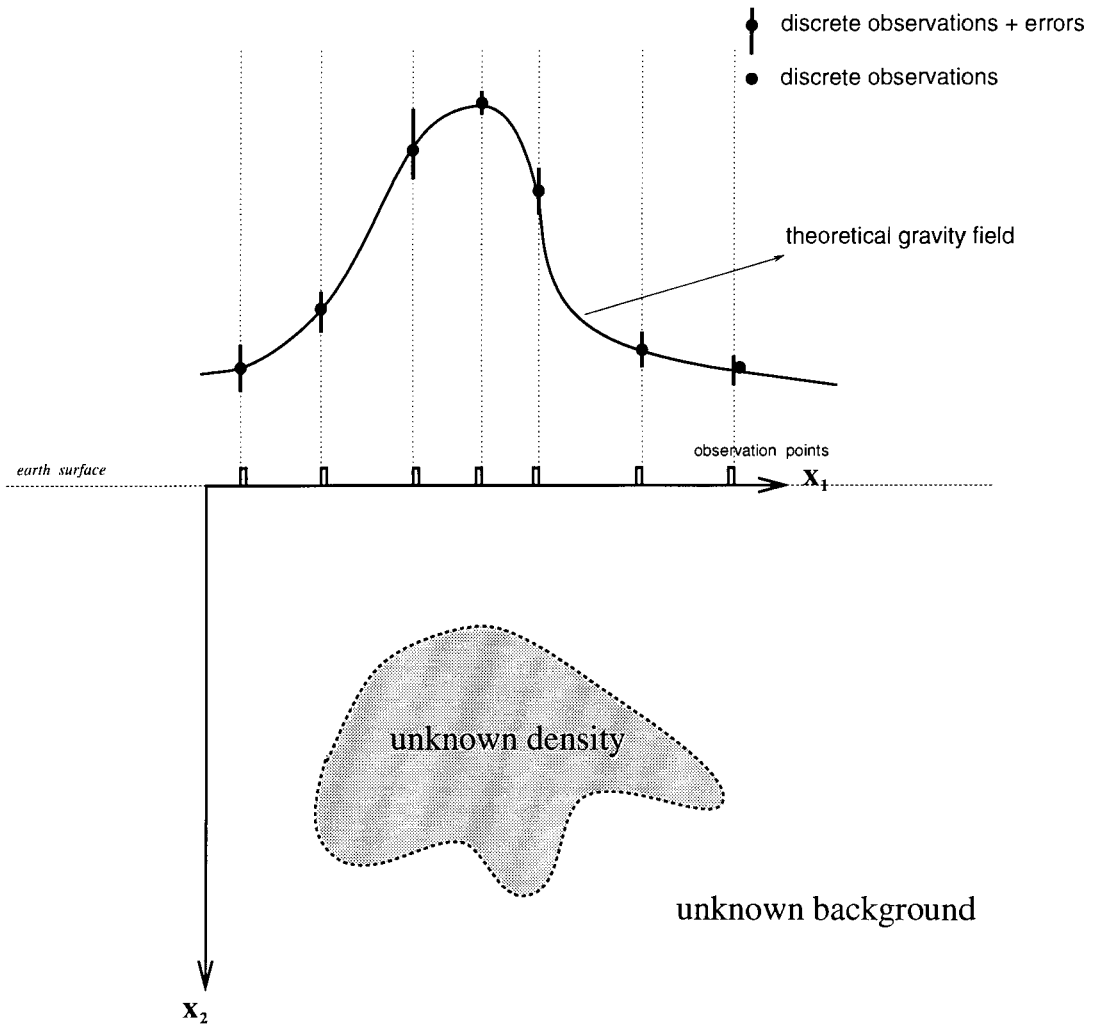


Figure 1.3. Inverse Gravimetric Scheme

formulated as an inverse problem for a completely continuous operator. Unfortunately it can be shown ([4]) that the inverse operator K^{-1} is not continuous. This implies that the solution (ρ) does not depend continuously on the measured vertical component of the gravitational field.

1.5 Ill-Posed Problem

According to (Hadamard, 1923) a mathematical model for a physical problem is well posed if:

- 1) The solution to the problem exists (existence)
- 2) There is only one solution to the problem (uniqueness)
- 3) The solution continuously depends on the data (stability)

The solution for the equation (1.8) fails the third condition (stability), as well as the second (uniqueness). This is illustrated in figure 1.4.

Hence the gravity problem is ill-posed in the Hadamard sense. In this work we will concentrate on recovering a feasible physical solution when the problem is unstable. Also, the lack of stability can be considered as the most important obstacle for the solution of equation (1.8). The existence of the solution can be obtained by enlarging the solution space, and uniqueness, by increasing the restriction to the solution, but the lack of stability will require changes on the topology of the spaces. The theoretical background for the understanding and solution of ill-posed problems was stated by Tikhonov in 1943 [13] and in many publications by different researchers since then. In our work we will use Tikhonov approach for the solution of (1.8).

1.5.1 Noisy data

In this work we want to recover the density function distribution from an observed data. The first consideration is that any instrument used to measure these responses have limited accuracy, hence we have

$$\textit{observed_data} = \textit{theoretical_data} + \textit{instrument_error}$$

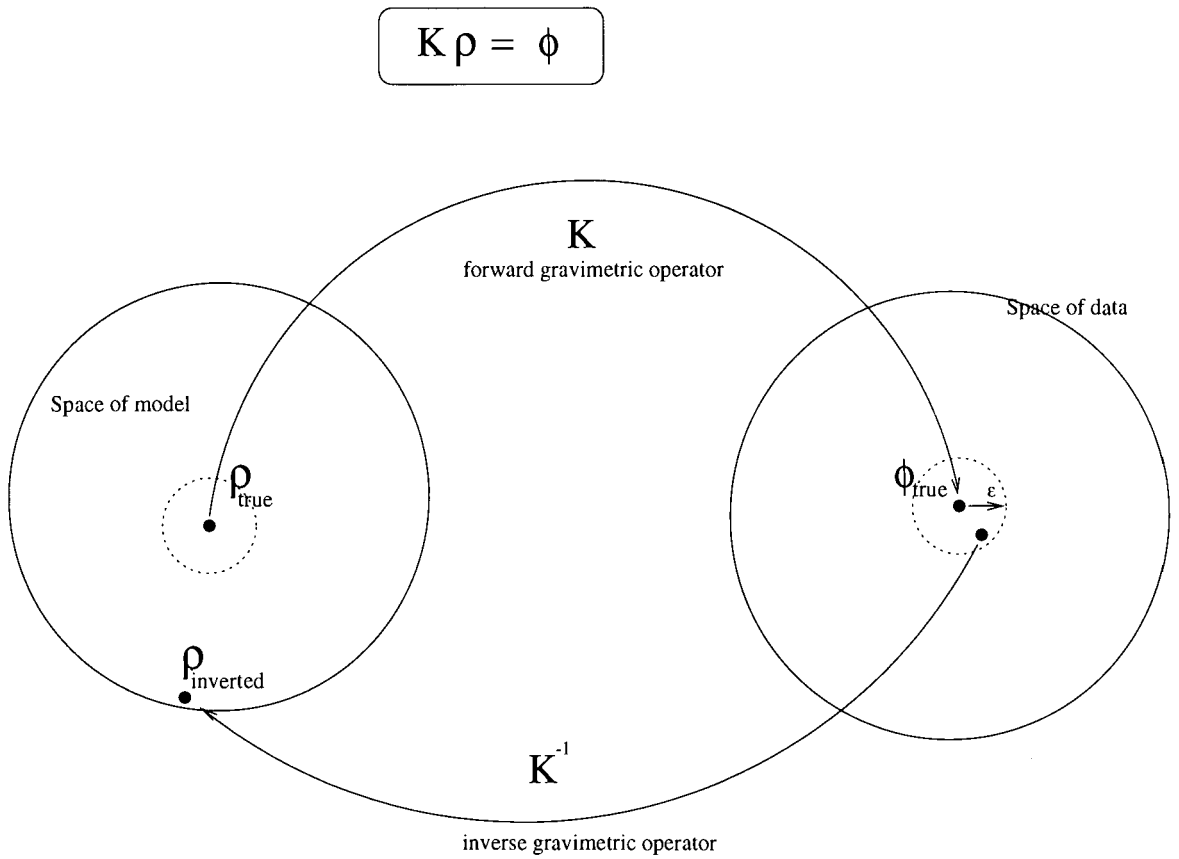


Figure 1.4. Instability of the inverse gravimetric operator

In practice, the observed readings are subject to many other sources of error, such as error of positioning, measuring fields components slightly deviated from the vertical, cultural noise, etc.. We just write

$$\textit{observed_data} = \textit{theoretical_data} + \textit{noise}$$

where the noise term is the sum of contribution of errors from different sources. In most real situations there is not available much information about the noise characteristics in the observed data, due to the complexity involved in the field reading operation process. In our work, we will consider that the noise level is bounded by a known value (ϵ) as the only assumption.

Then our inverse problem now can be written as

$$K(\rho) = b + b_\epsilon \tag{1.9}$$

with $\|b_\epsilon\| = \epsilon$.

Operator equation (1.9) is ill-posed (Lavrentev, [15]). This means that in the presence of a noise of small amplitude, we obtain a solution far away from the true one, due to the instability of the inverse operator K^{-1} . The problem requires a special technique for its solution.

CHAPTER 2

SOLUTIONS FOR THE INVERSE GRAVITY PROBLEM

2.1 No Regularization

The inverse gravimetric problem was developed intensively in the 60's, when potential methods were in use in exploration geophysics [29], due to the fact that these methods were not very expensive and they gave good structural information about the subsurface. Since then, many regularization and optimization techniques were introduced to solve different types of inverse gravimetric problems. Most of the published works up to 1977 discussed mainly Minimum Least Square approaches. Then later papers were presented which used Linear Programming to solve this problem [17]. Later in 1980 some works solving the inverse gravimetric problem were published using Quadratic Programming [16].

One of the important references for the ill-posed problems arising in mathematical models of physical problems was presented in Tikhonov, 1977 [14]. Since then many inverse gravimetric schemes were approached using the term "general smooth regularization".

2.2 General Smooth Regularization

The main idea behind regularization is to find the solution of the inverse problem transforming one ill-posed inverse problem, given by the operator equation (1.9)

$$K(\rho) = b, \quad \rho \in X, \quad b \in D \tag{2.1}$$

where X and D are Hilbert spaces of density functions and the data, respectively, and $b = b_{true} + b_{noise}$, with $\|b_{noise}\| = \epsilon$

in a sequence of well posed inverse problems depending on a parameter (α), with the property that when ($\alpha \rightarrow 0$) the solution ($\rho^\alpha \rightarrow \rho$). In other words regularized algorithm of solution of (1.9) provides a stable solution such that small variations in the data generate small variations in the solution.

We will introduce some concepts for the understanding of this work, but the complete theoretical details can be found in [14].

2.2.1 Tikhonov Regularization

Let distance between functions b and b_{true} in the space of data D be $\rho_D(b, b_{true})$ and distance between the models ρ and ρ_{true} in the space of models X be $\rho_X(\rho_\alpha, \rho_{true})$.

Definition

An operator $R(\rho, \alpha)$, α being a scalar parameter, is called the regularizing operator in some vicinity of the element $b_{true} = K(\rho_{true})$ if there exist a function $\alpha(\delta)$ such that for any $\epsilon > 0$ it can be found a positive number $\delta(\epsilon)$ such that if

$$\rho_D(b, b_{true}) < \delta(\epsilon)$$

then

$$\rho_X(\rho_\alpha, \rho_{true}) < \epsilon$$

where

$$\rho_\alpha = R(b, \alpha(\delta)) \tag{2.2}$$

and it is illustrated in (figure 2.1).

Then the problem of finding an approximate solution for the inverse ill-posed problem (2.1) is reduced to constructing a regularization operator (2.2) and solving the problem for this operator (figure 2.1). Having introduced supplementary information about the solution, a regularizing operator can be constructed substituting the original ill-posed problem (2.1) by a sequence of well posed equations

$$K_\alpha(\rho) = b$$

where the inverse operators K_α^{-1} are continuous.

The regularization parameter α , can be obtained from the amplitude of the noise in the data. A method of construction of a regularized operator was developed in Tikhonov which is based on selection of *Stabilization Functional*.

Definition

Let $J(\rho)$ be a non negative functional in some metric space (X) . $J(\rho)$ is called *Stabilization Functional*, if for every number $m > 0$, the subset of elements ρ in X for which $J(\rho) < m$ is a compact set of (X) and contains the solution (ρ_{true}) .

The main application of the Stabilization Functional is to select from all possible solutions the ones that continuously depend on the data so that the problem can be reduced to the problem of minimization of stabilization functional on the correctness set or subset of possible solutions F_c ,

$$\min_{\rho \in F_c} J(\rho) \tag{2.3}$$

with

$$F_c = \{\rho, \rho_D(K(\rho), b) \leq \varepsilon\}$$

This gives a clear interpretation of J as known in advance or prescribed properties of the solution, such as belonging to specified class of functions, for example, smooth ones.

2.2.1.0.1 Regularized Minimization Problem, Tikhonov Approach It can be proved ([30]) that if the problem has a solution, the solution occurs on the boundary of the constrained region. Thus, we can solve the problem of minimization of (2.3) subject to

$$\rho_D(K(\rho), b) = \varepsilon$$

Introducing the Lagrange multiplier α we can write the *Tikhonov Parametric Functional* as an unconstrained functional $P^\alpha(\rho, b)$, $\rho \in X$, $b \in D$, given by

$$P^\alpha(\rho, b) = \rho_D^2(K(\rho), b) + \alpha J(\rho)$$

and solve the unconstrained problem

$$\min P^\alpha(\rho, b) \tag{2.4}$$

where b is observed gravitational data and α is an unknown regularization parameter, which can be determined using the condition,

$$\rho_D^2(K(\rho_\alpha), b) = \epsilon^2$$

Here ϵ^2 is the noise level and ρ_α is the solution of the minimization problem (2.4).

Minimization problem (2.4) is a regularized problem. Its solution defines the operator $R(\alpha, b)$ such that the solution ρ can be obtained as

$$\rho^\alpha = R(\alpha, b)$$

$R(\alpha, b)$ is a regularization operator for the original ill-posed problem (2.1). Now we can use this approximation of the solution of 2.1 as a new minimization problem ($P^\alpha(\rho, b) \rightarrow \min$) and take smaller values of the errors ϵ closer to the original problem. We have replaced the initial ill-posed problem, by a sequence of problems where the operator $R(\alpha, b)$ is well posed. Our next consideration will be the selection of the stabilization functional.

2.2.2 Smoothing Stabilization Functional

Based on the smoothness of the solution the following quadratic stabilization functionals are commonly used [14], [15]

$$J_{mn}(\rho) = \int_{\Omega} \rho^2(x) dx$$

or

$$J_B(\rho) = \int_{\Omega} |\nabla \rho(x)|^2 dx$$

with $|\nabla \rho(x)|^2 = \left(\frac{\partial \rho(x)}{\partial x_1}\right)^2 + \left(\frac{\partial \rho(x)}{\partial x_2}\right)^2 + \left(\frac{\partial \rho(x)}{\partial x_3}\right)^2$, or

$$J_H(\rho) = \int_{\Omega} |\Delta \rho(x)|^2 dx$$

with $\Delta \rho(x) = \left(\frac{\partial^2 \rho(x)}{\partial x_1^2} + \frac{\partial^2 \rho(x)}{\partial x_2^2} + \frac{\partial^2 \rho(x)}{\partial x_3^2}\right)$.

2.3 Regularized non-linear gradient minimization

Different optimization schemes can be developed to minimize the Tikhonov functional. We will illustrate the solution for the first case (MN), and analogously the methods were obtained for the other stabilization functionals presented in this work, in all cases using the gradient technique. In chapter 4, the implemented Adaptive Gradient Minimization algorithm will be described.

2.3.1 Euler Lagrange Equations

Let us consider a general non-linear forward operator F and the inverse problem for this operator. The minimum norm stabilization functional $J(\rho) = \|\rho\|_2^2$ is sometimes used in a form $J(\rho) = \|\rho - \rho_0\|_2^2$, where ρ_0 is some apriori model.

We want to minimize the Tikhonov parametric functional

$$\min P^\alpha(\rho) = \min \|F(\rho) - b\|_2^2 + \alpha \|\rho - \rho_0\|_2^2 \quad (2.5)$$

where F is the forward non-linear operator, and

ρ_0 is the apriori model.

Written in terms of inner products, the minimization problem is:

$$\min \langle F(\rho) - b, F(\rho) - b \rangle + \alpha \langle \rho - \rho_0, \rho - \rho_0 \rangle$$

The optimality conditions state that the solution of the minimization problem should satisfy the requirement that the variation of the functional with respect to ρ equal 0, $\delta_\rho P^\alpha(\rho) = 0$. Let δ_ρ be the variational operator with respect to ρ , $\delta_\rho J = J(\rho + \delta\rho) - J(\rho)$. Varying we will have,

$$\delta_\rho P^\alpha(\rho) = 2 \langle \delta_\rho (F(\rho) - b), F(\rho) - b \rangle + 2\alpha \langle \delta_\rho (\rho - \rho_0), \rho - \rho_0 \rangle$$

and finally,

$$= 2 \langle \delta_\rho F(\rho), F(\rho) - b \rangle + 2\alpha \langle \delta_\rho, \rho - \rho_0 \rangle$$

For differentiable F we can write in terms of the Frechet derivative F'_ρ ,

$$\delta_\rho F(\rho) \cong F(\rho + \delta\rho) - F(\rho) = F'_\rho \delta\rho$$

Then

$$\delta_\rho P^\alpha(\rho) = 2 \langle F'_\rho \delta\rho, F(\rho) - b \rangle + 2\alpha \langle \delta\rho, \rho - \rho_0 \rangle$$

using the definition of adjoint operator,

$$= 2 \langle \delta\rho, (F'_\rho)^* (F(\rho) - b) \rangle + 2\alpha \langle \delta\rho, \rho - \rho_0 \rangle$$

then we obtain,

$$= 2 \langle \delta\rho, (F'_\rho)^* (F(\rho) - b) + \alpha(\rho - \rho_0) \rangle \quad (2.6)$$

The requirement $\delta_\rho P^\alpha(\rho) = 0$ for any $\delta\rho$, implies that;

$$(F'_\rho)^* (F(\rho) - b) + \alpha(\rho - \rho_0) = 0 \quad (2.7)$$

These are the Euler-Lagrange equations for the minimization problem (2.5).

2.3.2 Gradient technique

To construct an iterative process to find the solution, let us take the $\delta\rho$ in (2.6) as a linear part of the $\delta_\rho P^\alpha(\rho)$, which corresponds to the steepest ascent direction of $P^\alpha(\rho)$

$$\delta\rho = -\theta^\alpha \left[(F'_\rho)^* (F(\rho) - b) + \alpha(\rho - \rho_0) \right]_\alpha = -\theta^\alpha g^\alpha(\rho)$$

where $-\theta^\alpha$ is the stepsize and

$$g^\alpha(\rho) = \left[\left(F'_\rho \right)^* (F(\rho) - b) + \alpha(\rho - \rho_0) \right]_\alpha$$

and $-g^\alpha(\rho)$ is the steepest descent direction of the functional $P^\alpha(\rho)$.

To see that this is a decreasing direction of the functional $P^\alpha(\rho)$, let us calculate $\delta_\rho P^\alpha(\rho)$;

$$\delta_\rho P^\alpha(\rho) = 2 \langle \delta \rho, g^\alpha(\rho) \rangle = 2 \langle -\theta^\alpha g^\alpha(\rho), g^\alpha(\rho) \rangle < 0$$

because $\langle g^\alpha(\rho), g^\alpha(\rho) \rangle \geq 0$.

The step size (for a fixed value of α) can be determined using one dimensional minimization procedures for the parametrical functional.

Let ρ_k be a solution constructed on the k iteration step and ρ_{k+1} be the next approximation, $\rho_{k+1} = \rho_k - \theta_k^\alpha g_k^\alpha(\rho_k)$, where g_k^α is the gradient of the parametrical functional P^α at the point ρ_k . In order to find the stepsize θ_k^α we need to solve the following unconstrained minimization problem:

$$\min \Theta(\theta_k^\alpha) = P^\alpha(\rho_{k+1}) = P^\alpha(\rho_k - \theta_k^\alpha g_k^\alpha(\rho_k))$$

The regularization parameter α is one from a sequence of real numbers $(\alpha_0 \dots \alpha_n)$, with $\alpha_0 > N$, and $\alpha_n < M$, where N and M are usually a big real value and a small one, respectively, and depend on each specific problem.

2.3.2.1 Euler Lagrange Equations for gravitational problem

In the gravitational problem we deal with linear operator (1.8) and we assume no apriori model is given, then the regularized inverse problem can be formulated as a minimization problem,

$$\min \|K(\rho) - b\|_2^2 + \alpha \|\rho\|_2^2$$

The E-L equations for this problem are

$$K^*(K\rho - b) + \alpha(\rho) = 0 \tag{2.8}$$

2.4 Choosing the regularization parameter

The automatic choice of the regularization parameter will influence the performance of the iterative minimization process of the Tikhonov parametrical functional. This is an important research area and many works have been published in this direction. In this work, we will not determine the regularization parameter automatically. We will do it, graphically (figure 2.2), following properties of the parametrical functional, stabilizer and misfit functional [14].

Figure 2.2 [14] shows behavior of the misfit functional $\|K(\rho) - b\|_2^2$ and the stabilization functional $\|\rho\|_2^2$ (minimum norm problem). When the parameter of regularization α tends to zero, the misfit goes to zero, however the norm of the solution becomes arbitrarily large.

This demonstrates clearly the ill-posedness of the inverse gravitational problem.

As it was mentioned in the previous chapter the gravity measurements of the vertical derivative of the potential field, b_{true} are observed with some noise ϵ .

$$b = b_{true} + b_\epsilon$$

Here b_{true} is the true solution of the forward gravimetric problem and ϵ the level of error in the observed data:

$$\rho_D(b, b_{true}) \leq \epsilon$$

The regularization parameter α can be obtained using the misfit constrained functional as a constraint in a minimization procedure

$$M(\alpha) = \rho_D(K(\rho_\alpha), b) = \epsilon$$

2.5 Discrete inverse gravimetric problem

Assuming smoothness of the solution we obtained the density distribution function for the inverse gravimetric problems solving the Tikhonov functional for different stabilization operators.

2.5.1 Regularized Gravimetric Minimization Problems

Let K be the matrix obtained from the linear operator (2.1) to reduce the problem to a finite dimensional one.

In this work we will consider the following smooth regularization to solve the 3D inverse gravimetric problems, with the density function constant in the x_3 direction.

◦ The Minimum Norm Problem [MN] is

$$\min_{\rho} P^{\alpha}(\rho) = \min \|K\rho - b\|_2^2 + \alpha \|\rho\|_2^2$$

when the stabilization functional is the l_2 norm of the solution.

◦ The 2D ∇ minimum norm problem is

$$\min \|K\rho - b\|_2^2 + \alpha \left(\left\| \frac{\partial(\rho)}{\partial x_1} \right\|_2^2 + \left\| \frac{\partial(\rho)}{\partial x_2} \right\|_2^2 \right)$$

when the stabilization functional is a norm of the gradient of the solution.

The gravimetric operator is linear with respect to (ρ) . In more general non-linear geophysical application the operator can be linearized and the following solutions still can be used.

2.5.2 Regularized Direct solution

If K is a linear operator, then for the previous stabilization functional the direct Tikhonov solution of the minimization parametrical functional

$$\min_{\rho} P^{\alpha}(\rho) = \min \|K\rho - b\|_2^2 + \alpha \|\rho\|_2^2$$

is unique ([14]) and can be expressed from the Euler-Lagrange equations (2.8) as:

1) For MN problem.

$$\rho^* = (K^T K + \alpha I)^{-1} K^T b \quad (2.9)$$

2) Generally when the stabilization functional $J(\rho) = B\rho$ with a given matrix B , the Euler-Lagrange equations are

$$K^T (K\rho - b) + \alpha B^T B \rho = 0 \quad (2.10)$$

from where

$$\rho^* = (K^T K + \alpha B^T B)^{-1} K^T b$$

2.5.3 Analysis of the discrete Tikhonov solution

The generalized singular value decomposition (GSVD) analysis of the Tikhonov solution gives us a good understanding of the effects of regularization.

Let $K \in \mathfrak{R}^{m \times n}$ be matrix; $B \in \mathfrak{R}^{p \times n}$ matrix; $\rho \in \mathfrak{R}^n$, $b \in \mathfrak{R}^m$, $m \succeq n$, and the discrete Tikhonov minimization problem be,

$$\min_{\rho} P^{\alpha}(\rho) = \min \|K\rho - b\|_2^2 + \alpha \|B\rho\|_2^2 \quad (2.11)$$

We can write the discrete Euler-Lagrange equations for (2.11) as (2.10),

$$(K^T K + \alpha B^T B) \rho^* = K^T b \quad (2.12)$$

Let us assume that $p < n$, which means that the matrix B has rank smaller than n , and has non zero null space.

The stabilization functional described by the matrix B cannot be minimized in the directions corresponding to the null space of the matrix B . We will show that the solution ρ^* can not be regularized in these directions. It means that this functional violates the requirements of compactness of the set of ρ such that $\|B\rho\|_2^2 < m$. Hence using such a functional one needs to be sure that the solution ρ^* does not have components in this directions.

In our case, the second stabilization functional, which is the norm of the gradient of the solution has a one-dimensional null-space consisting of constant functions. The same will be true for the Total Variation stabilization functional, which we consider in chapter 3. It will follow from construction of our numerical scheme that the computed solution does not have a constant component.

Using the GSVD for the matrix K and B [19], we can write

$$K = U \begin{pmatrix} \text{diag}(\xi_i) & 0 \\ 0 & I_{n-p} \\ 0 & 0 \end{pmatrix} W^{-1}$$

and,

$$B = V \begin{pmatrix} \text{diag}(\tau_i) & 0 \end{pmatrix} W^{-1} \quad (2.13)$$

with $0 \geq \xi_1 \geq \xi_2 \geq \dots \geq \xi_p$ and $0 \geq \tau_1 \geq \tau_2 \geq \dots \geq \tau_p$

where

$U \in \mathfrak{R}^{m \times m}$, $U = (u_1, \dots, u_m)$, is orthogonal matrix, $U^T U = I_n$,

$V \in \mathfrak{R}^{p \times p}$, $V = (v_1, \dots, v_p)$, is orthogonal matrix, $V^T V = I_p$,

and

$W \in \mathfrak{R}^{n \times n}$, $W = (w_1, \dots, w_n)$, is invertible, W^{-1} exists.

We show in the next section that the solution ρ^* can be written as

$$\rho^* = \sum_{j=1}^p \frac{\xi_j}{\xi_j^2 + \alpha \tau_j^2} (u_j^T b) w_j + \sum_{j=p+1}^n u_j^T b w_j$$

The elements ξ_j and τ_j , are usually normalized via

$$(\xi_j^2 + \tau_j^2 = 1), \{j = 1, \dots, p\}$$

then the generalized singular values can be written as the ratio

$$\sigma_j = \frac{\xi_j}{\tau_j} \quad (2.14)$$

We assume the generalized singular values are ordered as

$$\sigma_1 \geq \sigma_2 \geq \dots \geq \sigma_{p-1} \geq \sigma_p$$

Then we can write

$$\rho^* = \sum_{j=1}^p \frac{\frac{\xi_j^2}{\tau_j^2}}{\frac{\xi_j^2}{\tau_j^2} + \alpha} \frac{u_j^T b}{\xi_j} w_j + \sum_{j=p+1}^n u_j^T b w_j$$

and using (2.14) we obtain

$$\rho^* = \sum_{j=1}^p \frac{\sigma_j^2}{\sigma_j^2 + \alpha} \frac{u_j^T b}{\xi_j} w_j + \sum_{j=p+1}^n u_j^T b w_j$$

We can see that the solution consists of two parts. The first one depends on the regularization

$$\sum_{j=1}^p \frac{\sigma_j^2}{\sigma_j^2 + \alpha} \frac{u_j^T b}{\xi_j} w_j$$

From here we can see the effect of regularization on the solution ρ^* . A good choice of the parameter of regularization α will damp the effect of the small eigenvalues in the solution ρ^* (where $\sigma_j^2 \rightarrow 0$).

The second part of the solution is

$$\sum_{j=p+1}^n u_j^T b w_j \tag{2.15}$$

which does not depend on the regularization. This is particular important because, it can be proved that $w_{p+1} \dots w_n$ form the basis for the null space of B and it will be shown in the next section. This gives us the part of the solution that can not be regularized.

Also the following characteristics were observed in the forward gravimetric operator which are typically seen in problems arising from the discretizations of the integral equations for physical models:

a) the singular values $\sigma_1 \geq \sigma_2 \geq \dots \geq \sigma_{p-1} \geq \sigma_p$ decay exponentially to zero (figure 2.3).

This behavior of the singular values σ_j introduce significant instability in the solution when noise is present in the data. This can be easily seen from representing the solution in the basis of the matrix K .

b) the singular vectors u_j, v_j and w_j tend to have more sign changes as j increases (figures 2.4, 2.5, 2.6).

2.5.4 Derivation of GSVD of Tikhonov solution

Let us take a block matrix $R \in \mathfrak{R}^{p \times p}$, as the first p columns and rows,

$$R = \begin{pmatrix} \xi_1 & & 0 \\ & \xi_i & \\ 0 & & \dots \\ & & & \xi_p \end{pmatrix}$$

and in analogous way, let us take a block matrix $M \in \mathfrak{R}^{p \times p}$ as,

$$M = \begin{pmatrix} \tau_1 & & 0 \\ & \dots & \\ 0 & & \tau_p \end{pmatrix}$$

then we can rewrite $K^T K$ using the defined block matrices as,

$$K^T K = (W^T)^{-1} \begin{pmatrix} R & 0 & 0 \\ 0 & I_{n-p} & 0 \end{pmatrix} U^T U \begin{pmatrix} R & 0 \\ 0 & I_{n-p} \\ 0 & 0 \end{pmatrix} W^{-1} =$$

or

$$= (W^T)^{-1} \begin{pmatrix} R^2 & 0 \\ 0 & I_{n-p} \end{pmatrix} W^{-1}$$

Let us also rewrite $B^T B$ as

$$B^T B = (W^T)^{-1} \begin{pmatrix} M \\ 0 \end{pmatrix} V^T V \begin{pmatrix} M & 0 \end{pmatrix} W^{-1} = (W^T)^{-1} \begin{pmatrix} M^2 & 0 \\ 0 & 0 \end{pmatrix} W^{-1}$$

Using these expressions in the Euler-Lagrange equations (2.12) we obtain:
for the left hand side

$$(W^T)^{-1} \left[\begin{pmatrix} R^2 & 0 \\ 0 & I_{n-p} \end{pmatrix} + \alpha \begin{pmatrix} M^2 & 0 \\ 0 & 0 \end{pmatrix} \right] W^{-1} \rho^* =$$

and for the right hand side

$$(W^T)^{-1} \begin{pmatrix} R^2 & 0 & 0 \\ 0 & I_{n-p} & 0 \end{pmatrix} U^T b$$

Rearranging the left hand side and multiplied by (W^T) from the left in both sides we obtain

$$\begin{pmatrix} R^2 + \alpha M^2 & 0 \\ 0 & I_{n-p} \end{pmatrix} W^{-1} \rho^* =$$

and for the right hand side

$$\begin{pmatrix} R^2 & 0 & 0 \\ 0 & I_{n-p} & 0 \end{pmatrix} U^T b$$

Let $y = W^{-1} \rho^*$; $y \in \mathfrak{R}^n$. Modifying the previous equation we obtain the left hand side

$$\begin{pmatrix} R^2 + \alpha M^2 & 0 \\ 0 & I_{n-p} \end{pmatrix} y = \begin{pmatrix} R & 0 & 0 \\ 0 & I_{n-p} & 0 \end{pmatrix} U^T b$$

and for the right hand side

$$\begin{pmatrix} R & 0 & 0 \\ 0 & I_{n-p} & 0 \end{pmatrix} U^T b = \begin{pmatrix} R & 0 & 0 \\ 0 & I_{n-p} & 0 \end{pmatrix} \begin{pmatrix} u_1^T b \\ u_2^T b \\ \vdots \\ \vdots \\ u_m^T b \end{pmatrix} = \begin{pmatrix} \xi_1 u_1^T b \\ \xi_2 u_2^T b \\ \vdots \\ \xi_p u_p^T b \\ \xi_{p+1} u_{p+1}^T b \\ \vdots \\ \xi_m u_m^T b \end{pmatrix}$$

Now we can express the left hand side as

$$(R^2 + \alpha M^2) y = \begin{pmatrix} \xi_1^2 + \alpha \tau_1^2 & & \\ & \xi_2^2 + \alpha \tau_2^2 & \\ & & \ddots \\ & & & \xi_p^2 + \alpha \tau_p^2 \end{pmatrix} y$$

Joining both sides we obtain

$$\begin{aligned} y_1 &= \frac{\xi_1 u_1^T b}{\xi_1^2 + \alpha \tau_1^2} = \frac{\xi_1}{\xi_1^2 + \alpha \tau_1^2} u_1^T b \\ y_2 &= \frac{\xi_2 u_2^T b}{\xi_2^2 + \alpha \tau_2^2} = \frac{\xi_2}{\xi_2^2 + \alpha \tau_2^2} u_2^T b \\ &\dots \\ y_p &= \frac{\xi_p u_p^T b}{\xi_p^2 + \alpha \tau_p^2} = \frac{\xi_p}{\xi_p^2 + \alpha \tau_p^2} u_p^T b \\ y_{p+1} &= u_{p+1}^T b \\ y_{p+2} &= u_{p+2}^T b \\ &\dots \\ y_n &= u_n^T b \end{aligned}$$

also we had $y = W^{-1} \rho^*$; $y \in \mathfrak{R}^n$. Then the solution for ρ^* can be written as

$$\rho^* = Wy = y_1w_1 + y_2w_2 + \dots + y_nw_n$$

or

$$\rho^* = \sum_{j=1}^p \frac{\xi_j}{\xi_j^2 + \alpha\tau_j^2} (u_j^T b) w_j + \sum_{j=p+1}^n u_j^T b w_j$$

Now we show (2.15) form the basis for the null space of B . Let $W \in \mathfrak{R}^{n \times m}$

$$W = (w_1, w_2, \dots, w_j, \dots, w_n)$$

We can write the identity matrix as

$$I = W^{-1}W = (W^{-1}w_1, W^{-1}w_2, \dots, W^{-1}w_j, \dots, W^{-1}w_n)$$

and using the result of the GSVD of B from (2.13) we have

$$Bw_j = [V (M | 0) W^{-1}] w_j$$

or

$$Bw_j = V (M | 0) (W^{-1}W)_j$$

Then for $j = p + 1, \dots, n$ we have

$$V (M | 0) \begin{pmatrix} 0 \\ \cdot \\ 0 \\ 1 \\ 0 \\ \cdot \\ 0 \end{pmatrix} = 0$$

Therefore for $j \geq p + 1$, $Bw_{p+1} = Bw_{p+2} = \dots = Bw_n = 0$. Hence $w_{p+1} \dots w_n$ form the basis for the null space of B .

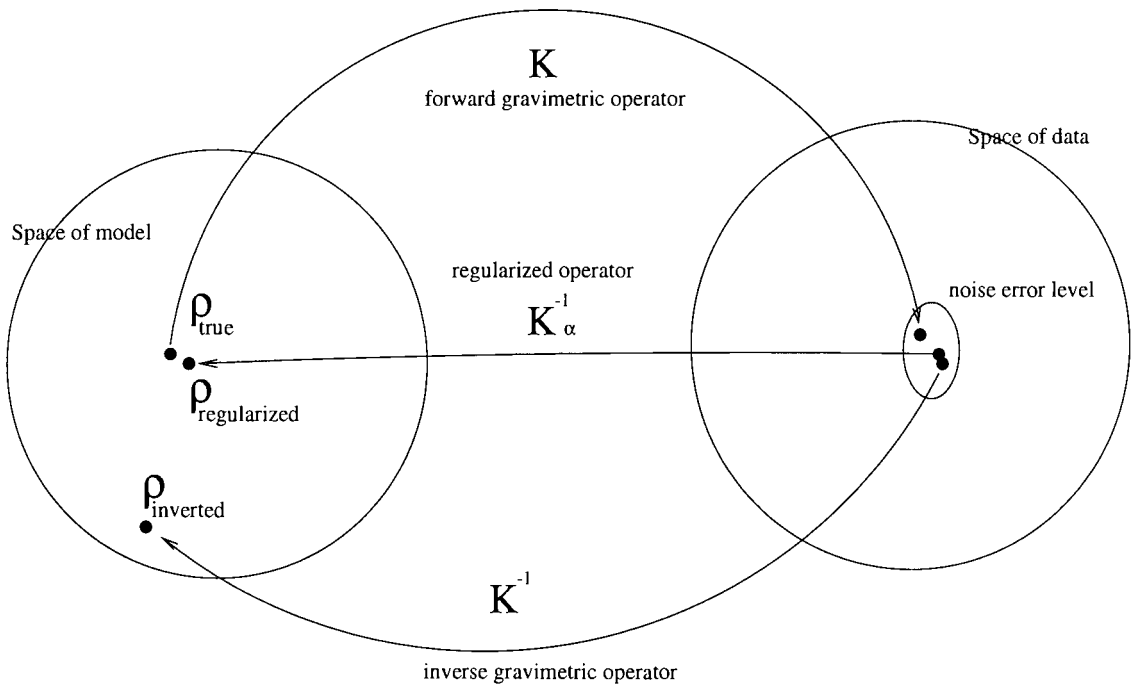


Figure 2.1. Regularized operator for the gravimetric problem

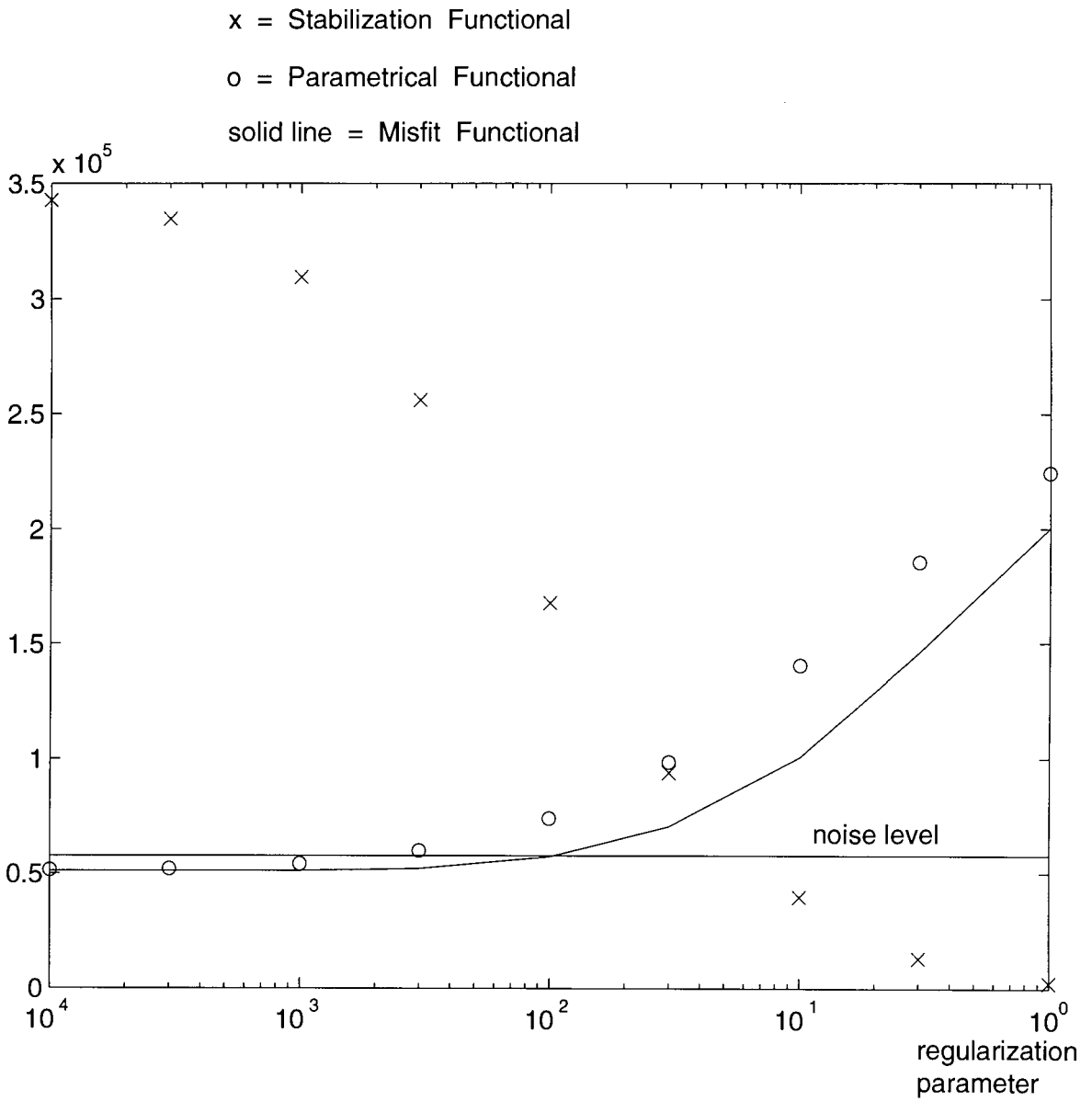


Figure 2.2. regularization parameter choice

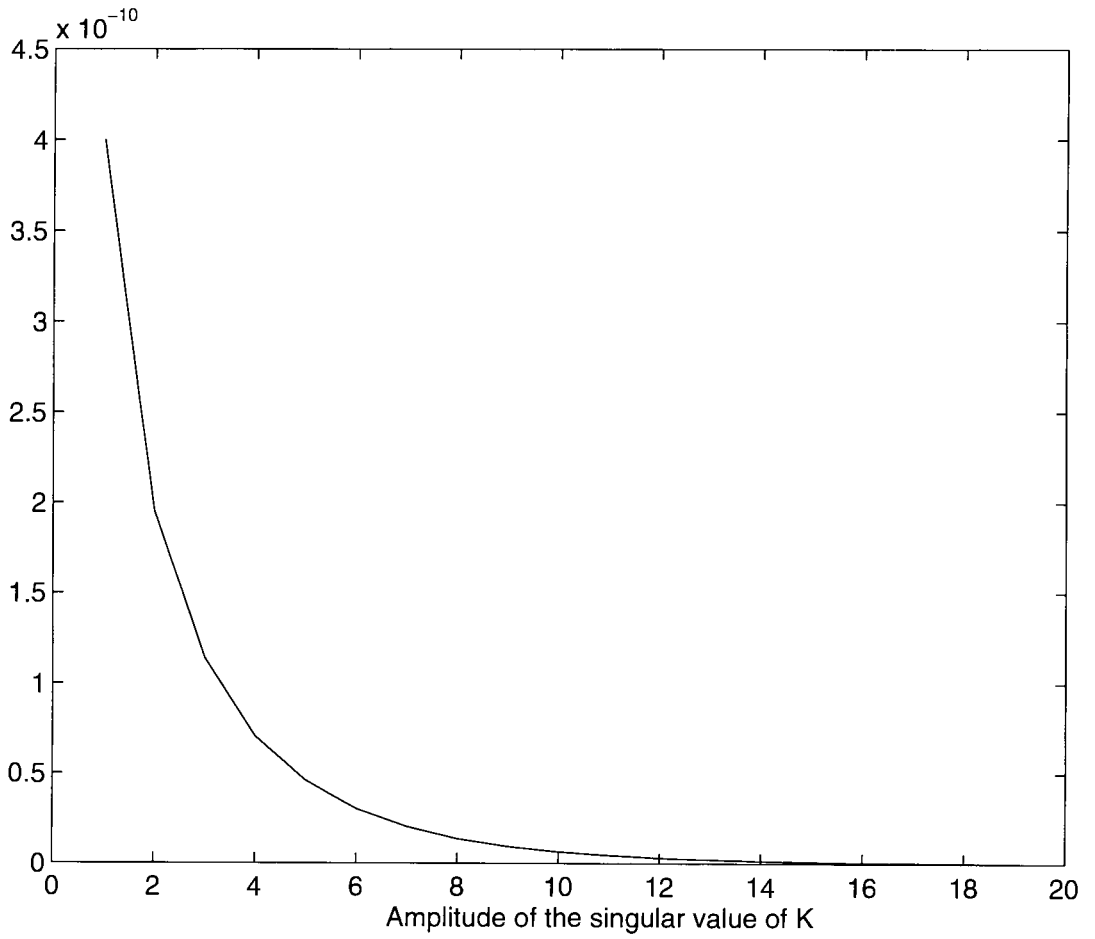


Figure 2.3. Exponential decay of singular values of K (60×20)

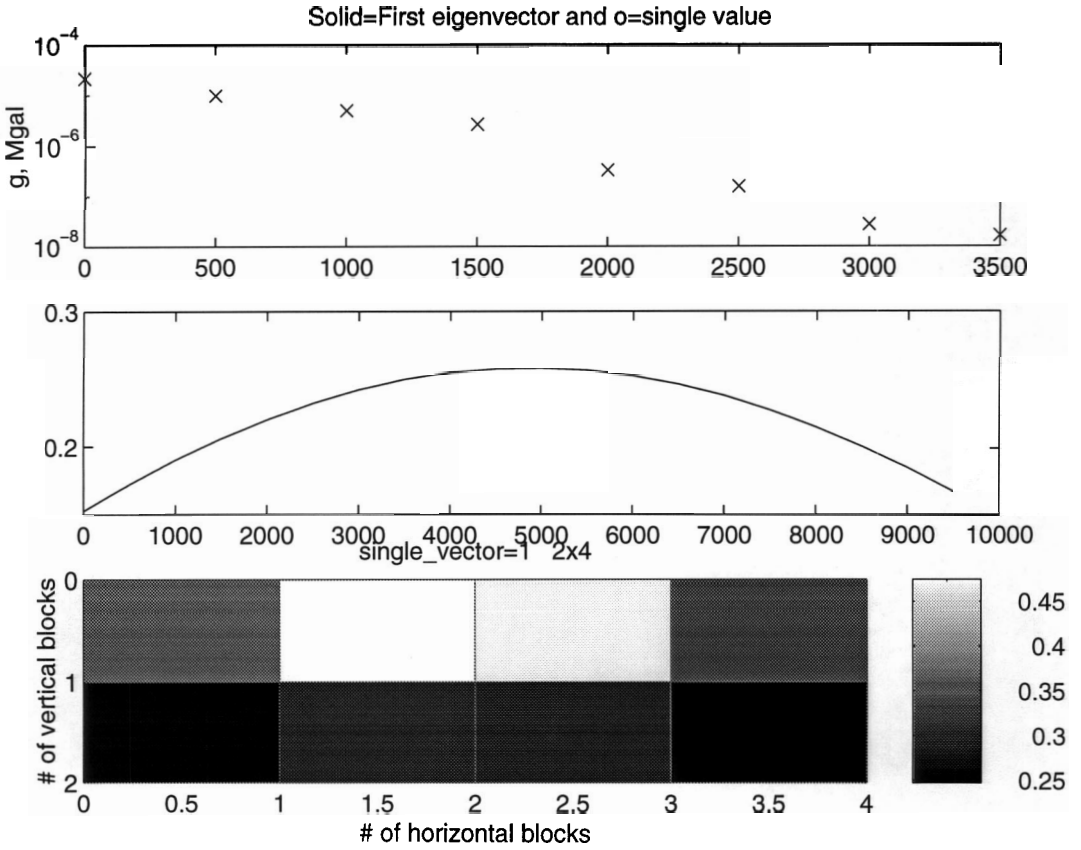


Figure 2.4. Singular values and first left and right singular vectors of the discretized operator K (8×20)

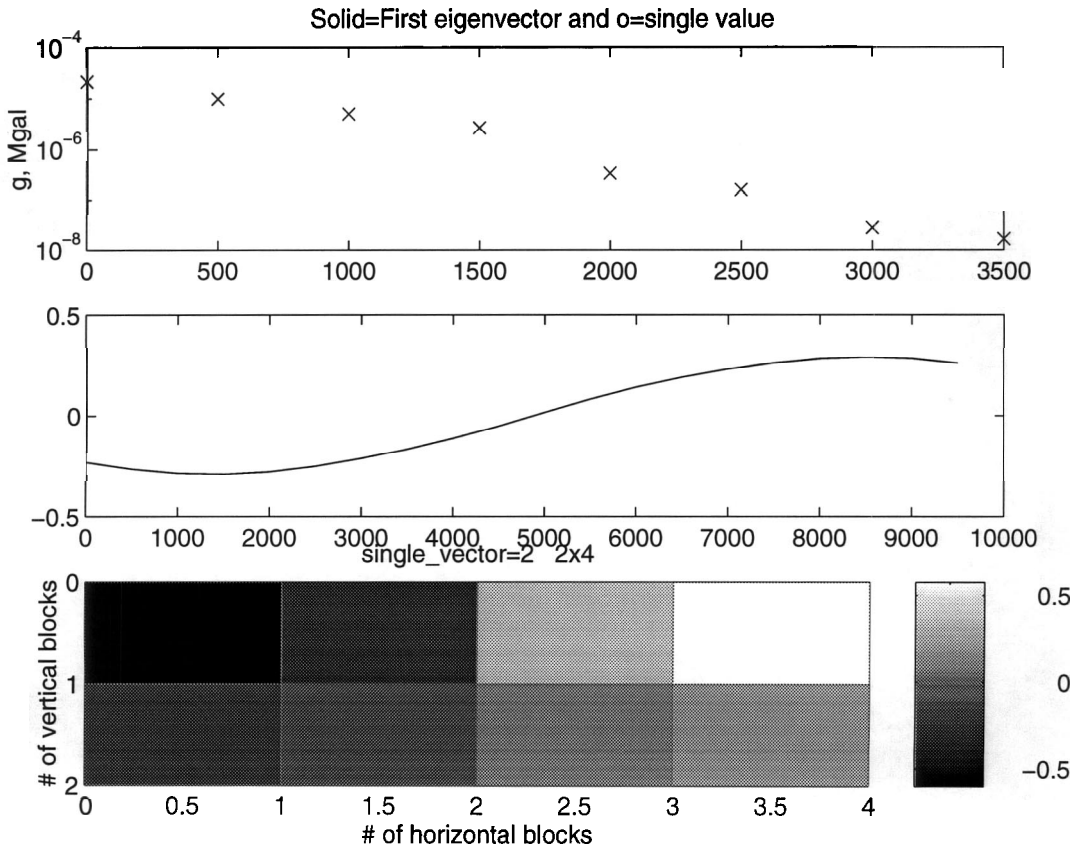


Figure 2.5. Singular values and first left and right singular vectors of the discretized operator K (8×20) corresponding to the second singular value

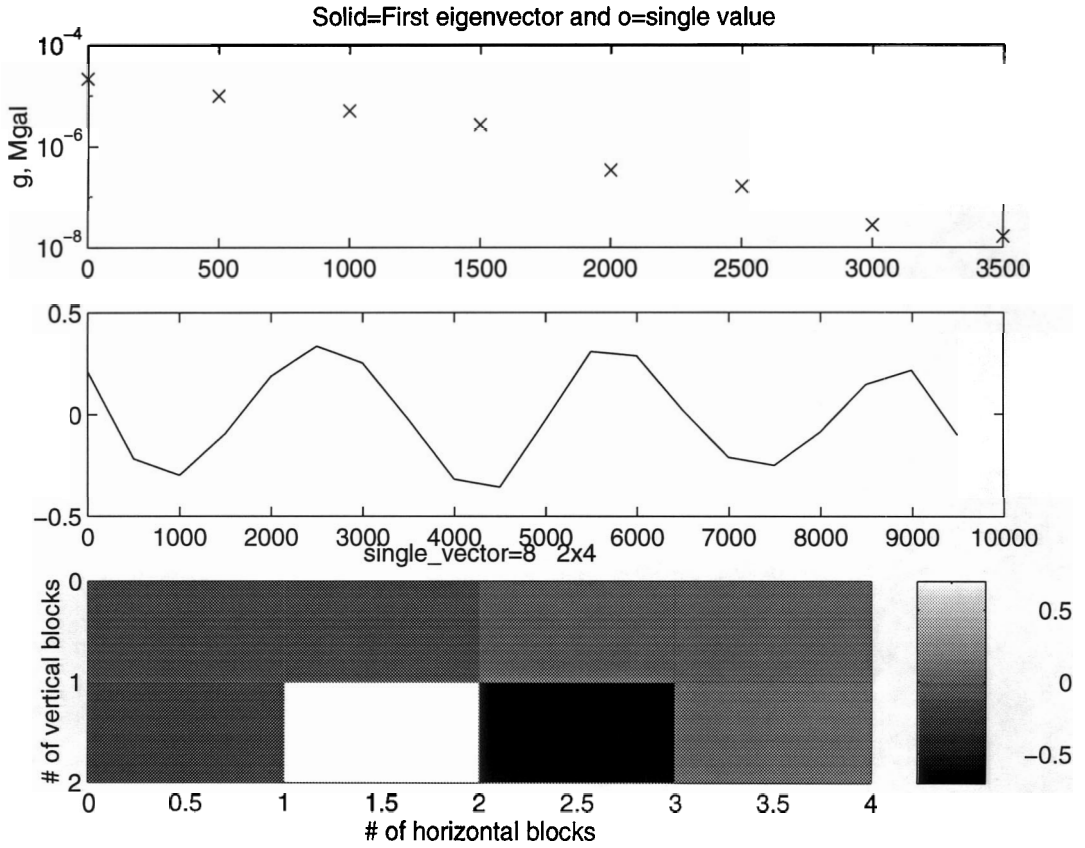


Figure 2.6. Singular values and first left and right singular vectors of the discretized operator K (8×20) corresponding to the last singular value

CHAPTER 3

NON-SMOOTH ALTERNATIVE REGULARIZATION

3.1 Previous Reference Work

In 1992 Total Variation method was proposed in [5] to solve the denoising problem. A typical problem in image denoising is to determine an unknown image from noisy observed data. Some examples are shown in figure 3.1 and figure 3.2. The problem of image denoising can be written mathematically as

$$(\epsilon + z) = B_{blur} u$$

where

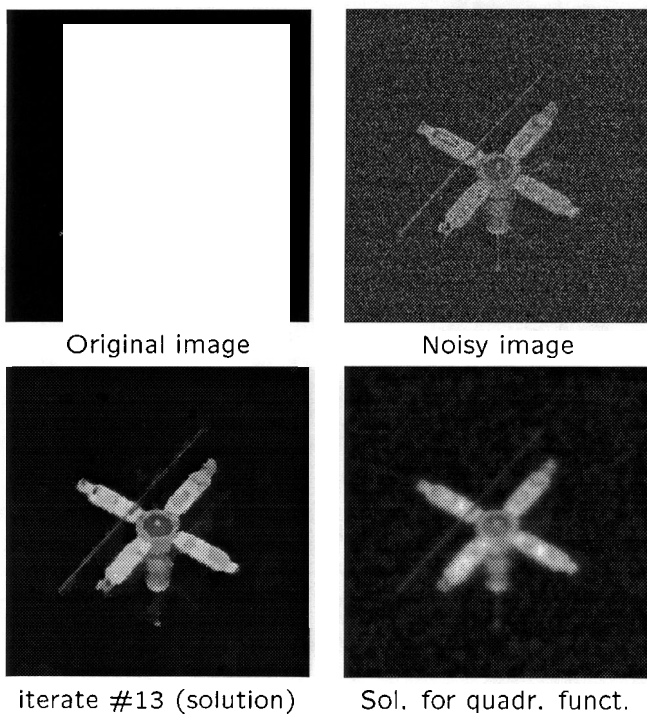
$B_{blur} = I$ is Identity Operator for non-blurred images, or an integral operator (usually with gaussian kernel) for blurred images,

u is real image; and

$(\epsilon + z)$ is noisy observed data.

Hence for non-blurred images the problem of denoising is

$$(\epsilon + z) = I \cdot u \tag{3.1}$$

Sample Denoising

Data provided by the Phillips Air Force Lab. at Kirkland AFB NM, through Prof. Bob Plemmons.

Figure 3.1. Denoising problem, example 1



Figure 3.2. Denoising problem, example 2

Total variation methods do better at restoring the edges of the original image in comparison with L^2 -based algorithms.

3.1.1 Inverse Gravitational Problem for a non-smooth density function

The inverse gravimetric problem can be written in a way similar to the image processing problem (3.1) when the operator K_{grav} is used instead of the identity operator.

$$(b_\varepsilon + b_{true}) = K_{grav}\rho \quad (3.2)$$

where

K_{grav} is Forward Gravimetric Operator,

$\rho(x)$ is true density function distribution

$(b_\varepsilon + b_{true})$ is noisy observed data of the vertical component of the gravimetric field.

Our goal is to be able to recover non-smooth density distributions in geophysical problems which is difficult with standard regularization operators. Standard methods give results that are poor approximations when the original structure is "blocky" (non-smooth), which occurs in many geological structures.

In this work we propose the minimization of the Total Variation norm of the density distribution, subject to noise constraints based on Tikhonov approach presented in chapter 2. We first discuss some properties of the Total Variation seminorm.

3.2 Definition of Bounded Variation seminorm or Total Variation (TV)

The Bounded Variation seminorm or Total Variation (TV) of a function u is [3]

$$J_{tv} =^{def} \sup_{v \in \nu} \int_{\Omega} (-u \operatorname{div} v) \, dx \quad (3.3)$$

where v is a d -dimensional test function defined in Ω , which is at least once differentiable and is zero on the boundaries, so that

$$\nu = \left\{ v \in C_0^1(\Omega, R^d) \mid |v(x)| \leq 1 \text{ for all } x \in \Omega \right\}$$

To analyze the Total Variation semi-norm, consider first the case of a continuous 1D function (fig. 3.3).

3.2.1 TV for continuous functions

Let $u \in C^1(\Omega_{0,1})$, then the TV of u on $[0,1]$ is from definition (3.3)

$$J_{tv} = \sup_{v \in \mathcal{V}} \int_{\Omega} -u \ v_x \ dx = \sup_{v \in \mathcal{V}} - \int_{\Omega} (-u_x \ v) \ dx + uv|_0^1$$

where the second equality follows from integrating by parts.

Since $v \in C_0^1(\Omega, R^d)$, it vanishes on the boundary, and

$$J_{tv} = \sup_{v \in \mathcal{V}} \int_{\Omega} v \ u_x \ dx$$

If we could have

$$v \equiv \begin{cases} +1, & u_x > 0 \\ -1, & u_x < 0 \end{cases}$$

then we obtain

$$J_{tv} = \int_{\Omega} |u_x| \ dx \tag{3.4}$$

From (3.4) we can easily see that the definition (3.3) gives the variation of the function on the domain Ω .

Consider now the case of a 1D discontinuous function (fig. 3.4).

3.2.2 TV for discontinuous functions

Let $u \in C^1(\Omega_{0,1})$, (fig. 3.4) then from definition (3.3) gives

$$J_{tv} = \sup_{v \in \mathcal{V}} \int_{\Omega} -u \ v_x \ dx$$

Dividing the integral around the discontinuity,

$$J_{tv} = \sup_{v \in \mathcal{V}} \left\{ \lim_{\hat{a} \rightarrow a^-} - \int_0^{\hat{a}} -u \ v_x \ dx + \lim_{\hat{a} \rightarrow a^+} \int_{\hat{a}}^1 -u \ v_x \ dx \right\}$$

integrating both terms by parts

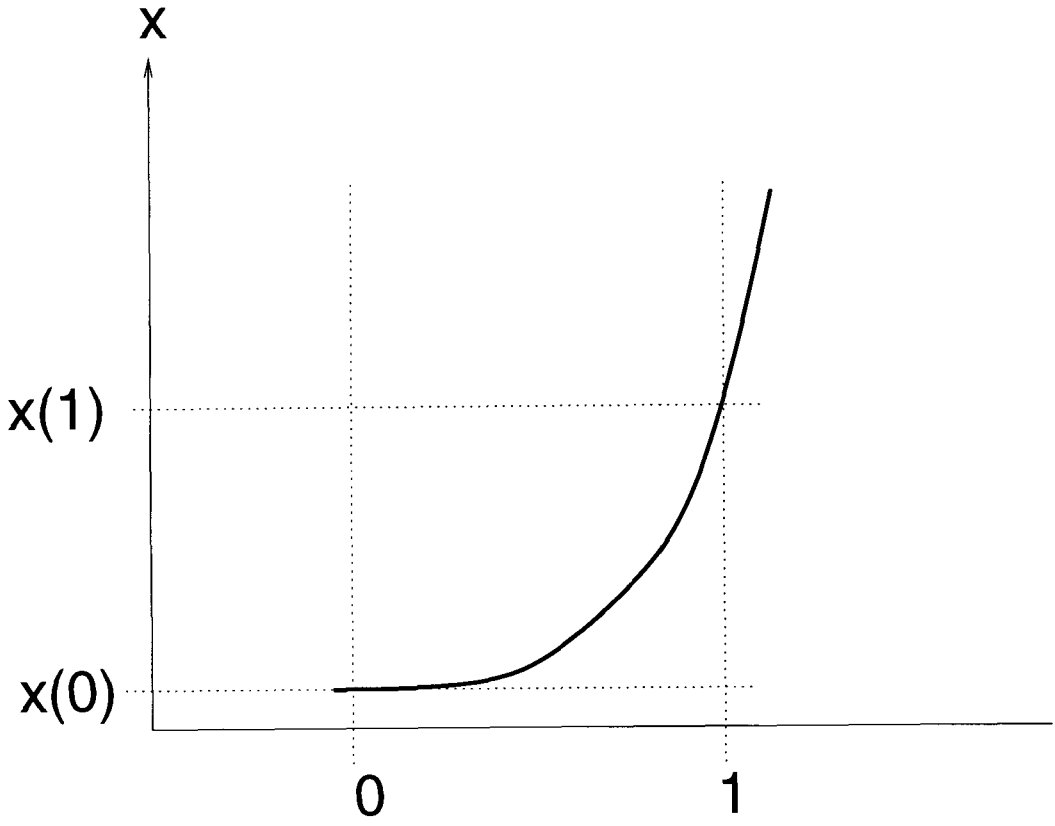


Figure 3.3. 1D continuous example

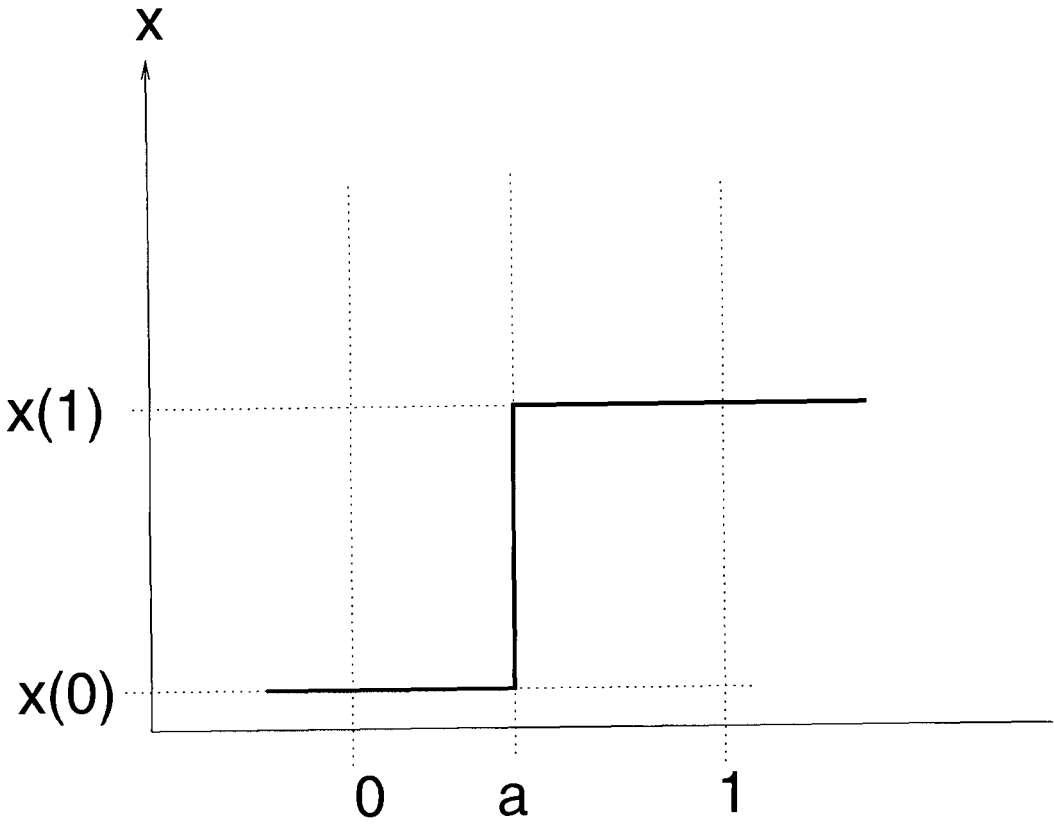


Figure 3.4. 1D discontinuous example

$$J_{tv} = \sup_{v \in \nu} \left\{ \lim_{\dot{a} \rightarrow a^-} \int_0^{\dot{a}} u \ v_x \ dx - u(\dot{a})v(\dot{a}) + \right. \\ \left. \lim_{\ddot{a} \rightarrow a^+} \int_{\ddot{a}}^1 u \ v_x dx + u(\ddot{a})v(\ddot{a}) \right\}$$

Because $v \in C_0^1(\Omega, R^d)$

$$J_{tv} = \sup_{v \in \nu} \left[-v(a)u(a^-) + v(a)u(a^+) \right]$$

or

$$J_{tv} = \sup_{v \in \nu} \left[v(a) \left(u(a^+) - u(a^-) \right) \right]$$

Letting

$$v(a) \equiv \begin{cases} +1, & (u(a^+) - u(a^-)) > 0 \\ -1, & (u(a^+) - u(a^-)) < 0 \end{cases}$$

then

$$J_{tv} = \left| u(a^+) - u(a^-) \right|$$

In this case too, it can be seen definition (3.3) gives the variation of the function in the domain Ω . Therefore, TV of a function gives in all cases its variation, which is bounded, meanwhile the norm of the derivative for a discontinuous function is unbounded.

Let us formulate now the inverse gravimetric problem using the TV as a stabilizer.

3.3 TV minimization for the inverse gravity problem

Using TV norm of the solution as the stabilizing functional for the inverse gravimetric problem as the following minimization problem gives

$$\min P_{TV}^\alpha(\rho, b) = \min \|K\rho - b\|_2^2 + \alpha \int_\Omega |\nabla \rho| \ dx \quad (3.5)$$

where $|\nabla \rho| = \sqrt{\left(\frac{\partial(\rho)}{\partial x_1}\right)^2 + \left(\frac{\partial(\rho)}{\partial x_2}\right)^2}$, and Ω is the domain in the earth where density is allowed to vary.

3.3.1 Regularization and Discretization

One way to solve (3.5) is numerically to derive the corresponding Euler-Lagrange equations, and then solve the resulting partial differential equation (PDE) numerically using available PDE solvers.

This method is effective for images because of the large number of pixels involved. However it requires the expensive solution of a PDE on each step. We will consider an alternative method based on gradient minimization. The first step is to derive the Euler-Lagrange equations.

3.3.2 Euler-Lagrange Equations for the $P_{TV}^\alpha(\rho, b)$ problem

The derivation of the Euler-Lagrange equation for the first term in (3.5) proceeds as in chapter two. For the second term,

$$\delta_\rho TV(\rho) = \delta_\rho \int_\Omega \sqrt{\left(\frac{\partial \rho}{\partial x_1}\right)^2 + \left(\frac{\partial \rho}{\partial x_2}\right)^2} dx_1 dx_2 \quad (3.6)$$

putting the δ_ρ operator inside the integral gives

$$\int_\Omega \delta_\rho \sqrt{\left(\frac{\partial \rho}{\partial x_1}\right)^2 + \left(\frac{\partial \rho}{\partial x_2}\right)^2} dx_1 dx_2$$

Applying δ_ρ gives

$$\frac{1}{2} \int_\Omega \frac{1}{\sqrt{\left(\frac{\partial \rho}{\partial x_1}\right)^2 + \left(\frac{\partial \rho}{\partial x_2}\right)^2}} \left(2 \frac{\partial \rho}{\partial x_1} \delta_\rho \frac{\partial \rho}{\partial x_1} + 2 \frac{\partial \rho}{\partial x_2} \delta_\rho \frac{\partial \rho}{\partial x_2} \right) dx_1 dx_2$$

which is rearranged to,

$$\int_\Omega \frac{\frac{\partial \rho}{\partial x_1} \delta_\rho \frac{\partial \rho}{\partial x_1}}{\sqrt{\left(\frac{\partial \rho}{\partial x_1}\right)^2 + \left(\frac{\partial \rho}{\partial x_2}\right)^2}} + \frac{\frac{\partial \rho}{\partial x_2} \delta_\rho \frac{\partial \rho}{\partial x_2}}{\sqrt{\left(\frac{\partial \rho}{\partial x_1}\right)^2 + \left(\frac{\partial \rho}{\partial x_2}\right)^2}} dx_1 dx_2$$

or

$$\int_\Omega \frac{\nabla \rho}{\sqrt{\left(\frac{\partial \rho}{\partial x_1}\right)^2 + \left(\frac{\partial \rho}{\partial x_2}\right)^2}} \cdot \delta_\rho \left(\frac{\partial \rho}{\partial x_1}, \frac{\partial \rho}{\partial x_2} \right) dx_1 dx_2$$

Green's Theorem will recast the previous integral as the sum of a boundary integral

$$\int_{\partial\Omega} \delta\rho \left(\frac{\frac{\partial\rho}{\partial x_1}}{\sqrt{\left(\frac{\partial\rho}{\partial x_1}\right)^2 + \left(\frac{\partial\rho}{\partial x_2}\right)^2}}, \frac{\frac{\partial\rho}{\partial x_2}}{\sqrt{\left(\frac{\partial\rho}{\partial x_1}\right)^2 + \left(\frac{\partial\rho}{\partial x_2}\right)^2}} \right) \cdot \vec{n} \, ds \quad (3.7)$$

and an integral over Ω

$$\int_{\Omega} \delta\rho \left(\nabla \cdot \frac{\nabla\rho}{\sqrt{\left(\frac{\partial\rho}{\partial x_1}\right)^2 + \left(\frac{\partial\rho}{\partial x_2}\right)^2}} \right)$$

The optimality condition is satisfied when

$$\begin{cases} \frac{\partial\rho}{\partial n} = 0 & \text{on } \partial\Omega \\ \nabla \cdot \left(\frac{\nabla\rho}{|\nabla\rho|} \right) = 0 & \text{in } \Omega \end{cases}$$

Thus the Euler-Lagrange equations for (3.5) are

$$\frac{\partial\rho}{\partial n} = 0 \quad \text{on } \partial\Omega \quad (3.8)$$

$$(K^*K\rho - K^*\rho) + \alpha \nabla \cdot \left(\frac{\nabla\rho}{|\nabla\rho|} \right) = 0 \quad (3.9)$$

Equation (3.9) however is unstable because of the term $1/|\nabla\rho|$. This can be overcome by regularizing,

$$|\nabla\rho| \cong \sqrt{|\nabla\rho|^2 + \beta}$$

where β is a small positive number.

The resulting PDE system to be solved is

$$\begin{cases} \frac{\partial\rho}{\partial n} = 0 & \text{on } \partial\Omega \\ (K^*K\rho - K^*\rho) + \alpha \nabla \cdot \left(\frac{\nabla\rho}{\sqrt{|\nabla\rho|^2 + \beta}} \right) = 0 & \text{in } \Omega \end{cases} \quad (3.10)$$

Different approaches have been used to solve the PDE resulting from the Euler-Lagrange equations: Time Marching (Rudin, 1992) [5], Fixed-Point lagged diffusivity iteration (Vogel, 1995) [9], Primal-Dual algorithm (Chan, 1996).

These approaches were based on particular features of the problem, available code, and mathematical orientation of the group that developed the numerical solution. Time Marching (Rudin, 1992) [5], Fixed-Point lagged diffusivity iteration (Vogel, 1995) [9], Primal-Dual algorithm (Chan, 1996).

Three common features in these algorithms are:

- i) they derive analytically the iteration equations
- ii) they discretize the resulting PDE
- iii) they use an efficient and well established PDE solver in each iteration (finite elements, finite difference, etc.).

In this, the main idea will be to discretize the parametrical functional and then regularize the finite-dimensional problem.

CHAPTER 4

DISCRETIZATION AND REGULARIZATION

The minimization problem for the inverse gravity problem using the TV functional is:

$$\min \|K\rho - b\|_2^2 + \alpha \int_{\Omega} |\nabla\rho| \, dx \quad (4.1)$$

where $|\nabla\rho| = \sqrt{\left(\frac{\partial(\rho)}{\partial x_1}\right)^2 + \left(\frac{\partial(\rho)}{\partial x_2}\right)^2}$, and Ω is the domain of integration describing earth surface domain containing underground structures of interest.

4.1 Discretization of the forward operator

In figure (4.1) we show a scheme of a discrete model commonly used in many geophysical application for the domain Ω , which presents Ω as a union of small rectangular blocks: $\Omega = \{\Omega_{(ij)}, i = 1 \dots nx_1, j = 1 \dots nx_2\}$

The adopted discretization for Ω uses rectangular blocks with their principal axes oriented in the same direction as the gravitational attraction vector and its normal defined at the reference surface (see figure 1).

The function $\rho(x)$ is a given piece-wise constant function defined as:

$$\rho(x) = \sum_{i=1}^{i=nx_1} \sum_{j=1}^{j=nx_2} \rho_{ij} \chi_{ij}(x) \, , x \in \Omega$$

where $\chi_{i,j}(x) = \begin{cases} 1, & x \in \Omega_{i,j} \\ 0, & \text{otherwise.} \end{cases}$

The vector $b = \{b_j\}$ is the discrete data measured on some part of the boundary $\partial\Omega$, b_j is the discrete observation.

From the solution of Poisson equation we have

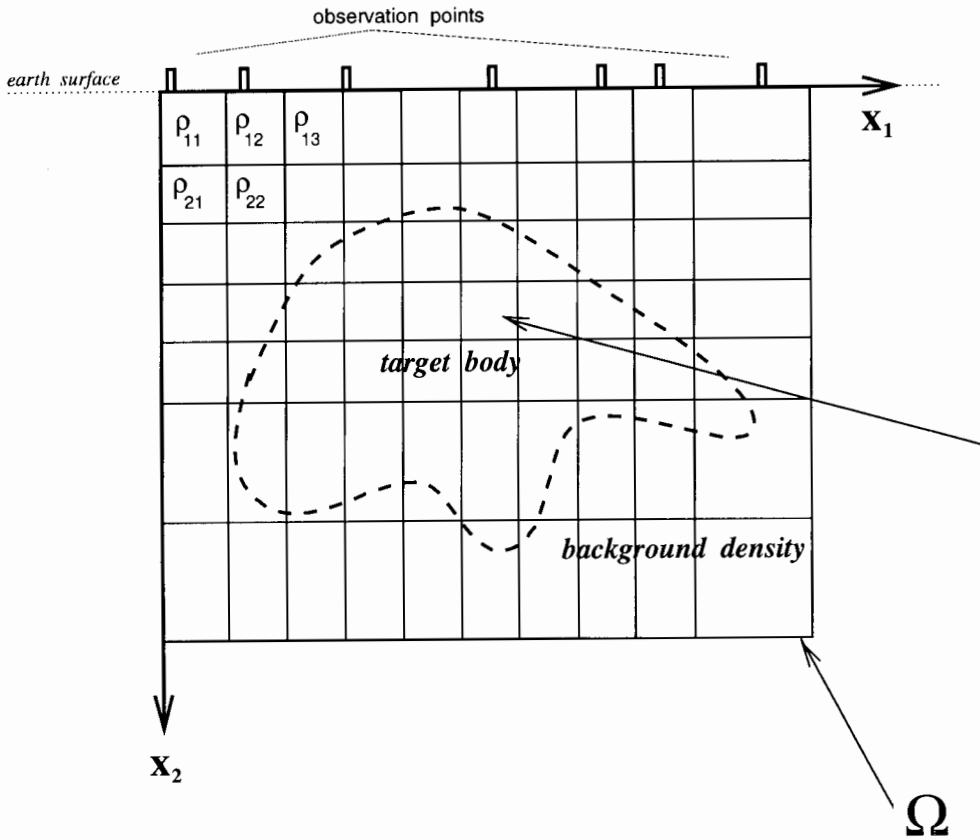


Figure 4.1. Discretization using rectangular blocks

$$\phi(y) = \gamma \int_{\Omega} \rho(x) \frac{1}{r} d\Omega = K(\rho)$$

and

$$\mathbf{g}(y) = \nabla\phi = \gamma \int_{\Omega} \rho(x) \nabla \frac{1}{r} d\Omega$$

As gravimeters measure the vertical component of the vector of gravity, the measured function is

$$b = \gamma \int_{\Omega} \frac{\partial}{\partial x_2} \frac{1}{r} \rho(x) d\Omega \quad (4.2)$$

The evaluation of this integral for different geometries is very well known, some examples are [18], [29]. A common approach to integrate (4.2) along the (x_3) axis in which ρ has constant density.

Then we obtain

$$b = \gamma \int_S \frac{\partial}{\partial x_2} \log \frac{1}{r} \rho(x) dS = \gamma \int_S f(x_1, x_2) dS$$

Using the observation that this surface integration is equivalent to a two-step integration around the boundary of the surface (F_x) , we have

$$b = \int_S f(x_1, x_2) dS = \oint_{\partial S} F_x(x_1, x_2) dx_2 \quad (4.3)$$

The numerical solution of (4.3) for a rectangular prism can be found in [18], [29], etc. and can be written as

$$b = 2\gamma \left[D\theta_2 - d\theta_1 - x \log \left(\frac{r_1 r_4}{r_2 r_3} \right) + b \log \left(\frac{r_4}{r_3} \right) \right] \rho \quad (4.4)$$

Figure 4.2 shows the quantities in (4.4).

Let b_j be discrete data in the observation point j , $j = 1, \dots, m$ and ρ_l be constant density inside the block l , $l = nx_1(i-1) + j$, for the block Ω_{ij} . Using matrix notation we can write

$$K(\rho) = \begin{pmatrix} k_{11} & \cdot & \cdot & k_{1n} \\ \cdot & \cdot & \cdot & \cdot \\ \cdot & \cdot & \cdot & \cdot \\ \cdot & \cdot & \cdot & \cdot \\ \cdot & \cdot & \cdot & \cdot \\ k_{m1} & \cdot & \cdot & k_{mn} \end{pmatrix} \begin{pmatrix} \rho^1 \\ \cdot \\ \cdot \\ \cdot \\ \rho^n \end{pmatrix} = \begin{pmatrix} b^1 \\ \cdot \\ \cdot \\ \cdot \\ \cdot \\ b^m \end{pmatrix} \quad (4.5)$$

where

$$k_{lj} = 2\gamma \left[D\theta_2 - d\theta_1 - x \log \left(\frac{r_1 r_4}{r_2 r_3} \right) + b \log \left(\frac{r_4}{r_3} \right) \right]$$

and the values of $b, D, r_1, r_2, r_3, r_4, \theta_1$ and θ_2 are shown in figure 4.2

4.2 Discretization of the TV semi-norm

In figure 4.1 the unknown density $\rho(x)$ is defined in a 2D domain, with $x = (x_1, x_2)$ and $\rho(x) = \rho(x_1, x_2)$. Representing the forward operator K in matrix form in the previous subsection we converted $\rho(x_1, x_2)$ in a 1D vector, using row-by-row ordering. We will use the same convention for the calculation of the discrete derivatives operators for the TV semi-norm in the second term of (4.1).

Figure 4.3 shows the row and column order in the 2D discretization.

In matrix notation we can write ρ as

$$\begin{pmatrix} \rho_{11} & \cdot & \cdot & \rho_{1X} \\ \cdot & \cdot & \cdot & \cdot \\ \cdot & \cdot & \cdot & \cdot \\ \cdot & \cdot & \cdot & \cdot \\ \cdot & \cdot & \cdot & \cdot \\ \rho_{Z1} & \cdot & \cdot & \rho_{ZX} \end{pmatrix}$$

where $X = nx_1$ are the number of blocks in the x_1 direction and $Z = nx_2$ are the number of blocks in the x_2 direction.

The 1D vector representation of is $\rho = [\rho_1, \rho_2 \cdots \rho_n]^T$, $n = nx_1 * nx_2$ and for $l = nx_1(i-1) + j$, $\rho_l = \rho_{ij}$ with ρ_{ij} be the density of the block Ω_{ij} :

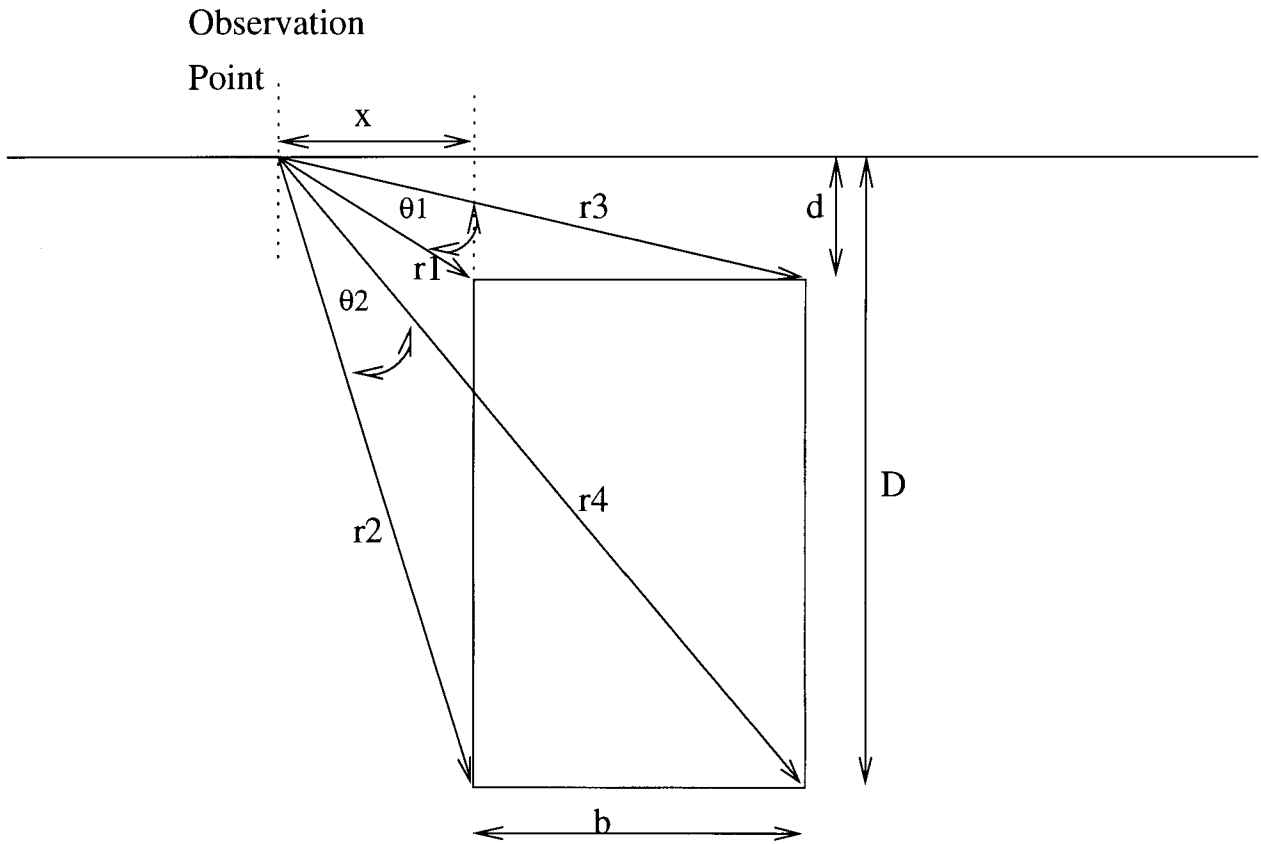


Figure 4.2. Quantities for calculation of a prism gravity effect

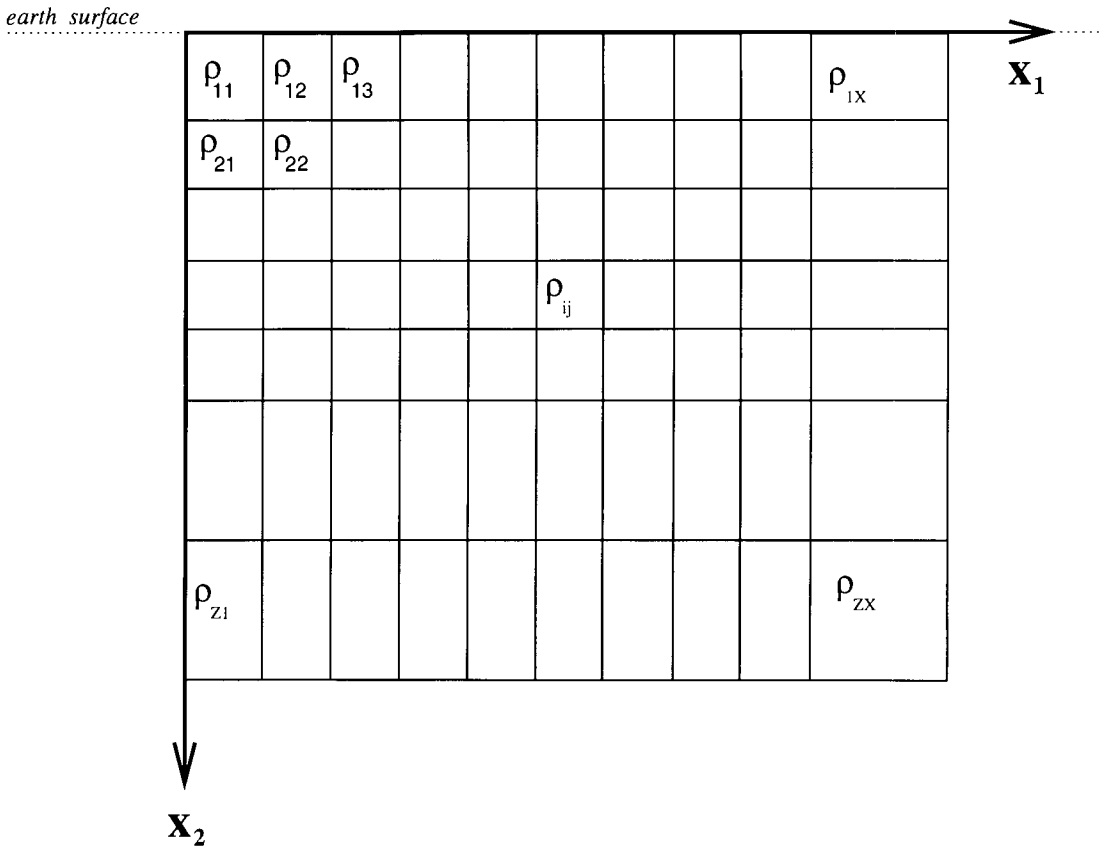


Figure 4.3. Row and Column order in the 2D discretization

$$\rho = \begin{pmatrix} \rho_{11} \\ \rho_{12} \\ \cdot \\ \rho_{1X} \\ \rho_{21} \\ \cdot \\ \cdot \\ \rho_{ZX} \end{pmatrix}$$

4.2.1 Discrete horizontal and vertical derivative operators

The horizontal and vertical direction the discrete derivative of the density distribution function at the point i, j can be written

$$\left(\frac{\partial(\rho)}{\partial x_1} \right)_{i,j} \cong \frac{\rho_{i,j} - \rho_{i,j+1}}{\Delta x_1}$$

and

$$\left(\frac{\partial(\rho)}{\partial x_2} \right)_{i,j} \cong \frac{\rho_{i,j} - \rho_{i+1,j}}{\Delta x_2}$$

where Δx_1 and Δx_2 are the block lengths in x_1 and x_2 directions.

We can build a discrete derivative operator DX_1 for the horizontal direction using the matrix

$$i \text{ row.} \rightarrow \begin{pmatrix} \cdot & \cdot & \cdot & \cdot & \cdot \\ \cdot & \cdot & \cdot & \cdot & \cdot \\ 0 & \frac{1}{\Delta x_1} & -\frac{1}{\Delta x_1} & 0 & 0 \\ \cdot & \cdot & \cdot & \cdot & \cdot \\ \cdot & \cdot & \cdot & \cdot & \cdot \\ \cdot & \cdot & \cdot & \cdot & \cdot \end{pmatrix} \begin{pmatrix} \rho_{11} \\ \cdot \\ \cdot \\ \rho_{ij} \\ \cdot \\ \cdot \\ \cdot \\ \rho_{ZX} \end{pmatrix} = \begin{pmatrix} \cdot \\ \cdot \\ \cdot \\ \frac{\rho_{i,j} - \rho_{i,j+1}}{\Delta x_1} \\ \cdot \\ \cdot \\ \cdot \\ \cdot \end{pmatrix}$$

Then having denoted this matrix as DX_1 we can write

$$\left(\frac{\partial(\rho)}{\partial x_1}\right) \cong DX_1 \begin{pmatrix} \rho_{11} \\ \cdot \\ \cdot \\ \rho_{ij} \\ \cdot \\ \cdot \\ \cdot \\ \rho_{ZX} \end{pmatrix} \quad (4.6)$$

And we can build a discrete derivative operator DX_2 for the vertical direction using the following matrix:

$$\begin{pmatrix} \cdot & \downarrow^{j \text{ col}} & \cdot & \downarrow^{j+1 \text{ col}} & \cdot \\ \cdot & \cdot & \cdot & \cdot & \cdot \\ 0 & \frac{1}{\Delta x_2} & 0 & -\frac{1}{\Delta x_2} & 0 \\ \cdot & \cdot & \cdot & \cdot & \cdot \\ \cdot & \cdot & \cdot & \cdot & \cdot \\ \cdot & \cdot & \cdot & \cdot & \cdot \end{pmatrix} \begin{pmatrix} \rho_{11} \\ \cdot \\ \cdot \\ \rho_{ij} \\ \cdot \\ \cdot \\ \cdot \\ \rho_{ZX} \end{pmatrix} = \begin{pmatrix} \cdot \\ \cdot \\ \cdot \\ \frac{\rho_{i,j} - \rho_{i,j+1}}{\Delta x_2} \\ \cdot \\ \cdot \\ \cdot \\ \cdot \end{pmatrix}$$

Hence

$$\left(\frac{\partial(\rho)}{\partial x_2}\right) \cong DX_2 \begin{pmatrix} \rho_{11} \\ \cdot \\ \cdot \\ \rho_{ij} \\ \cdot \\ \cdot \\ \cdot \\ \rho_{ZX} \end{pmatrix} \quad (4.7)$$

Using the derivatives operators for the horizontal and vertical directions (eqs. (4.6) and (4.7)) we can write the discrete total variation operator:

$$TV(\rho) \cong \sum_{ij} \sqrt{[DX_1(\rho)]_{ij}^2 + [DX_2(\rho)]_{ij}^2} \Delta x_1 \Delta x_2 \quad (4.8)$$

Now the discrete parametrical functional with a Total Variational functional can be written as

$$P_{dTV}^\alpha = \|K\rho - b\|_2^2 + \alpha \sum_{ij} \sqrt{[DX_1(\rho)]_{ij}^2 + [DX_2(\rho)]_{ij}^2} \Delta x_1 \Delta x_2 \quad (4.9)$$

and we want to minimize this functional with respect to ρ : $P_{dTV}^\alpha \rightarrow \min$.

4.3 Discrete calculation of variation of the TV semi-norm

Using the approximation of the first derivative of (4.8) the TV semi-norm can be evaluated at the cell kl as

$$\frac{\partial TV(\rho)}{\partial \rho_{kl}} \simeq \frac{1}{\delta \rho} TV(\rho + \eta^{kl} \delta \rho) - TV(\rho) \quad (4.10)$$

where $\eta_{ij}^{kl} = \begin{cases} 1, & \text{if } i = k, j = l \\ 0, & \text{otherwise} \end{cases}$ and $\delta \rho$ is a smaller number.

Substituting (4.8) in (4.10) we obtain the following expression,

$$\begin{aligned} \frac{\partial TV(\rho)}{\partial \rho_{kl}} \simeq & \\ & \frac{1}{\delta \rho} \left[\left\{ \sum_{ij} [DX_1(\rho + \eta^{kl} \delta \rho)]_{ij}^2 + \right. \right. \\ & \left. \left. [DX_2(\rho + \eta^{kl} \delta \rho)]_{ij}^2 \right\}^{\frac{1}{2}} \Delta x_1 \Delta x_2 - \right. \\ & \left. \sum_{ij} \left\{ [DX_1(\rho)]_{ij}^2 + [DX_2(\rho)]_{ij}^2 \right\}^{\frac{1}{2}} \Delta x_1 \Delta x_2 \right] \quad (4.11) \end{aligned}$$

The discrete Euler-Lagrange equations are

$$0 = \frac{\partial \rho}{\partial n} \quad \text{on } \partial \Omega$$

$$0 = l^\alpha(\rho) = (\widetilde{K}^* \widetilde{K} \rho - \widetilde{K}^* \hat{b}) +$$

$$\alpha \frac{1}{\delta \rho} \left[\left\{ \sum_{ij} [DX_1(\rho + \eta^{kl} \delta \rho)]_{ij}^2 + \right. \right.$$

$$\left[DX_2 \left(\rho + \eta^{kl} \delta_\rho \right) \right]_{ij}^2 \}^{\frac{1}{2}} \Delta x_1 \Delta x_2 -$$

$$\sum_{ij} \left\{ [DX_1(\rho)]_{ij}^2 + [DX_2(\rho)]_{ij}^2 \right\}^{\frac{1}{2}} \Delta x_1 \Delta x_2 \quad \text{in } \Omega$$

4.4 Solving the Euler-Lagrange equations

This work examined three different choices for the Tikhonov stabilization functional: a minimum norm operator, a 2D first derivative operator, and 2D Total Variation operator. Solutions for each individual problem could be obtained exploiting the individual structure of the specific problem in each situation, such as being linear, quadratic, etc.

Instead an algorithm was developed to solve the minimization problems for all the different parametrical functionals in a way that avoids particular computational difficulties for each case. The adaptive gradient minimization developed in this work fits the above requirements.

The algorithm minimize the parametrical functional for a fixed value of α then α is reduced using decreasing criteria. The iterations are performed until the stopping criteria are reached.

The gradient based algorithm can be summarized as follows:

take $\alpha = \alpha_L$ and $\rho = \rho_0$

do until stopping criteria for α ([14],[30],[15])

do until stopping criteria for ρ_{k+1} ([14],[30],[15])

set $(\rho_{k+1}) = \rho_k - \xi_k^\alpha g^\alpha(\rho_k)$

find ξ_k^α from $P^\alpha(\rho_{k+1}) = P^\alpha(\rho_k - \xi_k^\alpha g^\alpha(\rho_k)) = \min$

end do ρ_{k+1}

choose new α by decreasing criteria ([14],[30],[15])

end do α

Here α_L is a regularization parameter which should have the "right" size for the problem being solved. Too big an initial choice for α_L will make the minimization process slow and too small a value will make it unstable.

ρ_0 is a prior model. This is one critical point in the algorithm. Usually this prior model is provided from previous geological or geophysical study in the area. In this work we focus our attention on non-smooth geological structures.

ξ_k^α is the step length at the iteration k for a fixed value of α .

ρ_k is the value of the density function at the iteration k .

The importance of the prior model can be seen from the fact that *regularization is a smart way to introduce information to solve the ill-posed problem* [14]. Also important is the *smart* selection of the stabilization functional, which reflects the properties of the expected solution.

Three criteria are involved in the algorithm: stopping criteria for $[\alpha]$, stopping criteria for $[\rho_{k+1}]$, and decreasing criteria for $[\alpha]$, and they are based on the same common condition. Actions are taken (stop or decrease, etc.) when no improvements are verified in the solution for the density function. Some heuristic criteria were implemented to ensure this condition, they are small variation of the norm of the solution over several iterations, number of iterations, etc..

The following minimization is performed for each parametric functional,

$$\text{set } (\rho_{k+1}) = \rho_k - \xi_k^\alpha g^\alpha(\rho_k);$$

$$\text{find } \xi_k^\alpha \text{ from } P^\alpha(\rho_{k+1}) = P^\alpha(\rho_k - \xi_k^\alpha g^\alpha(\rho_k)) = \min$$

where P^α can be:

- $P_I^\alpha = \|K \rho - b\|_2^2 + \alpha \|I \rho\|$

- $P_{2D\nabla}^\alpha = \|K \rho - b\|_2^2 + \alpha \left(\left\| \frac{\partial \rho}{\partial x_1} \right\|_2^2 + \left\| \frac{\partial \rho}{\partial x_2} \right\|_2^2 \right)$

and

- $P_{2DTV}^\alpha = \|K \rho - b\|_2^2 + \alpha \sum_{ij} \sqrt{[DX_1(\rho)]_{ij} + [DX_2(\rho)]_{ij}} \Delta x_1 \Delta x_2$

The gradient $g^\alpha(\rho_k)$ of the parametrical functionals are, respectively,

$$g_I^\alpha(\rho_k) = \widetilde{K}^T (\widetilde{K} \rho - b) + \alpha I \rho$$

or

$$g_{2D\nabla}^\alpha(\rho_k) = \widetilde{K}^T (\widetilde{K} \rho - b) + \alpha (DX_1^T DX_1 + DX_2^T DX_2) \rho$$

or

$$g_{2DTV}^\alpha(\rho_k) = \widetilde{K}^T (\widetilde{K} \rho - b) + \alpha \frac{1}{\delta_\rho} \left[\left\{ \sum_{ij} [DX_1(\rho + \eta^{kl} \delta_\rho)]_{ij} + [DX_2(\rho + \eta^{kl} \delta_\rho)]_{ij} \right\}^{\frac{1}{2}} \Delta x_1 \Delta x_2 - \sum_{ij} \left\{ [DX_1(\rho)]_{ij} + [DX_2(\rho)]_{ij} \right\}^{\frac{1}{2}} \Delta x_1 \Delta x_2 \right]$$

where again

$$\eta_{ij}^{kl} = \begin{cases} 1, & \text{if } i = k, \quad j = l \\ 0, & \text{otherwise.} \end{cases}$$

For all functionals the adaptive gradient minimization performs the evaluation of the solution usually in less than a couple of minutes in the worst case (for the

largest discretizations, 240 cells). A typical convergence results for this algorithm is shown in figure 4.4.

This code was written in Matlab and is highly vectorized. A user friendly interface is under development.

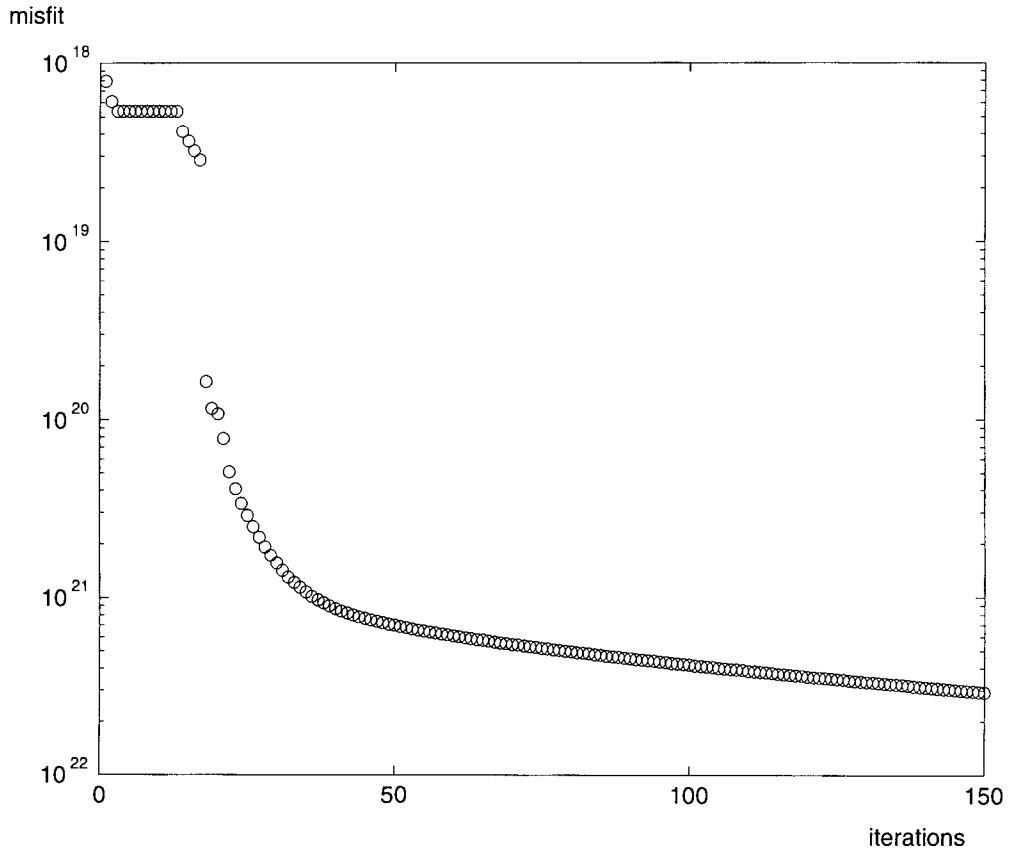


Figure 4.4. Convergence results

CHAPTER 5

ANALYSIS OF THE NUMERICAL RESULTS

5.1 Model considerations

The numerical results that follow were calculated for a piecewise density function that exhibits sharp density contrast and sharp edges (figure 5.1). This model was previously used in (Bassrei, 1993 [1]), where the author analyzes smooth regularization techniques, minimizing the second differences of the model parameters. The observations are performed on the earth surface in 20 stations aligned on the horizontal direction (x_1).

We will consider initially only computer noise added during the computing of the numerical solution, avoiding particular noise distributions influencing the inversion results. The regularization parameter was allowed to decrease until no improvement in the solution was obtained due to the presence of low level amplitude noise.

Discretization plays an important role in the inverse gravimetric problem, because in its continuous form this problem is already ill-posed. As shown in chapter 2, it will become even more ill-posed with the increasing the number of discretization cells. Hence regularization is required in order to obtain a stable solution ([14],[15]).

5.2 General Inversion results for large discretizations

Figure 5.2 shows an attempt to recover the density function when no regularization is used. The domain is divided in 240 cells, which turns the problem into highly ill-posed one. The result in figure 5.2 shows the correct amplitude of the recovered density function, but physically has no meaning.

Results of inversion using the 2D first derivative operator are shown in figure 5.3 and is an important improvement in the physical solution, when compared with figure 5.2. But this method fails to recover the non-smooth original density function distribution.

A second important improvement is shown in the next result (figure 5.4) , when for the same discretization, we use the minimization of the Total Variation of the density function. A closer image to the original non-smooth function is recovered due to the fact that the TV functional does not penalize sharp density contrast.

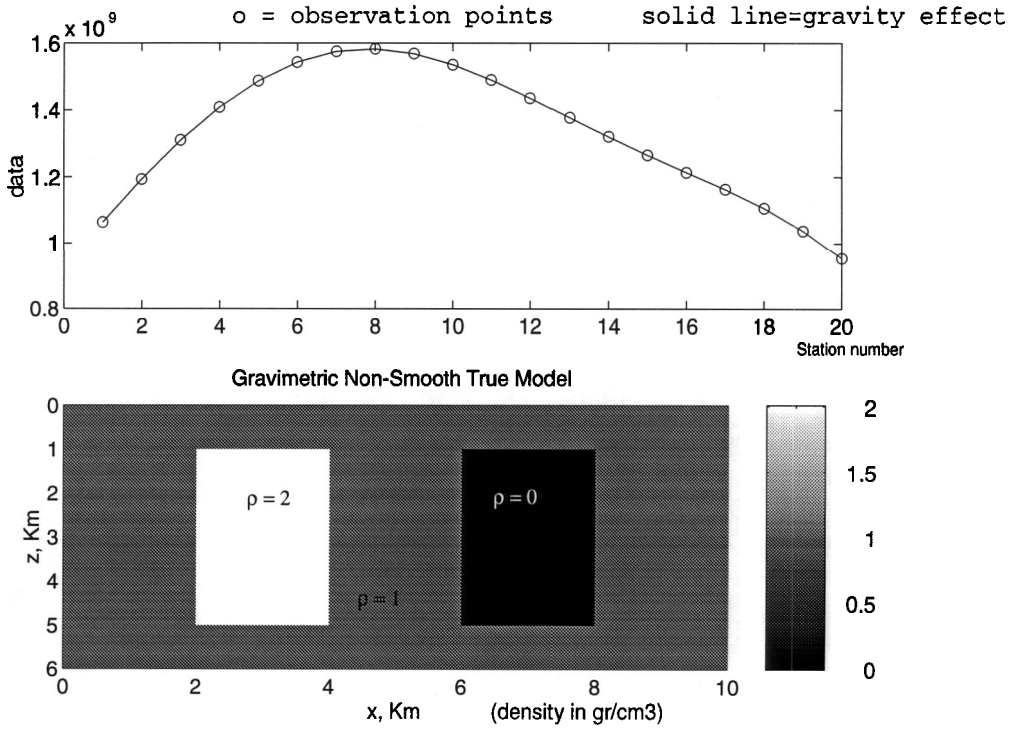


Figure 5.1. Non-Smooth density model

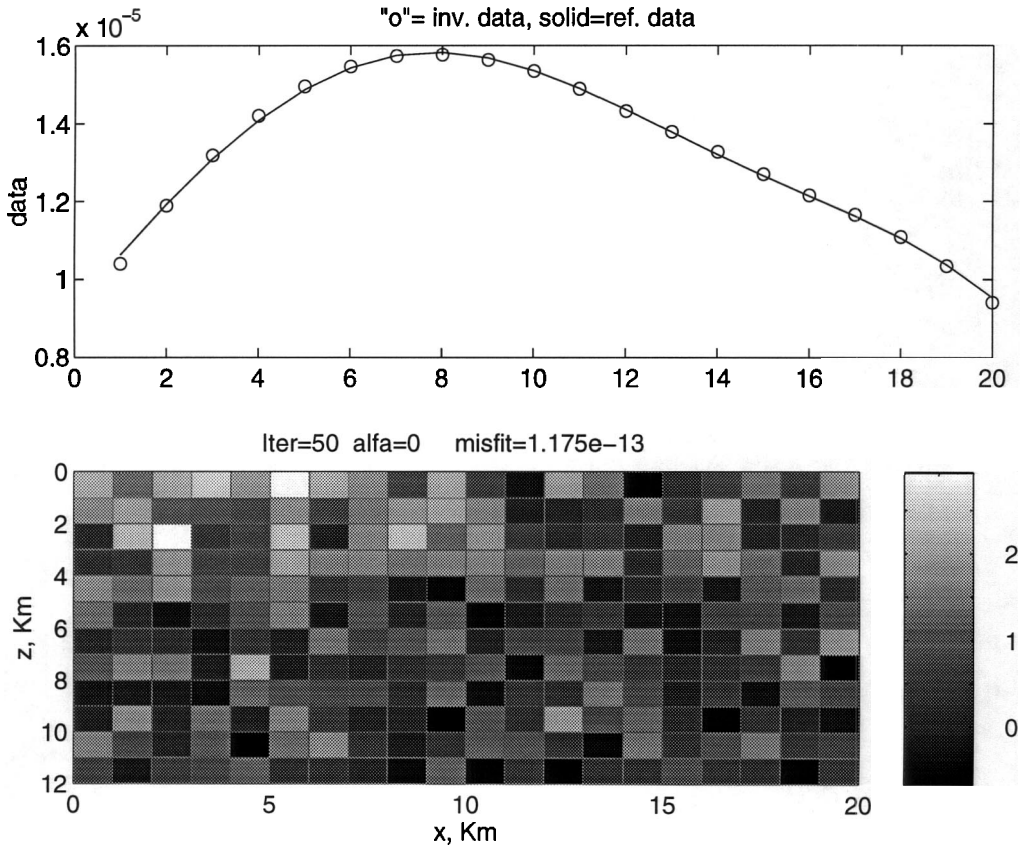


Figure 5.2. Solution for a Non-Regularized scheme

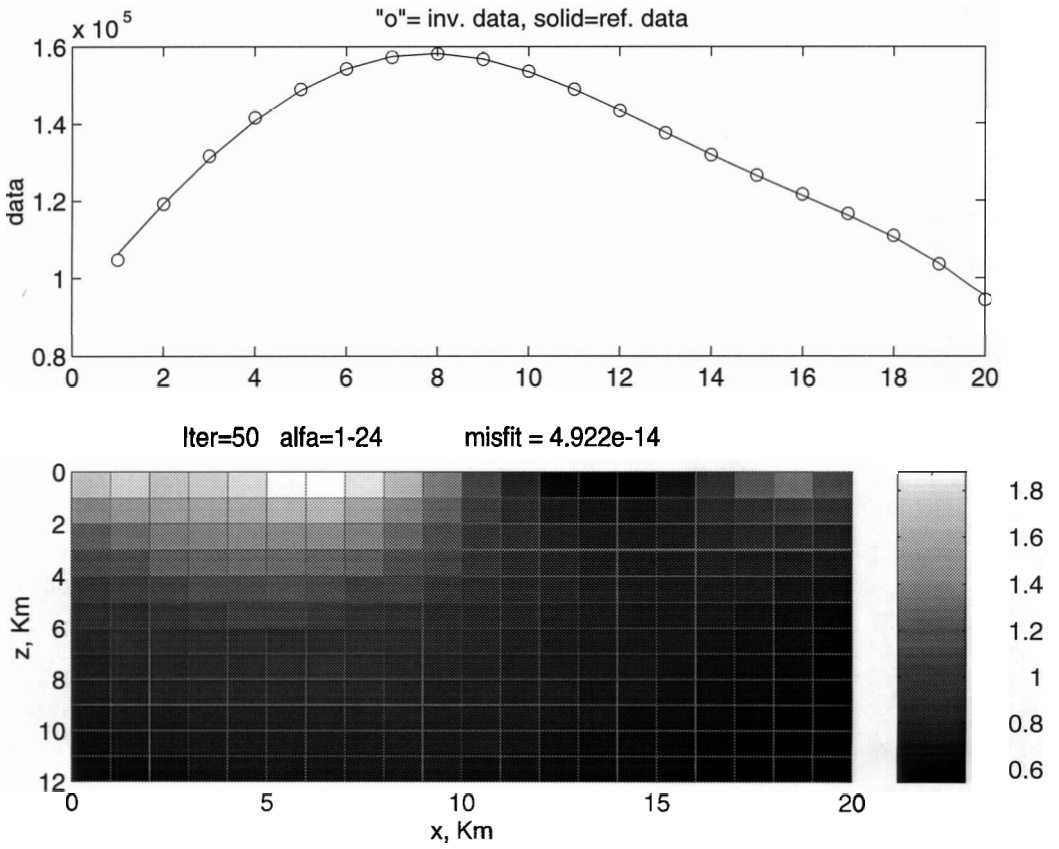


Figure 5.3. Solution for a 2D First Derivative scheme

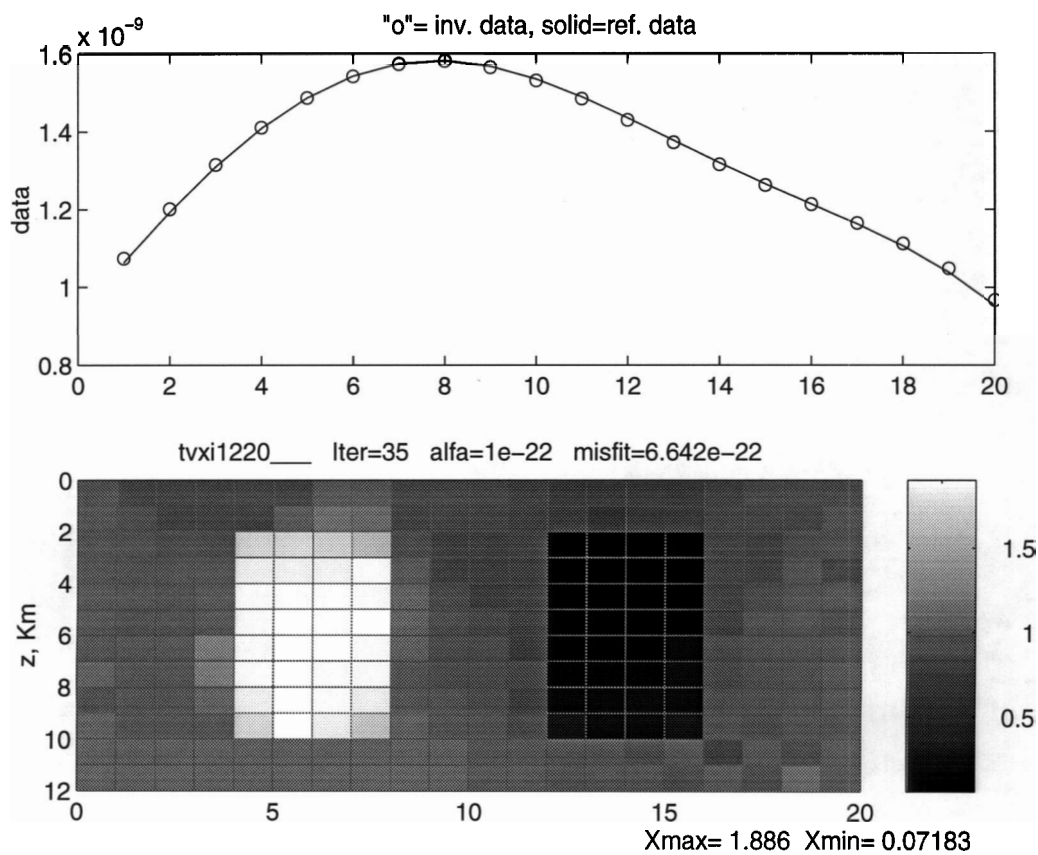


Figure 5.4. Solution for a 2D Total Variation Scheme

5.2.1 Comparison of the inversion schemes

A better understanding of the different regularization schemes and their solutions are given by the following results, which use the true density of the model as the starting point in the inversion procedure. A reduced discretization (60 blocks instead of 240) is used to improve the resolution for the smoothing regularization operators.

5.2.2 Smooth regularization results

Figure 5.5 shows the initial function density distribution used in the adaptive gradient minimization when a minimum norm and a 2D derivative operator are used as stabilizers in Tikhonov parametrical functional.

Figure 5.6 and figure 5.7 show the distribution of the density in the beginning of the iterative minimization process when a big penalty is imposed. This destroys all information about the solution by smoothing the density function during these iterations. Also, no improvement is observed in the misfit functional due to the large value of the regularization factor. Figure 5.6 shows the result for the case of the minimum norm used as a stabilizer, and figure 5.7 shows the results in the case of the 2D first derivative operator taken as the stabilization functional.

The density distributions are very smooth, which show these types of regularization destroy information about non-smooth features of the solution.

When the regularization factor is small enough, an improvement in comparison with previous iterations starts to be seen in the misfit. Figure 5.8 shows an intermediate result for the 2D first derivative stabilizer.

Figure 5.9 and figure 5.10 show the final result for the two inversion schemes, with the minimum norm stabilizer and 2D first derivative stabilizer, respectively. These results were obtained using regularization, and they better express feasible physical features than when no regularization is used (fig. 5.2). However these results did not preserve the non-smooth information that was contained in the starting point. Even when the starting point was the true density distribution function the solution

constructed in the process of minimization of the parametrical functional is very smooth.

As it was mentioned before, there are many practically important situations where non-smooth density distributions give a better picture of the earth model. Initial models presenting these features are often available from previous research in the area, but as it was shown by the previous results, smoothing techniques would not preserve this information.

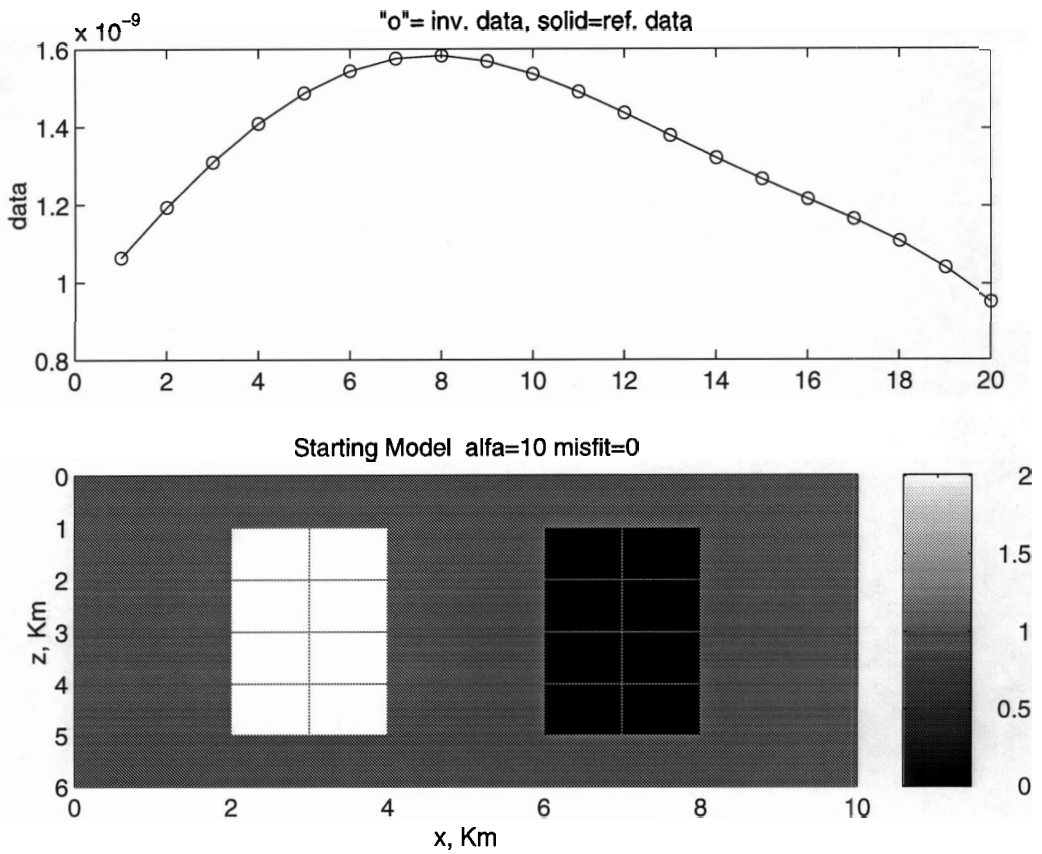


Figure 5.5. True initial density function

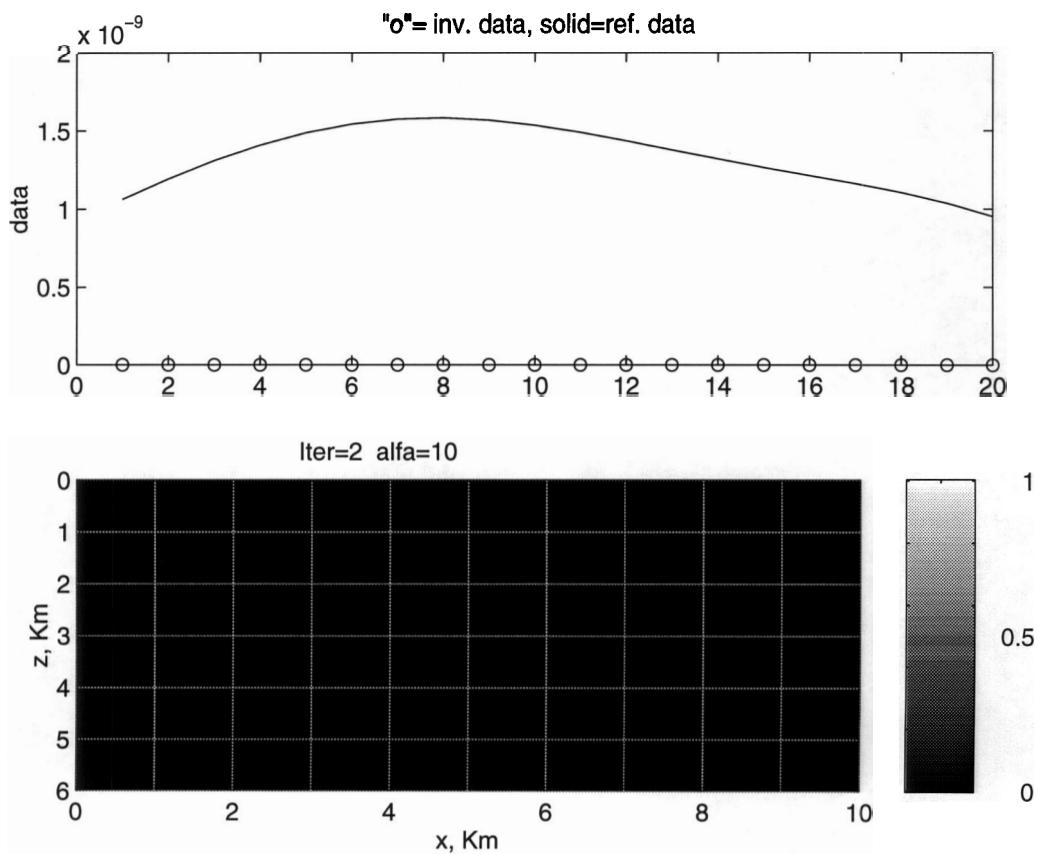


Figure 5.6. Minimum Norm Stabilizer, second iteration

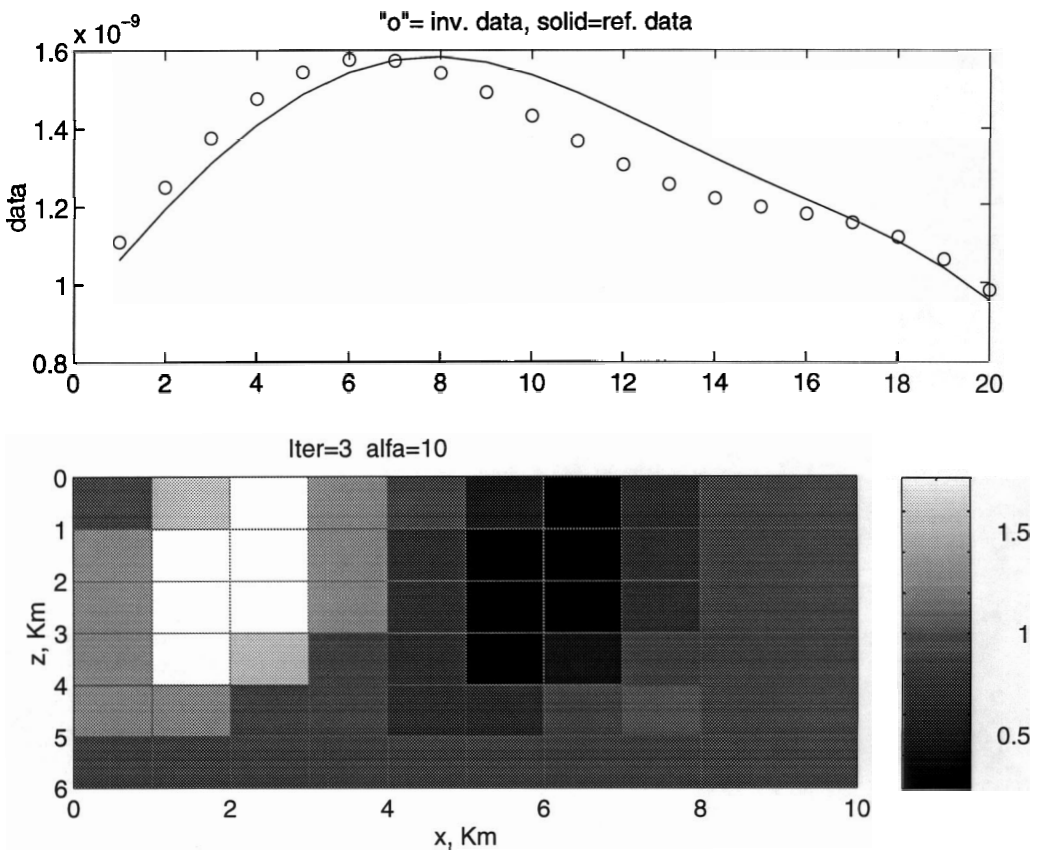


Figure 5.7. 2D First Derivative operator, third iteration

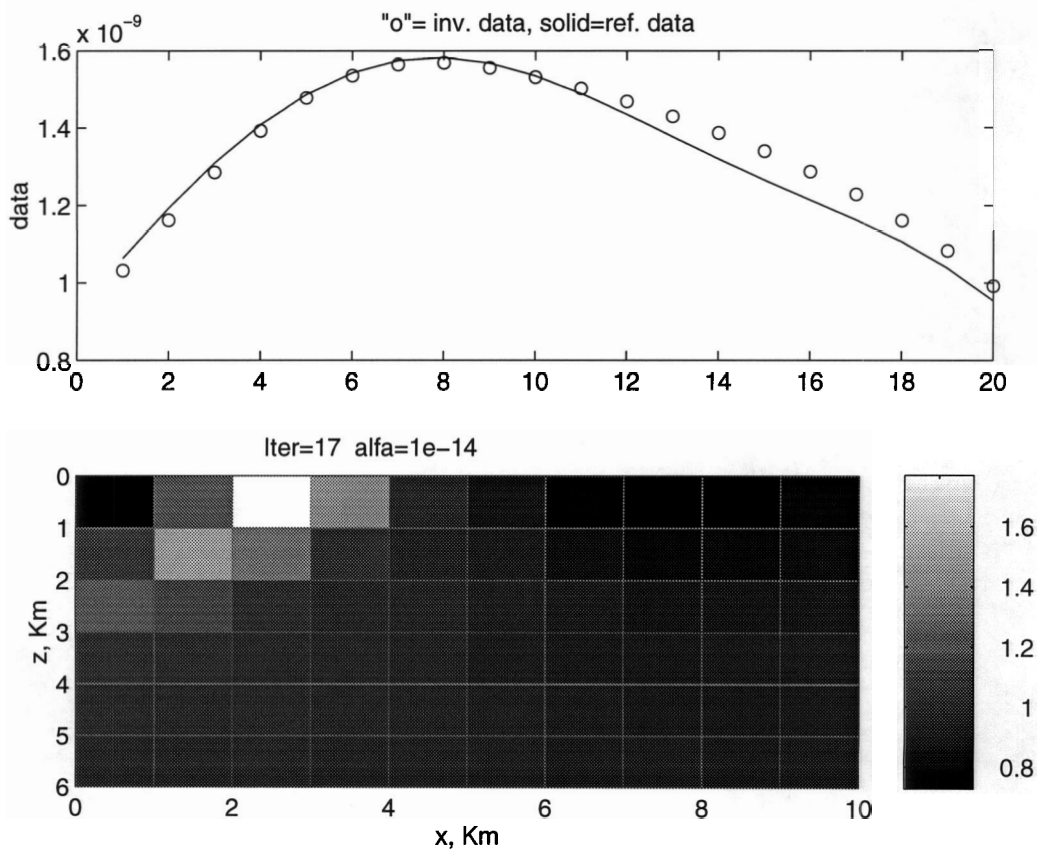


Figure 5.8. Intermediate smooth iteration (2D grad. stabilizer)

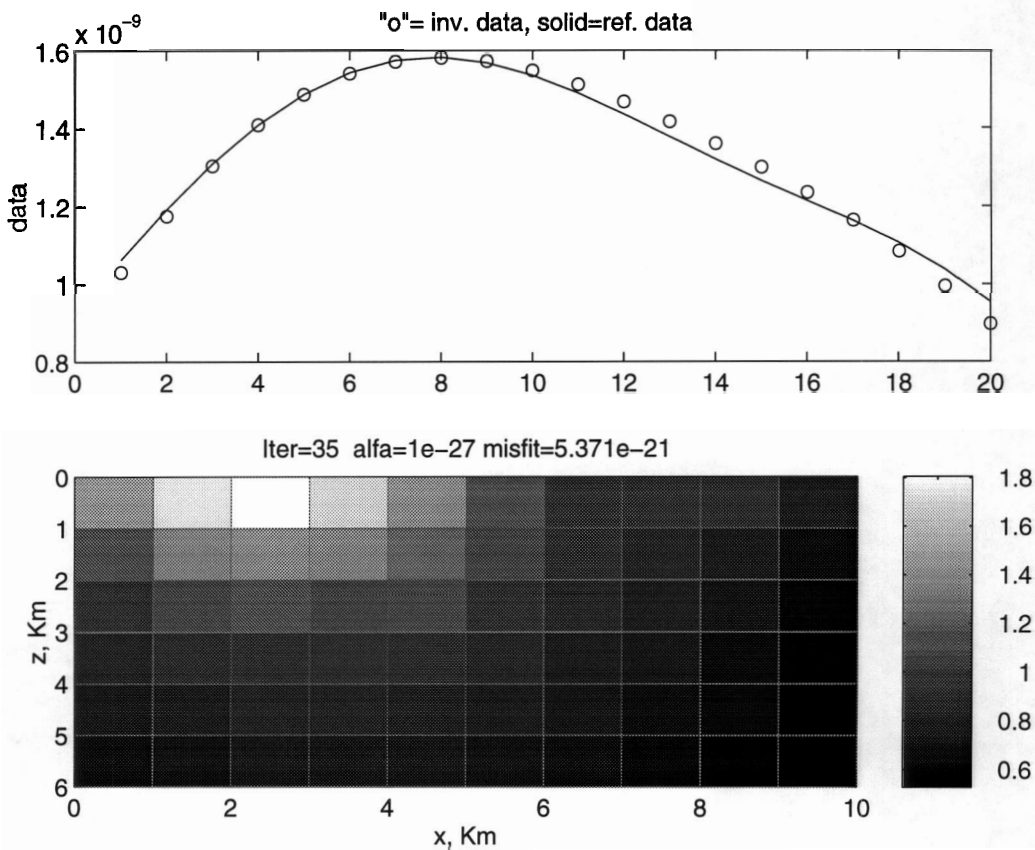


Figure 5.9. Minimum Norm Stabilizer, final iteration

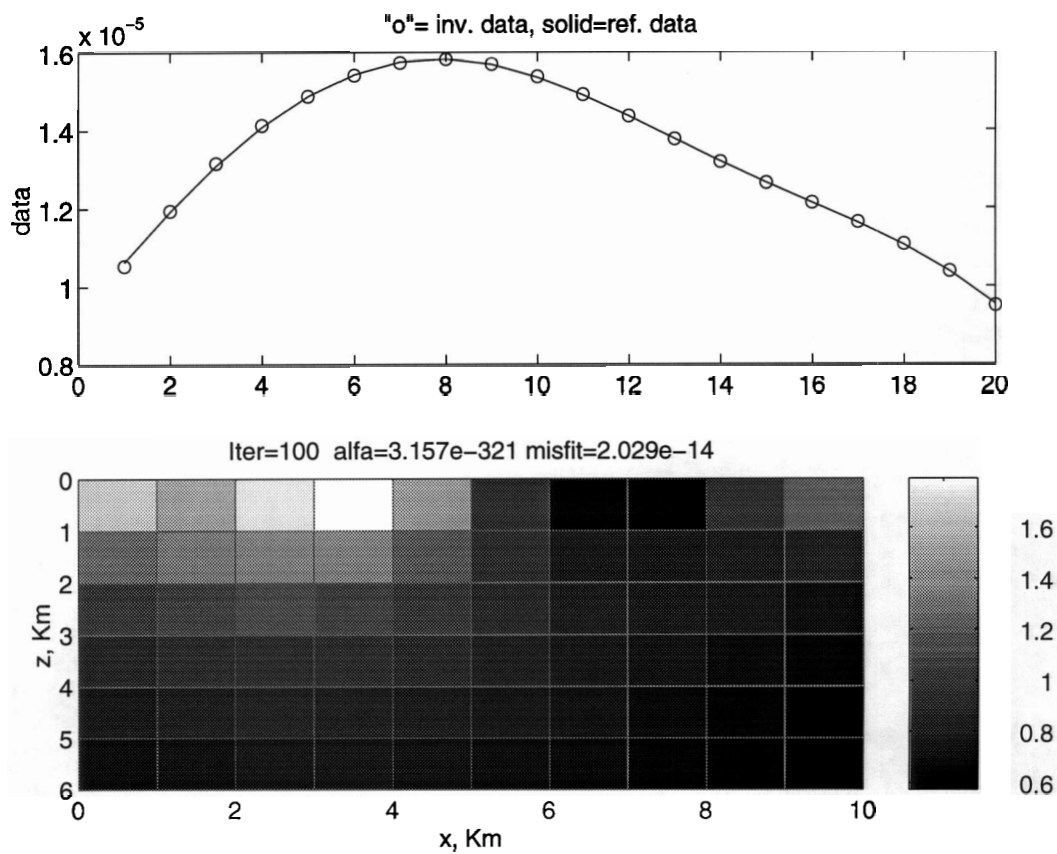


Figure 5.10. 2D First Derivative operator, final iteration

5.2.3 Non-smooth regularization results

Results presented in the previous section show that the penalty term will smooth the solution for large values of the regularization parameter, destroying the information even when we started from the true solution.

5.2.4 Large Discretization

In the next figures we show the results of the minimization of the Total Variation norm of the solution. The chosen initial model was finely discretized (240 cells) and it was an approximation of the true solution with 25% noise added (figure 5.11).

Fine discretization does not affect TV results, as much as the previously analyzed schemes do due to the fact that there is no smoothness requirement imposed on the solution.

Figure 5.12 shows the density distribution at the beginning of the adaptive gradient minimization. In the fifth iteration no improvement is made in the misfit due to the large value of the regularization factor. However, most of the noise in the solution is removed, preserving non-smooth information from the previous steps. The eventual minimization of the data misfit preserves those features (figure 5.16).

5.2.5 Reduced discretization

The next result presents a less ill-posed problem, with only 60 cells in the discretization of the model, but with smoothing because of the discrete approximation of the TV semi-norm. A starting model containing very poor a priori information is used.

The initial model is shown in figure 5.14.

Iteration 14 in the minimization of the total variation of the density function is shown in figure 5.15. The model still reflects the a priori information in "building" a non-smooth solution. Figure 5.16 shows the final result. The discrete approximation of the TV on a coarse grid introduces some smoothness in the solution, but still gives a "flatter" model than standard regularization schemes.

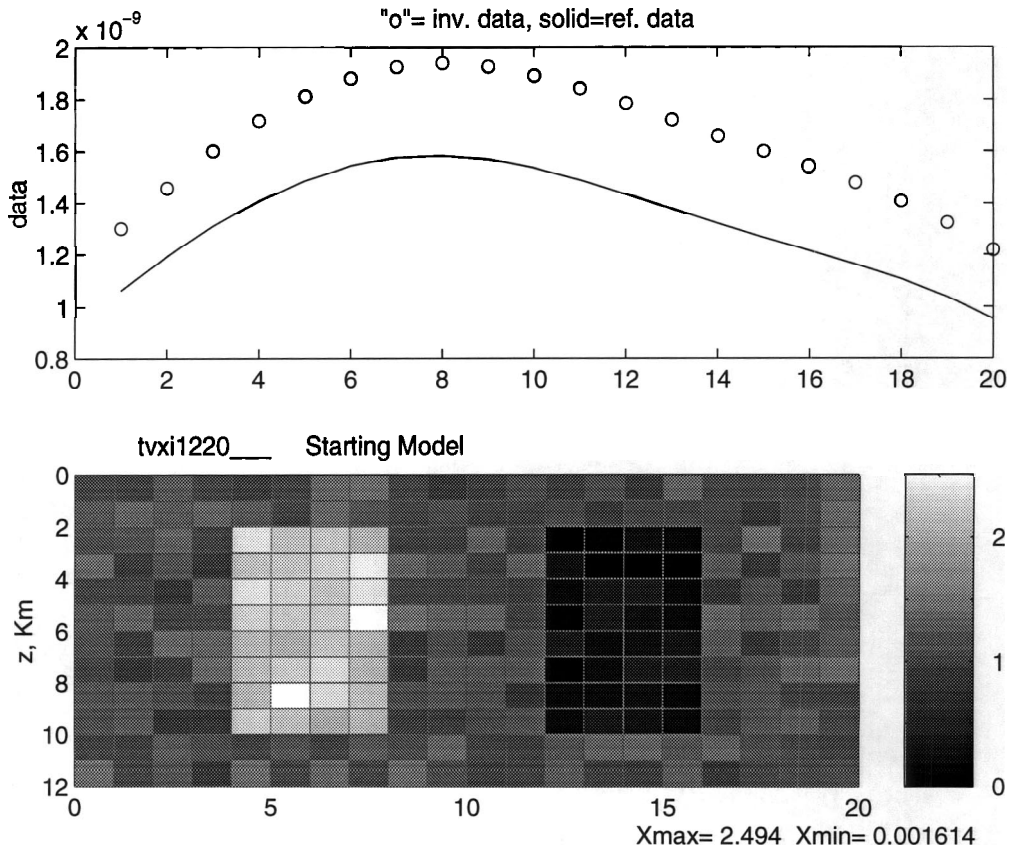


Figure 5.11. TV semi-norm Stabilizer, starting model (240 cells)

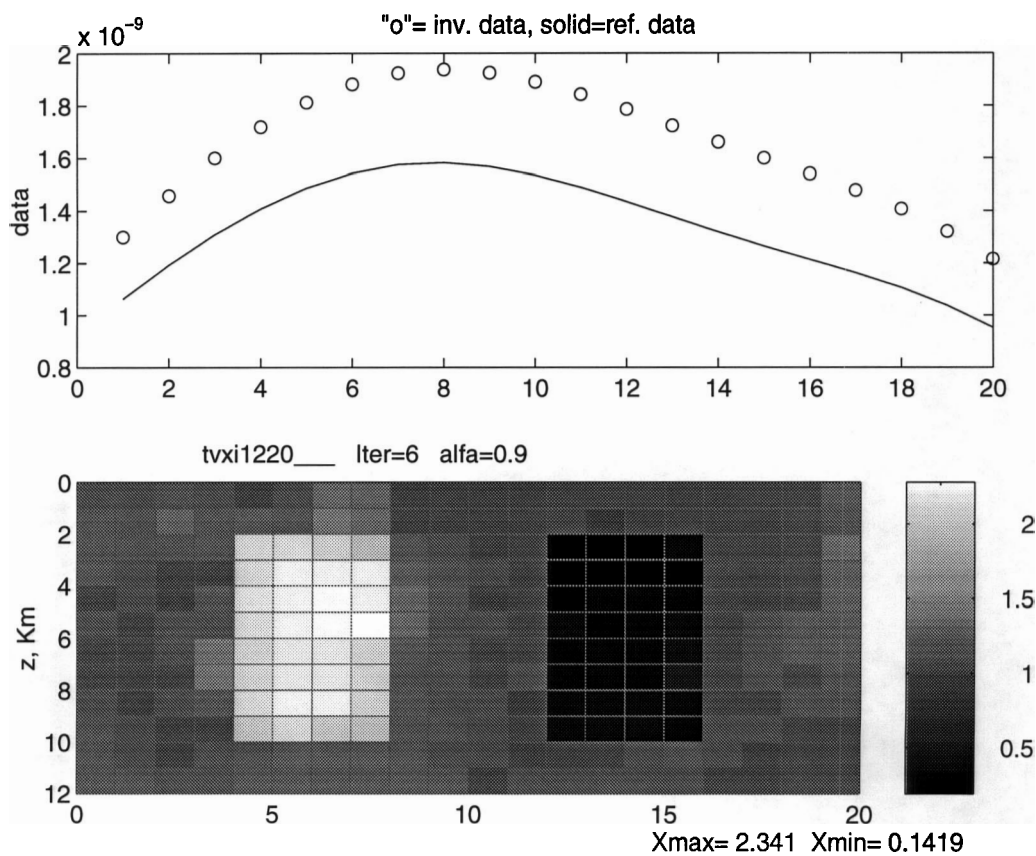


Figure 5.12. TV semi-norm stabilizer, intermediate iteration (240 cells)

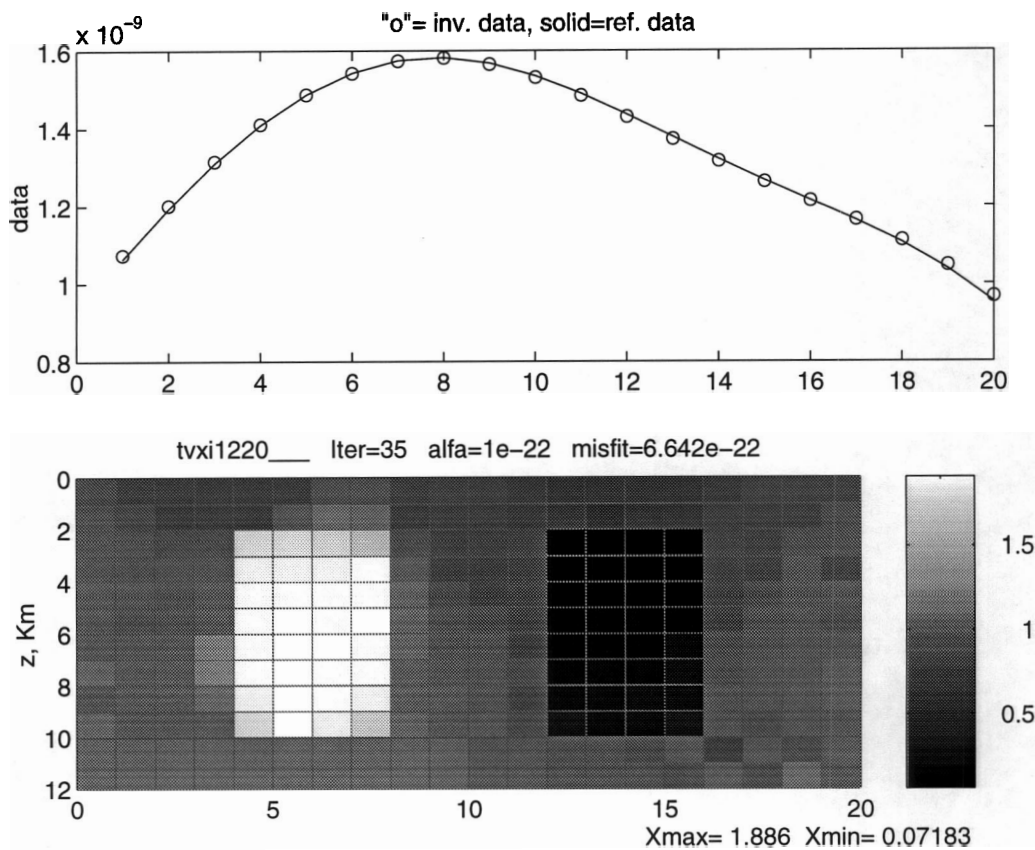


Figure 5.13. TV semi-norm stabilizer, final solution (240 cells)

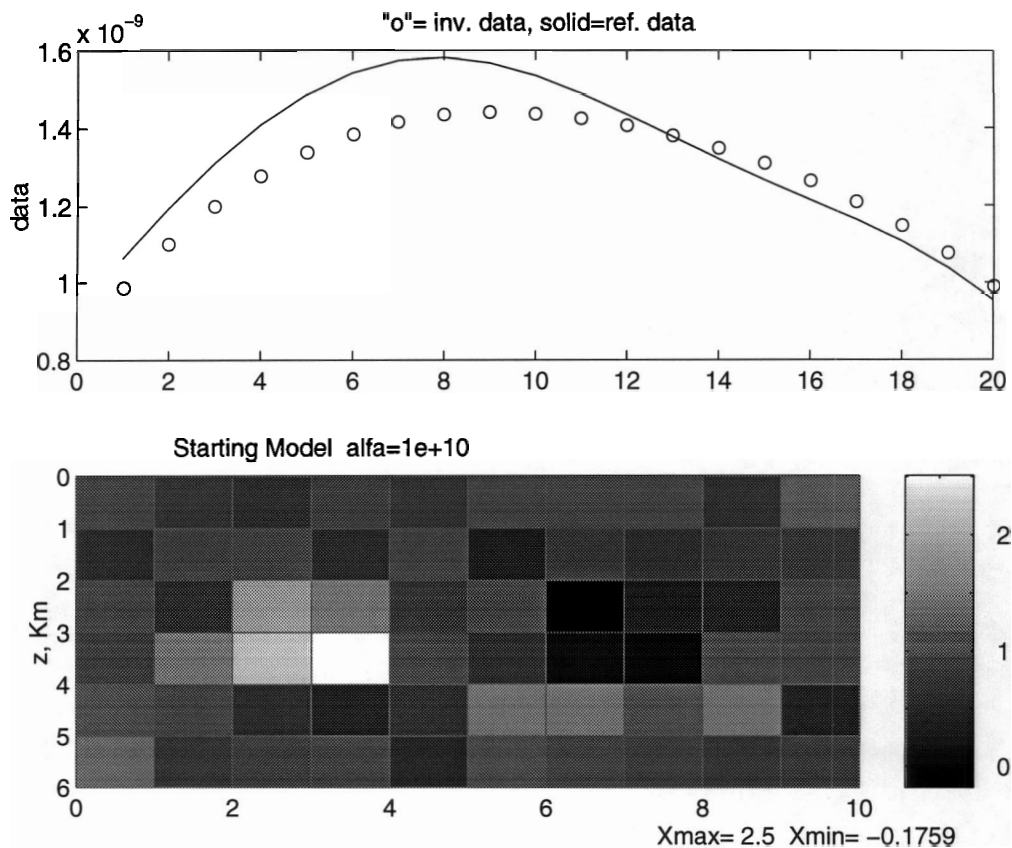


Figure 5.14. TV semi-norm Stabilizer, starting model (60 cells)

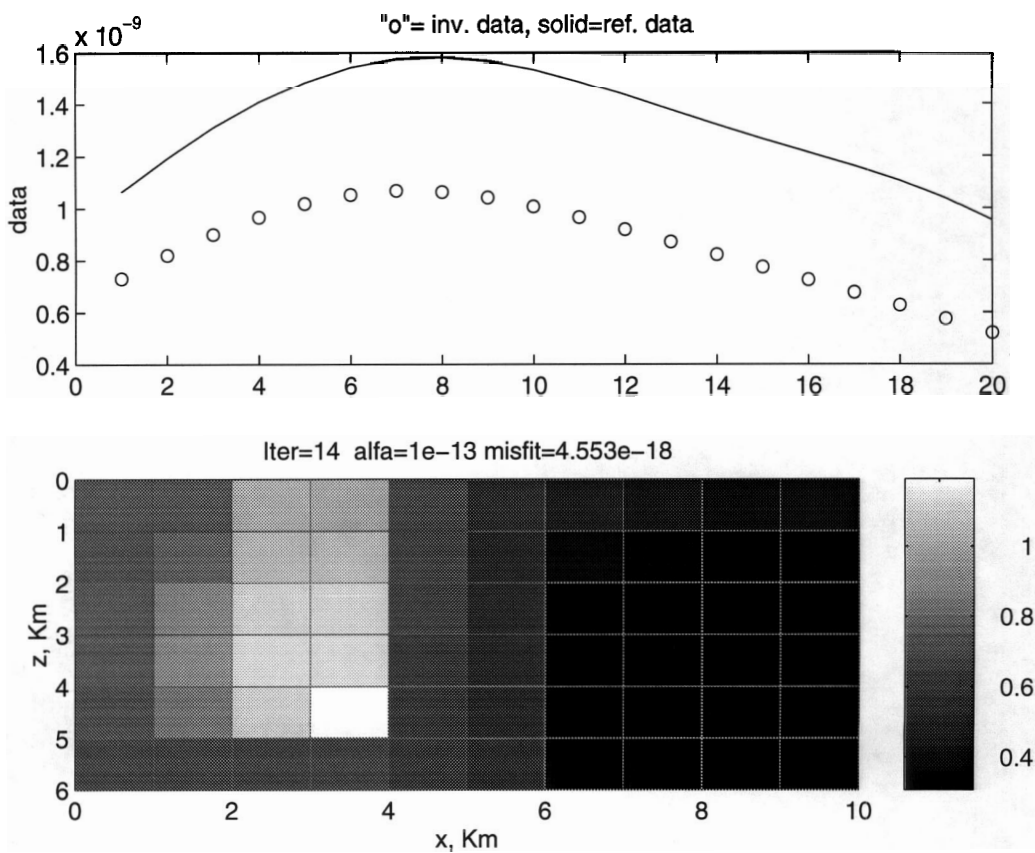


Figure 5.15. TV semi-norm stabilizer, intermediate iteration (60 cells)

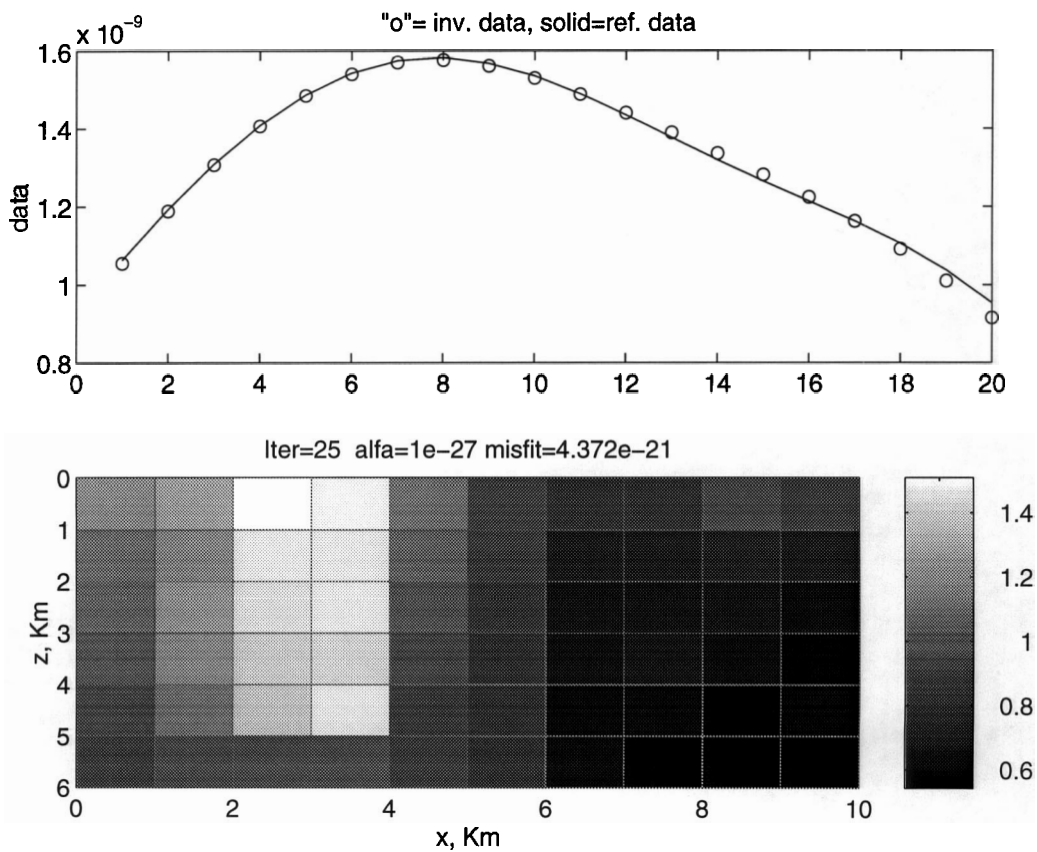


Figure 5.16. TV semi-norm stabilizer, final solution (60 cells)

5.3 Application of TV method to noisy data

The next two inversion results are obtained from models where 6% gaussian noise was added to the gravitational data calculated in 20 stations at the top reference surface.

The first 240 cells model is shown in figure 5.17. It roughly represents a geological fault separated by a low density structure. A second 240 cells model related to the shape of an oil reservoir is shown in figure 5.19. In this model, measurements are simulated to be taken in a borehole in the bottom of the reservoir. For convenience the display in figure 5.19 is flipped top to bottom, so that depth is increasing in positive vertical direction on this figure, and the zero-th layer of the blocks corresponds to the most deep undersurface structures. The measurements now take place at the top of the model.

The presence of noise in the gravity data limits the accuracy in the inversion scheme, which will be reflected in the quality of the recovered density distribution.

The inversion results are shown on figures 5.18 and 5.20. We can see that the method still is able to recover part of the non-smooth features of the true models. In spite of the presence of noise in the gravity data, the constructed solution is close to the true density distribution. This illustrates the stability of the reconstruction algorithm.

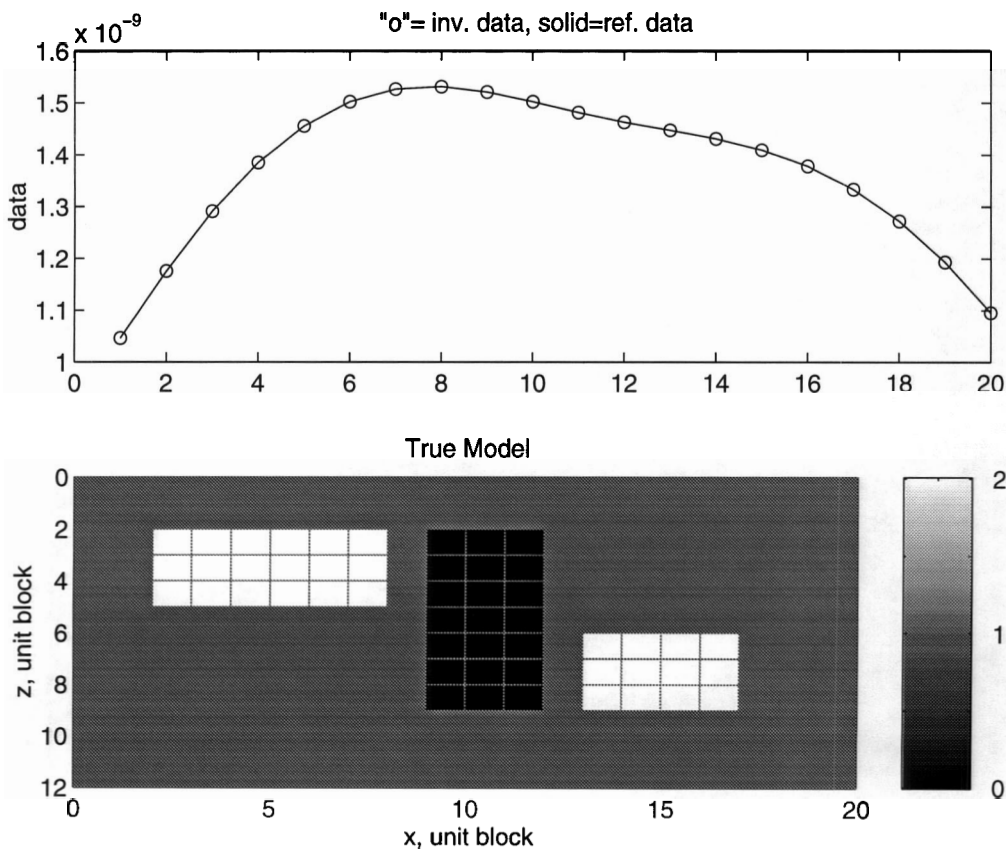


Figure 5.17. Fault model with noisy gravity data

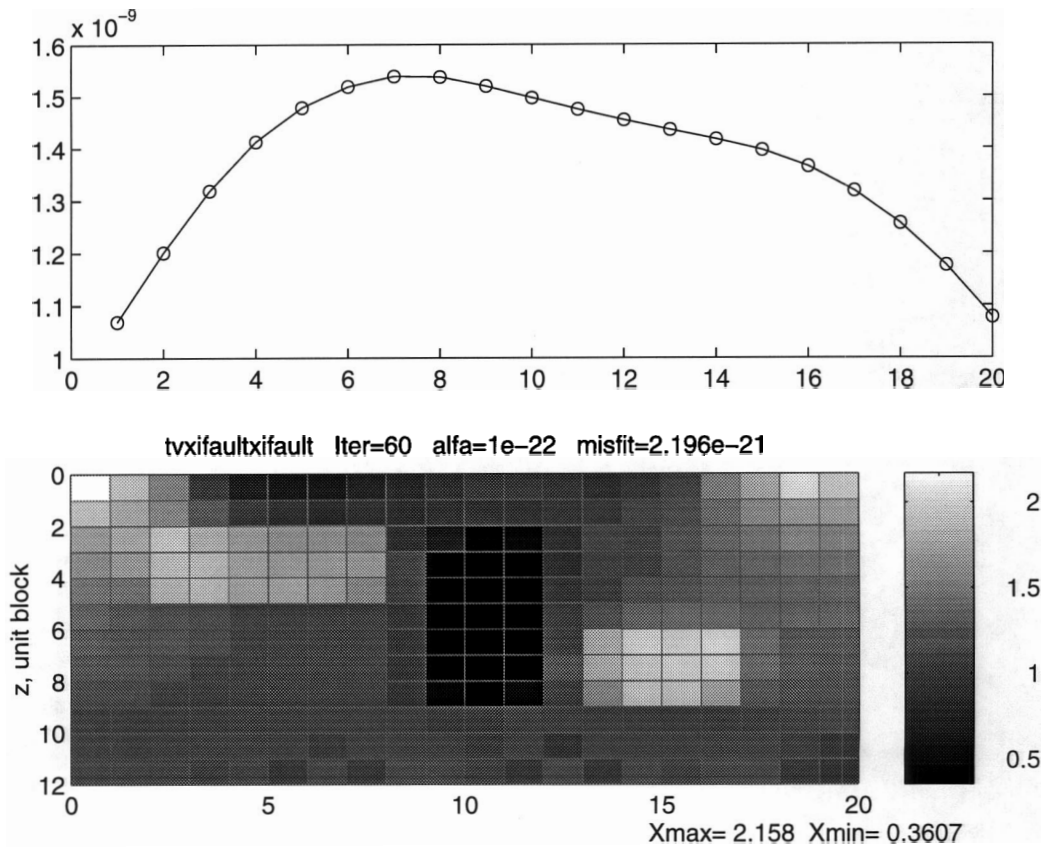


Figure 5.18. Inversion result, fault model with noisy data

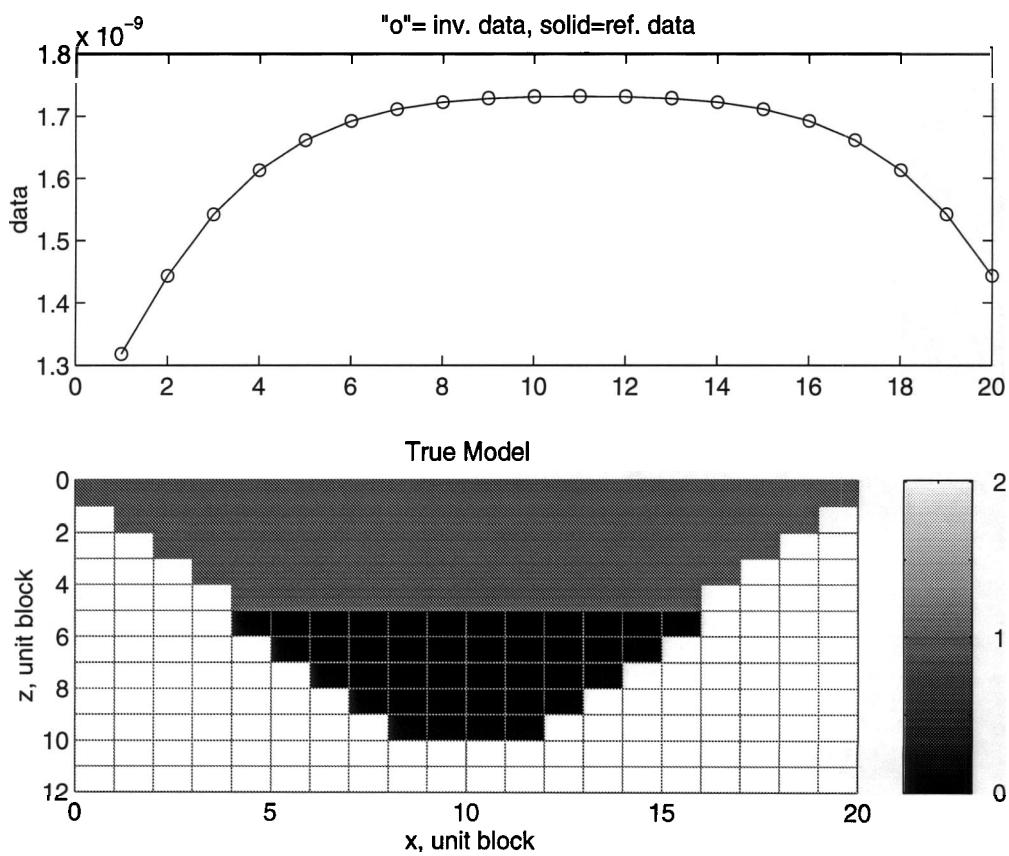


Figure 5.19. Oil reservoir model with noisy gravity data

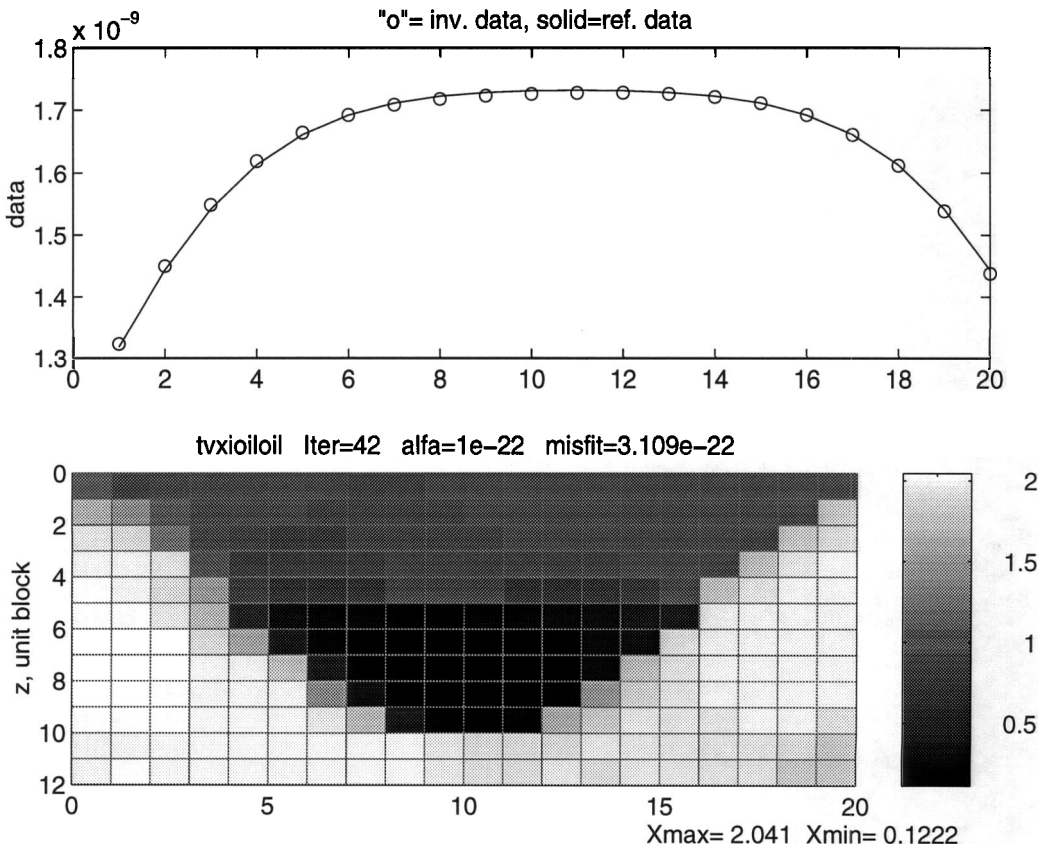


Figure 5.20. Inversion result, oil reservoir model with noisy data

CHAPTER 6

CONCLUSIONS AND FURTHER WORK

The approach in this work can be extended to other geophysical measurements. Here we present the fundamental equations for other geophysical applications, which can be formulated as operator equations analogous to the gravimetric problem.

6.1 Extension to other geophysical problems.

Electromagnetic fields are generated by Maxwell's equations which consist of Ampere's Law,

$$\nabla \times H = J + J_D + \frac{\partial D}{\partial t} \quad (6.1)$$

Faraday's Law,

$$\nabla \times E = -\frac{\partial B}{\partial t} \quad (6.2)$$

the compatibility equations,

$$\begin{aligned} \nabla \cdot B &= 0 \\ \nabla \cdot D &= Q + Q_D \end{aligned} \quad (6.3)$$

where

$$\nabla \cdot J = Q$$

$$\nabla \cdot J_0 = Q_D$$

and constitutive relations for linearized isotropic materials: Ohm's law,

$$j = \sigma E \quad (6.4)$$

and for D and B , reflecting the electromagnetic properties of a medium,

$$\begin{aligned} D &= \epsilon E \\ B &= \mu H \end{aligned}$$

Here,

E is the vector electric field, and D is the electric displacement field,

H is the vector magnetic field, B is magnetic induction,

J and Q are the electric density currents and the spatial density of impressed (source) charges,

J_D and Q_D are the electric density currents and the spatial density electric charges of the external charges,

ϵ , μ and σ are the permittivity, the magnetic permeability, and electric conductivity, respectively.

The forward electromagnetic problem is to calculate the solution of equation (6.1),(6.2),(6.3) and (6.4) for the given model parameters (ϵ, μ, σ) .

We can see that this is a system of linear differential equations. They can be summarized as an operator equation,

$$[E, H] = K_{em}(\epsilon, \mu, \sigma) \quad (6.5)$$

where the operator K_{em} is called the forward operator for the electro-magnetic problem.

The problems for static magnetic and static electric fields are particular case of this operator, so that the operator equation for the corresponding forward problems can be expressed analogously.

The inverse problem now is to determine the electromagnetic parameters of the medium. The difference with gravitational problem is that the equation (6.5) is not linear with respect to the parameters of the medium (ϵ, μ, σ) . However, if a good initial model is available, it can be linearized, and the linearized problem can be solved at each iteration step.

The basis of the study of the theory of seismic wave fields is described by the acoustic wave equation

$$\frac{\partial^2 p}{\partial t^2} = \frac{1}{v^2} \Delta p$$

where p is the pressure field and v is the velocity of the wave propagation. Solution of the acoustic wave equation for a given v describes the forward formulation for the seismic problem. The resulting operator equation for the forward problem can be expressed as

$$p = K_{seismic}(v) \tag{6.6}$$

where the operator $K_{seismic}$ is the forward operator for the seismic problem.

In this work we solved the operator equation for the gravitational potential problem. In the operator form this equation is analogous to the equations (6.5) and (6.6) arising in other geophysical fields, hence it can be expected that the results of this work can be extended to these fields as well.

6.2 Conclusions

One way to define regularization is as *a smart way to input a priori information in the inversion process*. This work has shown that regularization by the Total Variation method is a more appropriate than the standard regularization schemes, when the goal is to recover non-smooth solutions.

For the inverse problem of gravitational potential, functions with sharp density contrast and shapes are better reconstructed using TV norm as a stabilization functional instead of standard smoothing operators.

An effective computational algorithm is developed using a discrete approximation of the Euler-Lagrange equations, which avoids solving a PDE in each iterative step.

The adaptive gradient minimization is constructed to solve the problem numerically and it is shown to be efficient for this type of problems.

We expect that the results obtained in this work for the inverse gravity problem can be used in other geophysical applications.

6.3 Further Work

Further analysis of the effectiveness of different approaches such as discretization and regularization or regularization and discretization for the solution of large scale inverse problem.

Understanding of other effects of TV regularization on the solution besides the considered in the present work.

Extension to other geophysical problems.

Vector total variation norm applied to anisotropic non-linear geophysical problems.

Efficient optimization codes for large scale geophysical problems, performing automatic selection of the regularization parameter with an optimal decreasing criteria.

REFERENCES

- [1] A. BASSREI, *Regularization and Inversion of 2-D Gravity Data*, Expanded Abstracts of 63th. Annual Meeting, S.E.G., Washington, D.C., September 26-30, 1993
- [2] A. ACAR AND C. VOGEL, *Analysis of bounded Variation penalty methods for ill-posed problems*, Inverse Problems 10, (1994), 1217-1229.
- [3] E. GIUSTI, *Minimal Surfaces and Function of Bounded Variation*, Birkhäuser, (1984).
- [4] D. R. ADAMS, *Function spaces and potential theory*, Springer-Verlag Berlin Heidelberg New York, (1991).
- [5] L. RUDIN, *Nonlinear Total Variation Based Algorithms*, Physica D, 60 (1992), pp. 259-268.
- [6] L. ALVAREZ, P. LIONS AND J. MOREL, *Image selective smoothing and edge detection by nonlinear diffusion*, SIAM J. Numer. Anal. Vol. 29- 3, (1992), pp. 845-866.
- [7] D. DOBSON AND F. SANTOSA, *Recovery of blocky images from noisy and blurred data*, Tech. Report No. 94-7, Center for the Mathematics of Waves, University of Delaware (1994).
- [8] T. F. CHAN, H. M. ZHOU, AND R. H. CHAN, *Continuation method for total variation denoising problems*, Advanced Signal Processing Algorithms, Vol. 2563, (1995).
- [9] C. R. VOGEL AND M. E. OMAN, *Fast Numerical methods for total variation minimization in image reconstruction*, Advanced Signal Processing Algorithms, Vol. 2563, (1995).
- [10] H. BERTETE-AGUIRRE, E. CHERKAEVA, AND A. FOGELSON, *Comparison between total variation regularization operators and standard regularization operators for gravimetric inverse problems*, Fourth SIAM Conference on Mathematical and Computational Issues in Geosciences, June 16-19, Albuquerque, New Mexico, (1997)
- [11] H. BERTETE-AGUIRRE, E. CHERKAEVA, AND A. FOGELSON, *Total variation methods for finding non-smooth solutions to the inverse gravimetric problem*, II PanAmerican Workshop in Applied and Computational Mathematics, Gramado, Brazil, September 8-12 (1997).

- [12] H. BERTETE-AGUIRRE AND A. XAVIER, *Mínimos cuadrados aplicados à inversão geofísica*, Coppe-Sistemas report, UFRJ, (1994).
- [13] A. N. TIKHONOV, *On the stability of inverse problems*, Soviet. Math. Dokl., 39 (1943), pp. 1035–1038.
- [14] A. N. TIKHONOV AND V. Y. ARSEININ, *Solutions of ill-posed problems*, Willey, N.Y., 1977.
- [15] M. M. LAVRENTIEV, V. G. ROMANOV AND S. P. SHISHASKY, *Ill-posed problems in mathematical physics and analyses*, Nauka, Moscow, 1980.
- [16] N. J. FISHER, AND L. E. HOWARD, *Gravity interpretation with the aid of quadratic programming*, Geophysics, 45 (1980), pp. 403–419.
- [17] C. SAFON, G. VASSEUR, AND M. CUER, *Some applications of linear programming to the inverse gravity problem*, Geophysics, 42 (1977), pp. 1215–1229.
- [18] W. M. TELFORD, L. P. GELDART AND, R. E. SHERIFF, *Applied geophysics*, 2nd ed., Cambridge University Press, Cambridge (1990)
- [19] G. H. GOLUB AND C. F. VAN LOAN, *Matrix computations*, 2nd ed., The Johns Hopkins University Press, Baltimore (1989)
- [20] J. WERMER, *Potential theory*, Lecture Notes in Mathematics 408, (1974).
- [21] H. AIKAWA AND M. ESSEN, *Potential theory - Selected Topics*, Lecture Notes in Mathematics 1633, (1996).
- [22] O. P. GUPTA, *A least-squares approach to depth determination from gravity data*, Geophysics, 48, (1983), pp. 357-360.
- [23] E. M. ABDELRAHMAN, A. I. BAYYOUMI AND H. M. EL-ARABY, *A least-squares minimization approach to invert gravity data*, Geophysics, 56, (1991), pp. 115-118.
- [24] M. AL-CHALABI, *Some studies relating to nonuniqueness in gravity and magnetic inverse problems*, Geophysics, 36, (1971), pp. 835-855.
- [25] F. GUSPI, *Noniterative nonlinear gravity inversion*, Geophysics, 58, (1993), pp. 935-940.
- [26] C. T. BARNET, *Theoretical modeling of the magnetic and gravitational fields of an arbitrarily shaped Three-Dimensional Body*, Geophysics, 41, (1976), pp. 1353-1364.
- [27] R. E. CHAVEZ AND G. D. GARLAND, *On the application of the inverse theory to gravity interpretation*, Geophysics, 31, (1983), pp. 119-130.
- [28] D. W. OLDENBURG, *The inversion and interpretation of gravity anomalies*,

Geophysics, 39, (1974), pp. 526-536.

- [29] G. D. GARLAND, *The earth's shape and gravity*, Pergamon Press, London 1965
- [30] A. BJÖRCK, *Numerical methods for least squares problems*, SIAM, Philadelphia, (1996).
- [31] C. L. LAWSON AND R. J. HANSON, *Solving least squares problems*, Prentice Hall, Englewood Cliff, NJ, (1995).
- [32] C. L. LAWSON AND R. J. HANSON, *Solving least squares problems*, Classics in Applied Mathematics, SIAM, Philadelphia, (1995).